To the Graduate Council:

I am submitting herewith a dissertation written by Christopher Aaron Shelley entitled "The Kinetic Enhancement of Polymer-Supported Reagents for Organic Synthesis and Selective Metal Ion Complexation." I have examined the final copy of this dissertation for form and content and recommend that it be accepted in partial fulfillment of the requirements for the degree of Doctor of Philosophy, with a major in Chemistry.

Spiro D. Alexandratos, Major Professor

We have read this dissertation
and recommend its acceptance:

Accepted for the Council:

Associate Vice Chancellor and
Dean of the Graduate School

THE KINETIC ENHANCEMENT OF POLYMER-SUPPORTED REAGENTS FOR USE IN ORGANIC SYNTHESIS AND SELECTIVE METAL ION COMPLEXATION

A Dissertation

Presented for the

Doctor of Philosophy

Degree

The University of Tennessee, Knoxville

Christopher Shelley

May 2000

DEDICATION

This dissertation is dedicated to my wife Tracy

for her support, time, understanding and

unconditional love.

ACKNOWLEDGMENTS

I would first like to thank my major advisor Professor Spiro D. Alexandratos. His guidance, insight and encouragement were invaluable to my completion of this work. I would also like to thank Professors Jeff Kovac, Richard Pagni and Engin Serpersu for serving on my committee. I am grateful to the Department of Chemistry and Department of Energy, Office of Basic Sciences for their financial support. Finally, I owe many thanks to my co-workers Bob, Subu, Christy, Stephanie, Marc, Min, Dorothy, Vijay, Kelly, Robert, Latiff, Cheryl, Mike, Lenore and my parents. Their friendship, kindness and support over the years have meant more to me than words can express.

ABSTRACT

Polymers can be designed with specific chemical properties for application in organic synthesis and selective metal ion complexation. The chemical properties of the polymer-supported reagent are influenced by the structure of the polymer backbone. The focus of this dissertation is to investigate this relationship in the attempt to optimize the kinetics of the polymer-supported reagent for its specific application.

The influence of the polymer structure on the kinetics of an S_N2 displacement mechanism was evaluated by the Hammett correlation. Polymer-supported phenoxide resins were synthesized from polystyrene beads and used in the Williamson ether synthesis. The initial rate of the reaction between the phenoxide resins and benzyl chloride in ethanol decreased with increasing strength of the electron withdrawing group of the substituted phenoxide. A non-linear Hammett correlation of the kinetic data determined a change in the rate limiting step to occur between sigma -0.17 and 1.27. It is proposed that a change in the rate limiting step from ion-pair dissociation to nucleophilic attack is the result of an increased delocalization of the phenoxide electron density. Variations in the polarity of the polymer backbone did not alter the rate of ion-pair dissociation, but did influence the activation energy of nucleophilic attack. The initial reaction rate with polymer-supported p-nitrophenoxide was increased by a factor of 1.4 when the percentage of ionic monomer units was decreased from 100% to 50%. It is proposed that a decrease in the polarity of the local environment around the phenoxide increased the reactivity of the reactants, resulting in an increase in the initial rate.

Reactions with partially functionalized p-nitrophenoxide resins containing 50% methyl methacrylate in the copolymer were 1.4 times faster than resins containing 50% styrene. The enhanced reactivity of the methyl methacrylate resin was attributed to a decrease in anion solvation by ethanol which increased the reactivity of the nucleophile.

The yield of the Mitsunobu coupling reaction is significantly decreased when the pKa of the acidic reagent approaches 11. A series of polymer-supported phosphine resins were synthesized to evaluate the influence of the local environment within the macromolecule on the Mitsunobu etherification of m-cresol (pKa = 10.01) with benzyl alcohol. Resins with phenyl or ester groups neighboring the phosphine produced final yields of 20.8% and 0.0% respectfully. Due to competing side reactions, the ether yield was significantly influenced by the rate of the reaction. Reaction rates were determined to increase with the number of phenyl rings surrounding the phosphine (percent yield at 0.1 h: 4.2% and 15.7% for polymers with 0% and 82% phenyl groups). Similar behavior was observed in the Mitsunobu esterification of benzoic acid with benzyl alcohol. It is proposed that a non-polar microenvironment can be used to enhance the reactivity of ionic intermediates and increase the rate of product formation. Etherification kinetics were also determined to be enhanced by an increase in the electron-withdrawing substituent of the polymer-supported phosphine. Resins containing only triphenylphosphine or benzyldiphenylphosphine produced ether yields of 43.7% and 11.0% respectfully.

The selective complexation of metal ions by a polymer-supported reagent is hindered in highly acidic solutions due to a collapse of the micropores. A series of

phosphonic acid resins were synthesized with varying levels of crosslinking, and studied for their ability to complex Eu(III). Increased crosslinking of the phosphonic acid resin was unable to prevent pore collapse in 0.50 N nitric acid solutions . The hydrophobicity of crosslink levels between 12% and 25% DVB was determined to increase the matrix sensitivity to the solution pH and decrease the amount of Eu(III) complexed. Pore collapse of the phosphonic acid resin was prevented by sulfonating the ion-exchange resin. In highly acidic solutions, the sulfonic acid ligand of the bifunctional resin provided an access mechanism for metal ions, and prevented collapse of the microporous structure. Selective ion complexation was enabled by the recognition mechanism of the phosphonic acid ligands which selectively coordinated Eu(III) ions once inside the polymer.

TABLE OF CONTENTS

PAGE

1. INTRODUCTION....1

General....1

The polymer-support....2

Organic synthesis applications....5

Chemistry of polymer-supported reagents....10

Reagent accessibility....12

Site-site interaction....14

Microenvironmental effect....17

Research....19

2. THE STRUCTURAL INFLUENCE OF A POLYMER-SUPPORTED REAGENT ON THE KINETICS OF A S_N2 DISPLACEMENT MECHANISM....21

Introduction....21

Experimental....26

Synthesis of anion-exchange resins....26

Synthesis of benzyltrialkylammonium phenoxide resins....27

Williamson ether reaction conditions....27

Characterization of ether products....29

Results....30

Characterization....30

Reaction conditions....39

Kinetic study....42

Hammett analysis 57

Discussion 61

Non-linear Hammett correlations 61

Microenvironmental effect 71

Conclusion 73

3. THE APPLICATION OF POLYMER-SUPPORTED PHOSPHINE RESINS IN THE MITSUNOBU ETHERIFICATION REACTION.....74

Introduction 74

Experimental 79

Synthesis of phosphine resins 79

General procedure for the Mitsunobu reaction.....82

Characterization of ether product.....82

Results 85

Characterization 85

Etherification reaction conditions 85

Mitsunobu etherification 93

Mitsunobu esterification 96

Discussion 96

Conclusion 101

4. IONIC ACCESSIBILITY OF SELECTIVE ION-EXCHANGE RESINS.....102

Introduction 102

Experimental 107

Synthesis of ion-exchange resins 107

Metal ion studies 109

Results 112

Characterization 112

Metal ion studies 117

Discussion 124

Diethyl phosphonate ester resin (VBC-PE).....124

Phosphonic acid resins (VBC-PA and Sty-PA).....126

Monofunctional and bifunctional resins (VBC-PA and VBC-PA/SA) 126

Conclusion 127

5. EXPERIMENTAL PROCEDURES.....129

Synthesis 129

Copolymer synthesis 129

Washing of copolymer 130

Synthesis of benzyltrialkylammonium chloride resins.....131

Synthesis of benzyltrialkylammonium phenoxide resins.....131

Bromination of polystyrene beads 132

Synthesis of poly(vinylbenzyldiphenylphosphine) and poly(styrenediphenylphosphine) resins 132

Synthesis of diethyl phosphonate ester resins 133

Synthesis of poly(vinylbenzyl chloride)-supported phosphonic acid resins 133

Synthesis of polystyrene-supported phosphonic acid resins.....133

Sulfonation of ion-exchange resins with chlorosulfonic acid.....134

Sulfonation of ion-exchange resins with sulfuric acid.....135

Characterization 135

Nitrogen capacity 135

Chlorine capacity 136

Nitrophenoxide capacity 137

Phosphorus capacity 137

Swelling ratios 138

Percent solids 138

Acid capacity 138

Kinetic studies 139

Gas chromatography analysis of the organic reactions.....139

The Williamson ether synthesis 140

The Mitsunobu etherification and esterification.....141

Metal ion studies 141

Atomic absorption/emission spectroscopy.....142

REFERENCES.....143

APPENDIX.....151

VITA.....155

LIST OF TABLES

TABLE		PAGE
2.1	Composition of copolymer starting material	28
2.2	Characterization of benzyltrialkylammonium chloride resins	31
2.3	Characterization of benzyltrimethylammonium chloride resins	32
2.4	Characterization of benzyltrialkylammonium p-nitrophenoxide resins	33
2.5	Characterization of benzyltrimethylammonium p-nitrophenoxide resins	34
2.6	Characterization of benzyltrimethylammonium m-nitrophenoxide resins	35
2.7	Characterization of benzyltrimethylammonium phenoxide resins	36
2.8	Characterization of benzyltrimethylammonium p-methylphenoxide resins	37
2.9	Characterization of benzyltrialkylammonium p-chlorophenoxide and p-methylphenoxide resins	38
2.10	Reaction condition controls using benzyltrimethylammonium p-nitrophenoxide resins in toluene	40
2.11	Side-reaction controls using benzyltrimethylammonium resins in toluene	41
2.12	Side-reactions with benzyltrimethylammonium p-methoxyphenoxide resins in toluene	43
2.13	Non-reproducible data using benzyltrimethylammonium p-nitrophenoxide resins in toluene	44
2.14	Non-reproducible data using benzyltrimethylammonium [X]phenoxide resins in toluene	45
2.15	Williamson ether synthesis using benzyltrimethylammonium p-nitrophenoxide resins	48
2.16	Williamson ether synthesis using benzyltrimethylammonium m-nitrophenoxide resins	51

2.17 Williamson ether synthesis using benzyltrimethylammonium phenoxide resins 52

2.18 Williamson ether synthesis using benzyltrimethylammonium p-methylphenoxide resins 53

2.19 Williamson ether synthesis Hammett data 54

2.20 Accessibility controls with VBC supported benzyltrimethylammonium p-nitrophenoxide resins in ethanol 55

2.21 Swelling rations of [X]phenoxide resins 58

3.1 Composition of copolymer starting material 81

3.2 Characterization of phosphine resins 86

3.3 Reaction conditions using triphenylphosphine and a phosphine resin..... 88

3.4 Etherification accessibility controls 90

3.5 Swelling ratio of phosphine resins in THF 91

3.6 Etherification reactions using a different solvent or temperature..... 92

3.7 Percent yield of benzyl 3-methylphenyl ether in the Mitsunobu etherification..... 95

3.8 Percent yield of benzyl benzoate ether in the Mitsunobu esterification..... 97

4.1 Characterization of VBC diethyl phosphonate ester resins (VBC-PE)..... 113

4.2 Characterization of VBC phosphonic acid resins (VBC-PA)..... 114

4.3 Characterization of styrene phosphonic acid resins (Sty-PA)..... 115

4.4 Characterization of VBC phosphonic / sulfonic acid resins (VBC-PA/SA)..... 116

4.5 Characterization of VBC diethyl phosphonate ester / sulfonic acid resins..... 118

4.6 Characterization of styrene phosphonic / sulfonic acid resins..... 119

4.7 Sulfonation of styrene supported phosphinic acid resin..... 120

4.8 Complexation of Eu(III) from 10^{-4} $Eu(NO_3)_3$ / HNO_3 solutions.....121

4.9 Complexation of Eu(III) from 10^{-4} $Eu(NO_3)_3$ / HNO_3 solutions.....123

4.10 Complexation of Eu(III) from 10^{-4} $Eu(NO_3)_3$ / HNO_3 / 0.40 N $NaNO_3$ solutions 125

LIST OF FIGURES

FIGURES PAGE

1.1 Commercial synthesis of sulfonic acid ion-exchange resin 3

1.2 Synthesis of an acid chloride 6

1.3 Commercial synthesis of bisphenol A 7

1.4 Solid-phase peptide synthesis 9

1.5 Scavenger resin 11

1.6 Polymer-supports used to complex rhodium(I)....13

1.7 Polymer-supported benzenesulfonylhydrazide 15

1.8 Polymer-supported titanocene 16

1.9 Microenvironmental effect 18

2.1 Williamson ether synthesis 23

2.2 S_N2 mechanism 23

2.3 Application of an anion-exchange resin to the Williamson ether synthesis....24

2.4 Model polymer-supported phenoxide 24

2.5 Synthesis of polymer-supported phenoxide 25

2.6 Non-reproducible data using VBC:Sty supported benzyltrimethylammonium p-nitrophenoxide resins 46

2.7 Non-reproducible data using VBC:MMA supported benzyltrimethylammonium p-nitrophenoxide resins 47

2.8 Twelve phenoxide resins studied 49

2.9 Accessibility controls with VBC p-nitrophenoxide in ethanol at 65°C....56

2.10 Calculating the Hammett rate constant ratio from the initial rate data....59

2.11 Hammett plot of VBC support in ethanol at 65°C....60

2.12 Hammett plot of VBC:Sty support in ethanol at 65°C....62

2.13 Hammett plot of VBC:MMA support in ethanol at 65°C....63

2.14 Hammett plot of VBC, VBC:Sty and VBC:MMA supports in ethanol at 65°C....64

2.15 Desolvation vs. S_N2 rate limiting step....67

2.16 Dissociation vs. S_N2 rate limiting step....70

3.1 Mitsunobu etherification of m-cresol and benzyl alcohol....75

3.2 Mitsunobu esterification of benzoic acid and benzyl alcohol....76

3.3 Mechanism of the Mitsunobu reaction....77

3.4 Mechanism of the alkylated hydrazine side-reaction....78

3.5 Structures of polymer-supported phosphines....80

3.6 Synthesis of poly(vinylbenzyldiphenylphosphine) supports....83

3.7 Synthesis of poly(styrenediphenylphosphine) supports....84

3.8 GC analysis of the Mitsunobu etherification with triphenylphosphine at different reagent ratios....89

3.9 The Mitsunobu etherification with triphenylphosphine and polymer-supported phosphine resins....94

4.1 Non-selective sulfonic acid ion-exchange resin....103

4.2 Ion selective dithizone resin....104

4.3 Diphonix, an ion selective DMBP....106

4.4 Structures of ion-exchange resins....108

4.5 Synthesis of VBC-PE, VBC-PA and VBC-PA/SA....110

4.6 Synthesis of Sty-PA....111

Chapter 1

INTRODUCTION

GENERAL

Polymer-supported reagents are structurally defined as a reactant, catalyst or substrate covalently bound to an insoluble polymer. By rendering a reagent insoluble, the polymer-supported reagent is provided with a variety of practical advantages over its soluble counterpart, and is capable of several novel applications. Polymers designed with specific chemical properties are currently being utilized in important chemical applications such as catalysis,[1] organic synthesis,[2] and chromatography.[3]

The predominant advantage in using a polymer-supported reagent is the ability to separate the polymer from non-supported compounds. By using a polymer-supported reactant in an organic reaction, the spent polymer can be easily recovered by filtration. A novel application of this advantage is the adaptation of the reaction to a continuous flow process. Because the polymer-supported reaction is heterogenous, the reactive polymer can be packed into a column as a stationary phase, and the reagents pumped through the column as a mobile phase. The products of this reaction are collected as the solution exits the column.

There are numerous advantages to the continuous flow process. By adapting the reaction to this technique, product synthesis can be automated and upscaled to industrial applications. The commercial synthesis of bisphenol A using a polymer-supported

sulfonic acid catalyst is just one of many large scale applications currently in use.[4] Like the example of the polymer-supported catalyst, if the reactive polymer is not spent during the course of the reaction, the column can be reused and reduce the cost of production.

One final advantage of a polymer-supported reagent is the control of hazardous material. Because the polymer is insoluble and nonvolatile, it does not exhibit toxic or odor hazards. These characteristics of polymer-supported reagents have a large potential for waste management applications and improving the environmental compatible of industrial scale chemistry.[2,4]

THE POLYMER-SUPPORT

There are two conventional schemes used to synthesize a polymer-supported reagent. A functionalized monomer can be synthesized and then polymerized, or a functional ligand can be immobilized onto a polymer by synthetic means. Both synthetic schemes are commonly used, but the latter method is preferred because it does not require modification of the polymerization chemistry. An example of a commercially available polymer-supported reagent is the sulfonic acid ion-exchange resin. This resin is manufactured by the sulfonation of polystyrene lightly crosslinked with divinylbenzene[4] (Figure 1.1)

Reagents, catalysts and substrates have been immobilized onto crosslinked organic polymers like polystyrene, poly(4-vinylpyridine), and poly(vinyl acetate).[2] Of these polymers, polystyrene is the most common starting material used due to its superior physical and chemical versatility. Because all of the polymer-supported reagents in this

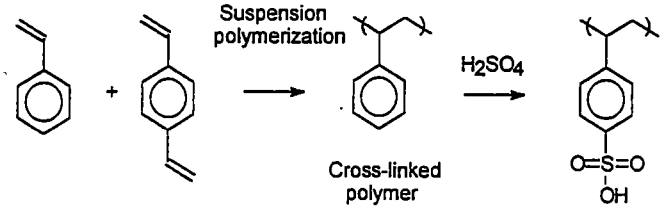


Figure 1.1. Commercial synthesis of sulfonic acid ion-exchange resin

dissertation were synthesized from polystyrene, most of the introduction content will involve polystyrene-based reagents.

In order to simplify handling and limit pressure drops in column applications, polymer-supported reagents are processed in the form of beads with a diameter >50μ. The suspension polymerization technique used to produce these beads involves the vinyl monomer, divinyl crosslinking agent and a free radical initiator mechanically dispersed in an aqueous phase to form spherical monomer droplets. A suspension stabilizer, such as polyvinylalcohol or calcium phosphate, is added to the aqueous phase to prevent agglomeration of the organic droplets. Initiation of the polymerization occurs inside the monomer droplets when free radicals are formed by the thermal fragmentation of the initiator. Because the monomer droplets are converted to hard beads during the course of the polymerization, the size of the bead is influenced by the stir speed, shape of the reactor, stabilizer, and organic:aqueous phase ratio. After the polymerization is complete, the beads are filtered from the solution and washed to remove the stabilizer and impurities.

Similar to the control of the particle size, the porosity of the bead is controlled during the polymerization before the monomer droplet is converted to the hard bead. Permanent porosity can be created by the addition of a diluent to the organic phase of the polymerization. Beads with pores several hundred angstroms in diameter are generated by the addition of a non-solvent to the polymerization. The non-solvent selected must be capable of solvating the monomer, but not the polymer formed. This difference in solvation causes phase separation to occur within the organic droplets, and thus forms

porous channels within the hard bead. Polymer beads produced using a non-solvent are classified as 'macroporous' resins (MR). In order to provide the polymer with physical stability, the highly porous resin generally contains 5% to 40% crosslinking agent.

Crosslinked beads formed without the use of a diluent are classified as 'gel' resins. The pore size of this glass-like polymer is determined by the distance between the polymer chains. The interchain distance is significantly influenced by the crosslink level of the polymer, and whether the beads can be swollen by the solvent or reactants. In order to maximize the swelling of a gel-type resin, the polymer is lightly crosslinked with 1% to 5% crosslinking agent.

ORGANIC SYNTHESIS APPLICATIONS

Polymer-supported reagents have been used as reactants, catalysts and protecting groups in organic reactions. There are hundreds of different examples of polymer-supported reactants in the literature.[2] Figure 1.2 is an example of a polymer-supported acid chloride used to convert acetic, acrylic, and benzoic acid into their acid chlorides.[5] Although the polymer-supported reactant cannot be reused in this application, the product can be separated by simple filtration when the excess reactant is the insoluble polymer.

The polymer-supported sulfonic acid catalyst used in the commercial synthesis of bisphenol A is an example of a polymer-supported reagent that can be reused[4] (Figure 1.3). Because the reactive polymer is not consumed by the reaction, the polymer-supported catalyst can be adapted to a continuous flow process and reduce the cost of production. This type of polymer can also be reused when performing benchtop scale

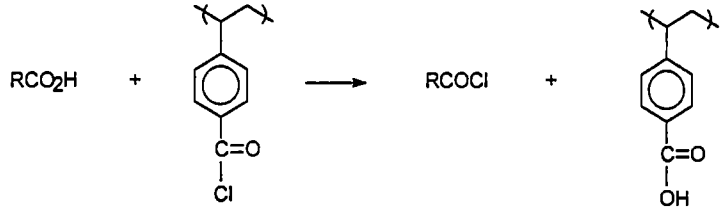


Figure 1.2. Synthesis of an acid chloride

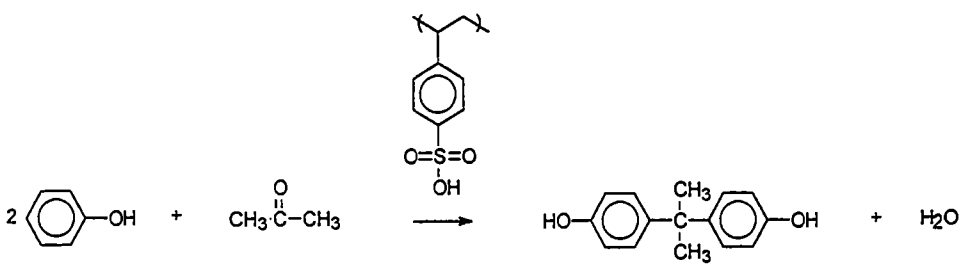


Figure 1.3. Commerical synthesis of bisphenol A

synthesis. However, the ability to separate the catalyst from the reaction by filtration is often the greatest advantage when working at this scale.

What is often referred to as the most significant discovery in polymer-supported reaction chemistry involves the first application of a polymer-supported protecting group. In 1963, Merrifield[6] introduced a scheme to synthesize a tetrapeptide using crosslinked chloromethylated polystyrene as a carboxylic acid protecting group (Figure 1.4). By temporarily immobilizing an amino acid onto the polymer-support, the amino acid was converted to a dipeptide by deprotecting the amine, and coupling it with a second amino acid. This process of deprotection and coupling amino acids was continued until the peptide of the desired amino acid sequence was obtained. The final peptide product was then cleaved from the polymer-supported with acid, and washed from the pores of the bead.

The significance of this solid-phase synthesis technique lies in the ability to temporarily render the amino acid insoluble. Because the synthesis of a peptide requires a purification step after the addition of each amino acid, the percent yield of the peptide would decrease after each step when using soluble reagents. However, by using a polymer-supported protecting group, Merrifield was the first to demonstrate that the loss of product associated with standard purification techniques in multi-step synthesis could be overcome.

Merrifield's novel approach to peptide synthesis earned him a Nobel prize in 1984, and revolutionized the fields of peptide and natural product synthesis. The application of polymer-supported protecting groups has also lead to the automation of

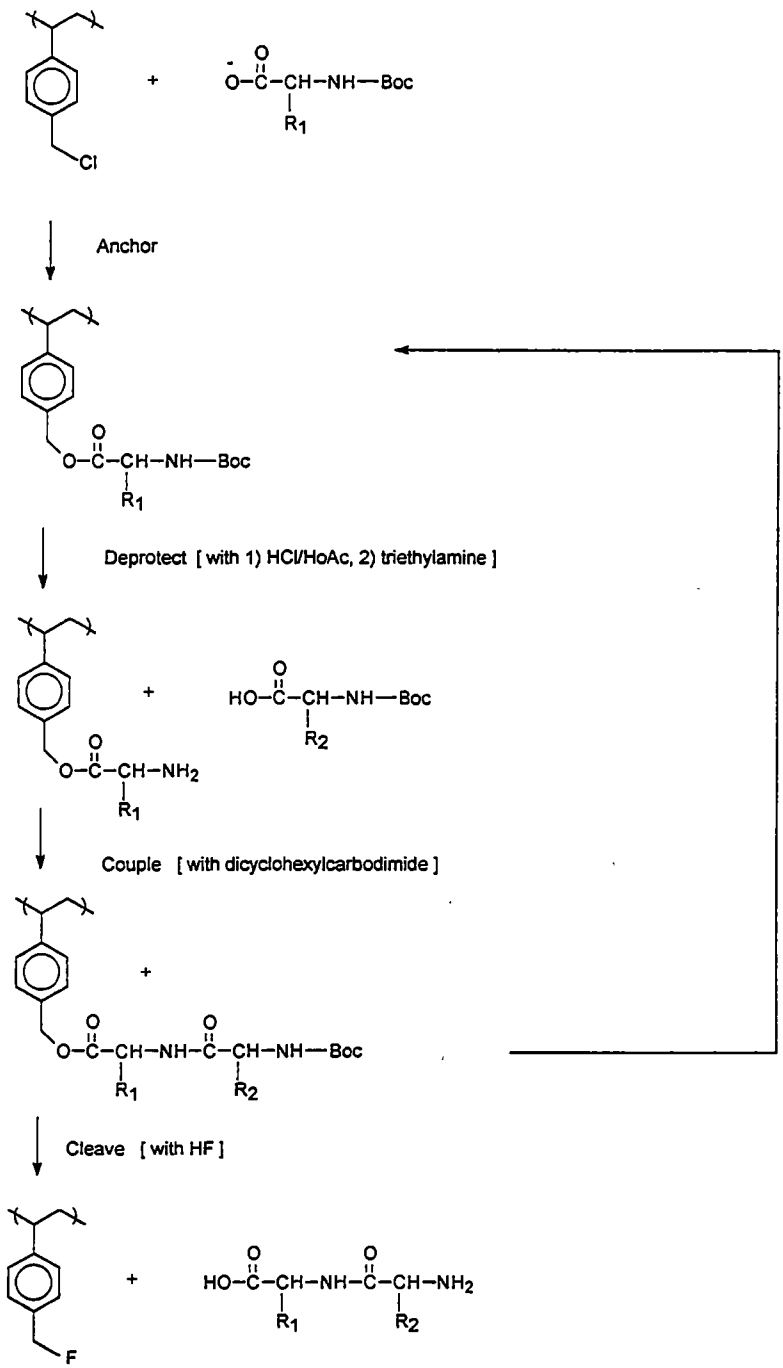


Figure 1.4. Solid-phase peptide synthesis

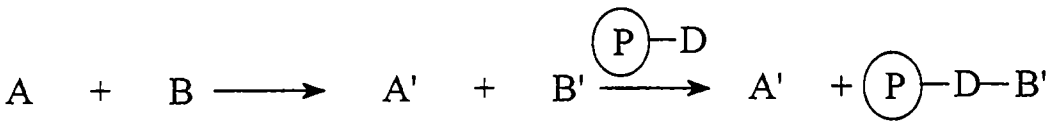
multi-step synthesis, and the development of a new field of chemistry know as combinatorial chemistry.[7-8]

The fourth, and newest, application of a polymer-supported reagent involves the isolation of a product from solution after an organic reaction has occurred. As outlined in Scheme 1 (Figure 1.5), after the reaction between compounds A and B, the desired product A' and byproduct B'are formed. The byproduct is then removed from the solution by adding a polymer-supported reactant that will covalently bond to the byproduct. Polymer-supported reactants used in this application are referred to as scavenger resins. A variety of scavenger resins are commercially available, and are characterized by the type of byproduct they will bond with.[9] Two examples of scavenger resins are: the isocyanate resin that will bond with nucleophiles like amines, alcohols, and alkoxides; and the trisamine resin that will react with electrophiles like acid chlorides, anhydrides, and isocyanates (Figure 1.5)

CHEMISTRY OF POLYMER-SUPPORTED REAGENTS

The organic chemistry of a polymer-supported reagent and its equivalent soluble reagent are not always identical. Polymer-supported reagents have been reported to exhibit enhanced or decreased kinetics, exhibit substrate selectivity, and produce different products when compared to their soluble analog.[10-13] Research has determined three unique properties of polymer-supported reagents that can explain these differences in reactivity: (1) reagent accessibility, (2) site-site interaction and (3) microenvironmental effects.[2]

Scheme 1



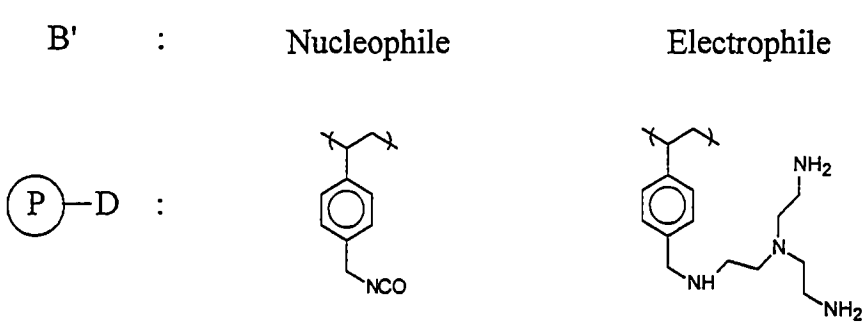
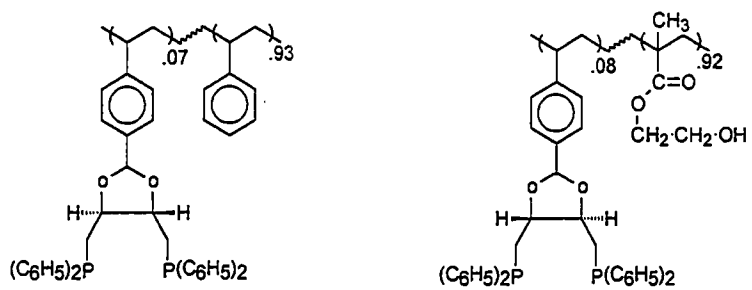


Figure 1.5. Scavenger resin

Reagent accessibility

Unlike a homogenous reaction, solvent and reactant molecules must diffuse into a polymer-supported reagent in order to react with the active site. If this diffusion process is impeded, then the rate limiting step of the polymer-supported reaction can be the accessibility of reagents. An example of this effect is the hydrogenation of asymmetric alkenes using a rhodium(I) supported catalyst (Figure 1.6). Kagan and coworkers[14] determined that rhodium(I) complex catalyst prepared from support **A** successfully hydrogenated α-acetamidoacrylic acid and α-phenylacrylic acid in benzene at 20°C. In an attempt to increase the percent enantiomeric excess, the reactions were repeated using a 1:5 benzene-ethanol mixture. Although no reaction occurred with support **A**, the results of the hydrogenation with support **B** were essentially identical to the reactions with the soluble catalyst. Kagan concluded that because support **A** could be swollen in benzene, but not in the benzene-ethanol mixture, the distance between the polymer chains of the 2% crosslinked gel beads were too close to allow reagents access to the catalyst. This limited accessibility in the mixed solvent was overcome by using the more hydrophilic support **B** which could be swollen by ethanol.

For polymer-supported applications where the solvent is incapable of solvating the polymer, macroporous resins have been used to maximize reagent accessibility. For example, a MR supported periodate ion-exchange resin has been successfully applied to the cleavage of 1,2-diols in water, ethanol, chloroform, diethyl ether, and benzene.[15] Although the increased porosity of the MR support improves reagent accessibility, the high crosslink level associated with these resins can result in steric hindrance around an



Support **A** Support **B**

Figure 1.6. Polymer-supports used to complex rhodium(I)

active site. Emerson and coworkers[16] demonstrated this in their study of a MR supported benzenesulfonylhydrazide used to synthesize hydrazones from aldehydes and ketones (Figure 1.7). Using a polymer-support containing 2.8 mmol g^{-1} of active sites, they determined acetone, 2-pentanone and cyclopentanone to react with 2.7, 1.9 and 1.8 mmol g^{-1} of the benzenesulfonylhydrazide respectively. When a polymer-support with 4.8 mmol g^{-1} of active sites was first treated with glucose to remove the more accessible ligands, cyclopentanone was determined to react with 0.4 mmol g^{-1} of active sites. Emerson concluded that approximately 1.0 mmol g^{-1} of the active sites are readily accessible in the MR bead, and the remaining active sites are located in less accessible, highly crosslinked regions.

Site-site interaction

Reagents can be immobilized onto a polymer-support to insure that the active sites are isolated and cannot interact. The potential of one active site to interact with another is influenced by the interchain distance, crosslink level, and the number of monomer units with a reactive functional group (also reported as percent functionalization).[2] For example, Grubbs and coworkers[17-18] have reported that the hydrogenation of 1-hexene with a 20% crosslinked macroporous polystyrene-supported titanocene was 25 times more active than the soluble catalyst (Figure 1.8). Because only dimeric titanium species were detected in the homogenous reaction, it was postulated that the higher activity of the polymer-support was due to permanent site isolation which enabled the existence of monomeric titanium species.

The ability to isolate an immobilized ligand was later supported by Hodge and

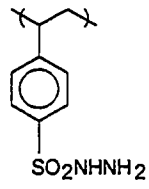


Figure 1.7. Polymer-supported benzenesulfonylhydrazide

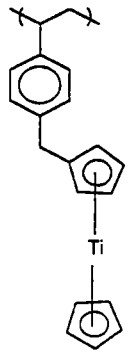


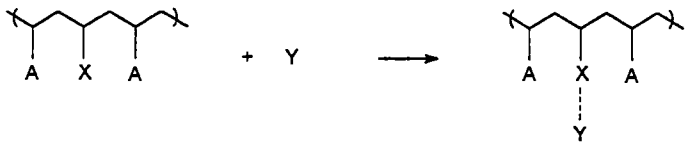
Figure 1.8. Polystyrene-supported titanocene

Khoshdel study of a polystyrene-supported phosphine used to synthesize ylides.[19] In their reaction of carbon tetrabromide with the polymer-support, the ylide could only be formed when two phosphine ligands were close enough to undergo a bimolecular nucleophilic substitution reaction. Ylides produced with a 1% crosslinked resin containing 2.5 mmol g^{-1} of phosphine determined at least 70% of the ligands reacted. When the percent crosslinking was increased to 2%, 8%, 15% and 37%, the number of phosphines able to react decreased to 47%, 14%, 2% and 0% respectively. This significant decrease in site-site interaction was attributed to an increase in the polymer rigidity as the crosslink level increased.

Microenvironmental effect

In organic synthesis applications, it was originally believed that the polymer-support onto which the ligand is immobilized was an inert spectator. However, research has determined that the structure of the polymer can significantly influence the chemical reaction. Unlike the homogenous reaction, interactions between the immobilized reagent and the polymer chain are enhanced due to the small volume they are confined to within the macromolecule.[2] As illustrated in Figure 1.9, the microenvironmental effect is defined as the influence of the polymer chain (A) on the interaction between the active site (X) and the reactant (Y).[20]

A clear example of the microenvironmental influence on reaction kinetics is the reaction of 1-octanol with carbon tetrachloride and triphenylphosphine.[21] The rate of the reaction with triphenylphosphine immobilized onto linear polystyrene was determined to be approximately twice as fast as the soluble phosphine. When the triphenylphosphine



X = Active site
A = Neighboring group
Y = Reactant

Figure 1.9. Microenvironmental effect

was immobilized onto a crosslinked polystyrene support, the reaction rate was determined to be approximately five times faster than the homogenous reaction. The increase in the reaction rate of the polymer-supports was attributed to local polar environment surrounding the active site. Because the rate limiting step of the reaction involves the formation of a phosphonium salt, a more polar environment would decrease the energy of activation and increase the reaction rate. The polarity around the active site was enhanced by decreasing the distance between the phosphine molecules through polymerization and crosslinking.

The structure of the polymer-support has also been reported to influence the reaction kinetics. Frechet and coworkers study of a crosslinked polystyrene-supported (dimethylamino)pyridine determined the catalyst activity to be significantly influenced by the polarity of the polymer backbone.[22-23] In the acetylation of 1-methylcyclohexanol with acetic anhydride, the catalytic activity of the polymer-support was optimized when the degree of functionalization was less than 50%. It was postulated that the decrease in polar monomer units of the copolymer produced a hydrophobic microenvironment which favored the rate limiting step of nucleophilic attack.

RESEARCH

Current research of polymer-supported reagents is being devoted to the design of versatile protecting groups, the development of novel applications, and optimizing reaction kinetics and product yields. Although the use of polymer-supported reagents has significantly grown in the last thirty years, research of the chemical factors that influence

these applications are limited. This dissertation focuses on investigating the structural influence of the polymer-support on reaction rates and product yields. First (Chapter 2), the microenvironmental influence on an S_N2 mechanism is evaluated by the Hammett correlation of aromatic substrates. By modifying the local environment of four different polymer-supported phenoxides used in the Williamson ether synthesis, the influence of three different microenvironments on the reaction transition state will be quantified for the first time. An established correlation between the microenvironmental effect and the S_N2 mechanism could provide important insight in the design of polymer-supported reagents. Next (Chapter 3), the product yield of a polymer-supported reaction is optimized by modifying the neighboring groups around the active site. The reaction rate and product yield of the Mitsunobu etherification reaction with triphenylphosphine and six different polymer-supported phosphines are reported. The influences of the microenvironment, crosslinking, solvent, and temperature are evaluated. Finally (Chapter 4), the influence of crosslinking on the ability of an ion-exchange resin to complex metal ions from a highly acidic solution is evaluated. Similar to the scavenger resin in organic synthesis applications, ion-exchange resins are used to remove metal ions from aqueous solutions. The percent complexation of Eu(III) by a series of phosphonic acid ion-exchange resins is used to evaluate the influence of the crosslink level, solution pH, structure of the active site, and bifunctionality. The concept of bifunctionality, along with the chemistry and application of ion-exchange resins, will be discussed in Chapter 4.

Chapter 2

THE STRUCTURAL INFLUENCE OF A POLYMER-SUPPORTED REAGENT ON THE KINETICS OF AN S_N2 DISPLACEMENT MECHANISM

INTRODUCTION

Over the past 30 years, polymer-supported reagents have developed from a novel organic synthesis technique to mainstream applications such as combinatorial chemistry,[7,8] micro scale synthesis,[24] and the automation of industrial scale synthesis[4]. This interest in polymer-supported reagent has also lead to a continuous growth of commercially available resins. Current research is being devoted to the design of new polymer-supported reagents, the development of new synthetic applications, and the improvement of current applications.

There are hundreds of examples of reactive polymers being used as reagents,[2] catalysts,[1] complexing agents,[25] and chromatography supports.[3] Although polymer-supported reagents are highly versatile, the reactivity and selectivity of the resin can be significantly limited by the physical and chemical structure of the polymer.[2] The relationship between the physical characteristics of the polymer-support and the reaction kinetics has been well documented, but little is known about how the chemical structure of the support influences the reaction kinetics.[26-28] If this correlation can be established, then polymer-supported reagents could be designed to maximize rates.

The objective of this research is provide a better understanding of the relationship

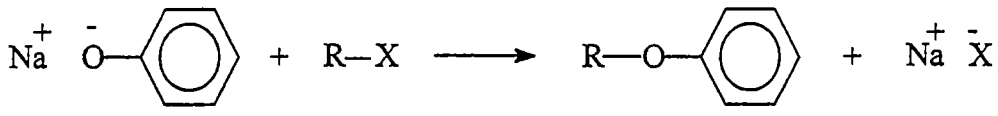
between the polymer matrix polarity and the reaction kinetics. Because many organic reactions involve an S_N2 displacement mechanism, a fundamental understanding of how the microenvironment can influence this mechanism would be extremely beneficial. An investigation of the Williamson ether synthesis using an anion-exchange resin will be used to evaluate this relationship. The Williamson ether synthesis has been applied to the synthesis of ethers[29], epoxides[30], water-soluble diarylsilanes[31], and polyethers[32]. By immobilizing a substituted phenoxide onto a polymer-support, the microenvironment influence on a single-step, S_N2 displacement mechanism will be investigated (Figures 2.1-2.3). A series of well defined polymer-supported phenoxides with varying microenvironments and differently substituted phenoxides will be synthesized (Figures 2.4 and 2.5). The reaction kinetics of these resins will be studied and the sensitivity of the transition state to changes in the phenoxide electron density will be evaluated by a Hammett correlation.[33]

The Hammett correlation is a well known empirical relationship used to correlate the substituent effects of meta- and para-substituted aromatic compounds with their reaction rates and equilibrium constants. The Hammett equation, equation 1, is derived from the ionization equilibrium of substituted benzoic acids. Written in this form, k_x and

$$\log (k_x / k_H) = \rho\sigma \qquad (1)$$

k_H are the equilibrium constant (or rate constant) for the substituted and unsubstituted aromatic compounds, σ is the substituent constant as defined by the standard reaction, and ρ is the reaction constant.

The benefit of the Hammett equation is that the sensitivity of the reaction to



X = Cl, Br, or I

Figure 2.1. Williamson ether synthesis

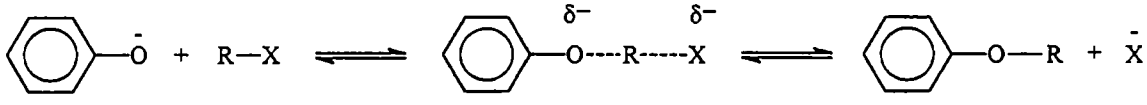


Figure 2.2. S_N2 Mechanism

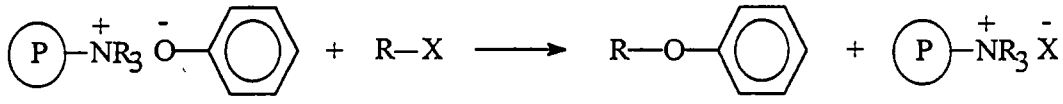
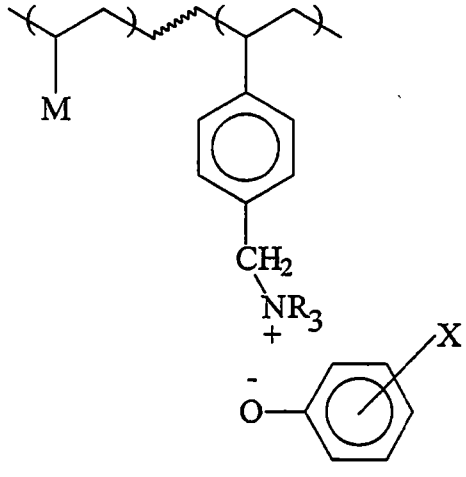


Figure 2.3. Application of an anion-exchange resin to the Williamson ether synthesis



M = Inert moiety that influences the microenvironment

X = Electron-withdrawing or donating substituent

Figure 2.4. Model polymer-supported phenoxide

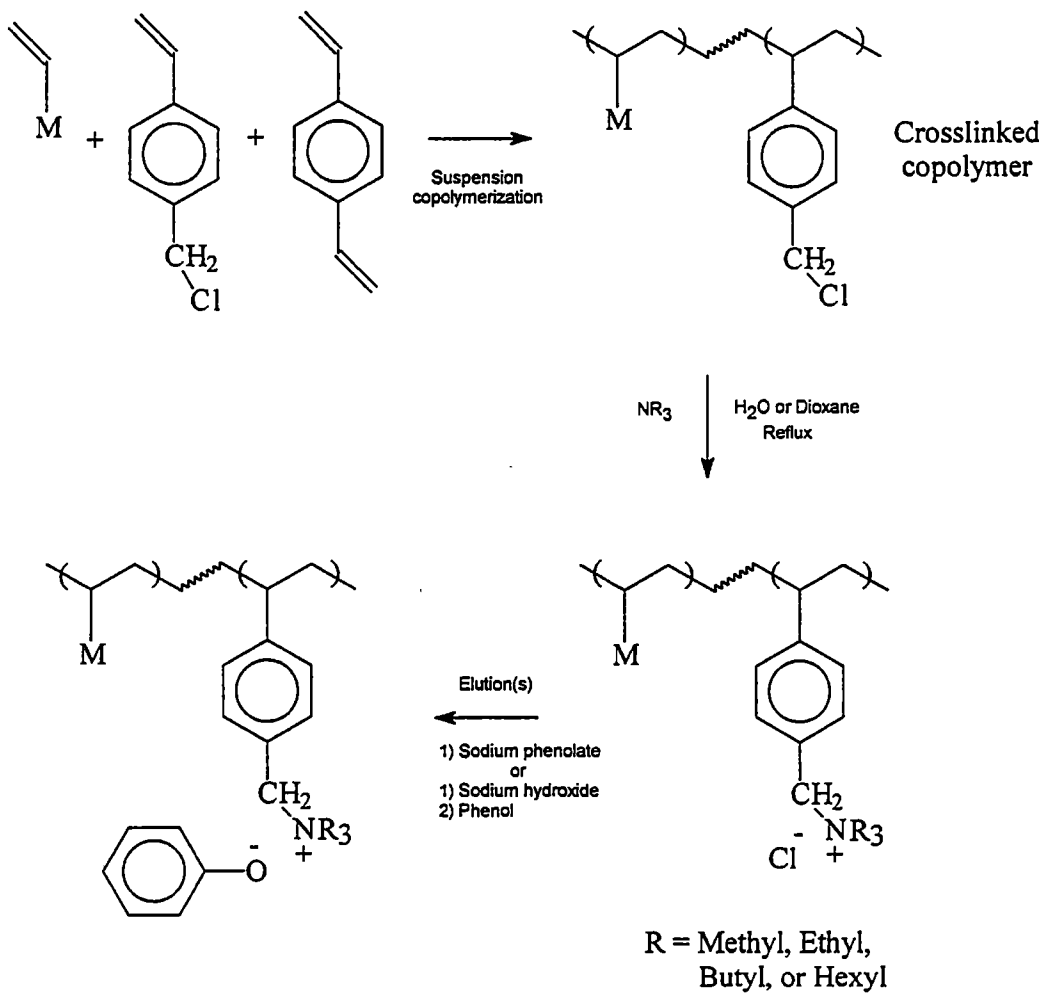


Figure 2.5. Synthesis of polymer-supported phenoxide

changes in aromatic substituents can be quantified by the ρ value. For example, the ionization of benzoic acid in water, methanol, and ethanol produced ρ values of 1.000, 1.537, and 1.957 respectively.[33] This phenomenon has be attributed to changes in the solvent polarity enhancing the substituent effect. The positive or negative value of the reaction constant also indicates the type of charge that develops in the transition state. In the example of benzoic acid ionization, the positive ρ value supports the fact that a negative charge formed at the acid site. The positive reaction constant also indicates that as the electron withdrawing effect of the substituent increases, the electron density at the reaction site will decrease, and the equilibrium constant for that substituted acid will increase. If a positive charge had formed at the reaction site, the resulting reaction constant would have been negative and the electronic effects would have been the opposite of the benzoic acid example.

The reaction constant in the Williamson ether synthesis will be determined for each polymer-support by plotting σ vs. log (k_x / k_H) where the slope of the line equals ρ. The value of ρ for the different polymer-supports will then be compared to evaluate the influence of the microenvironment on the reaction transition state.

EXPERIMENTAL

Synthesis of anion-exchange resins

Copolymer starting material was synthesized by the suspension copolymerization of vinylbenzyl chloride (VBC) and divinylbenzene (DVB). The porosity of the resulting insoluble beads was controlled by the monomer:diluent ratio used in the polymerization.

The polarity of the copolymer's microenvironment was adjusted by the addition of a third monomer to the copolymerization. Methyl methacrylate (MMA) and styrene (Sty) were used to change the polarity of the copolymer. The compositions of the various copolymers synthesized are summarized in Table 2.1. Copolymer materials were sieved using USA standard testing sieves, and only beads with a diameter between 0.15 to 0.25 mm were reacted with a tertiary amine to form the benzyltrialkylammonium chloride resin. The details of the anion-exchange resin synthesis are described in the Experimental section of this dissertation.

Synthesis of benzyltrialkylammonium phenoxide resins

The trialkylammonium chloride resin can be converted to an ammonium phenoxide resin by two different procedures.[34] In the one step method, the chloride form of the resin is packed into a column and eluted with a sodium phenoxide solution until all of the chloride ions have been replaced by phenoxide ions. In the two-step method, the chloride form of the resin is packed into a column as before, but is eluted first with a sodium hydroxide solution, and then with a solution of phenol. The details of converting the anion-exchange resin to the trialkylammonium phenoxide resin are described in the Experimental section of this dissertation.

Williamson ether reaction conditions

Small scale reactions were used to determine the suitable reaction conditions for the kinetic study. Alkyl halide was weighed into a 4 ml vial and diluted to 2 ml with toluene. The immobilized phenoxide resin was then added to the vial, a timer started, and the vial placed onto a wrist action shaker. A 1 μL sample of the mixture was analyzed at

Table 2.1
Composition of copolymer starting material

Copolymer	Support	Pore Size[a]	Precent DVB[b]	Mole Percent of Monomers[c]		
				VBC	Styrene	MMA
RB3-228	VBC	Gel	2	100	0	0
DQ6-254A	VBC	Gel	2	100	0	0
CS4-008	VBC	MR	5	100	0	0
CS4-052	VBC	MR	5	100	0	0
CS4-053	VBC	MR	5	100	0	0
CS4-187	VBC	MR	5	100	0	0
CS4-218	VBC	MR	5	100	0	0
CS5-062	VBC	MR	5	100	0	0
CS5-063	VBC	MR	5	100	0	0
CS4-009	VBC:Sty (18:82)	MR	5	18	82	0
CS4-009	VBC:Sty	MR	5	50	50	0
CS4-162	VBC:Sty	MR	5	50	50	0
CS5-018	VBC:Sty	MR	5	50	50	0
CS4-106	VBC:MMA	MR	5	50	0	50
CS4-161	VBC:MMA	MR	5	50	0	50
CS5-019	VBC:MMA	MR	5	50	0	50

[a] Gel resins contain micropores while MR resins contain macropores.

[b] The weight percent DVB, or divinylbenzene, indicates the amount of cross-linking agent.

[c] Mole percent of monomer repeating units excludes the cross-linking agent used.

timed intervals by GC.

Large scale reactions were used to accurately measure the initial reaction rate. The phenoxide resin (7.19 mmol) was weighed into a 100 ml 3-neck round bottom flask. A stir shaft, thermometer, septum, and 79.20 ml of toluene or ethanol was added to the flask. The solution was stirred at 150 rpm overnight to ensure swelling of the beads. The stir rate was increased to 353 rpm and the system heated to 75^{0}C using a water bath. Benzyl chloride (7.093 mmol, 0.80 ml) was then pipetted into the reaction, and a timer started. A 1 μL sample of the mixture was taken every 30 minutes for the first 5.5 h and the concentration of benzyl chloride determined by GC analysis.

A plot of benzyl chloride concentration (M) vs. time (seconds) was constructed for each reaction performed. The resulting curve was fit by a double or triple exponential decay equation with a regression greater than 0.99. The initial rate of the reaction was determined by calculating the derivative of the line equation at time zero. The details of the GC analysis and concentration calculations are provided in the Experimental section of this dissertation.

Characterization of ether products

Benzyl 4-methylphenyl ether ^{1}H NMR: δ 2.27(s, 3H), δ 5.04(s, 2H), δ 6.86 (d, 2H), δ 7.09 (d, 2H), δ 7.23-7.49(m, 5H). *Benzyl 3-nitrophenyl ether* ^{1}H NMR: δ 5.14(s, 2H), δ 7.24-7.46 (m, 7H), δ 7.83 (d, 2H). *Benzyl 4-nitrophenyl ether* ^{1}H NMR: δ 5.15(s, 2H), δ 7.02 (d, 2H), δ 7.26-7.45 (m, 5H), δ 8.21 (d, 2H). *Benzyl phenyl ether* ^{1}H NMR: δ 5.08(s, 2H), δ 6.94 (t, H), δ 6.98 (d, 2H), δ 7.22-7.46(m, 7H)

RESULTS

Characterization

Most polymers were characterized by nitrogen and chlorine elemental analysis. Ion-exchange resins containing m-nitrophenoxide or p-nitrophenoxide were characterized using a nitrophenoxide loading analysis technique. The details of these characterization techniques are described in the Experimental section of this dissertation.

The characterization of the anion-exchange resins, listed in Tables 2.2 and 2.3, showed that the degree of substitution varied with the type of amine and support used. Reactions with trimethylamine resulted in maximum percent functionalizations of 91% with VBC, 38% with VBC:Sty(18:82), 95% with VBC:Sty, and 94% with VBC:MMA. Reactions with trihexylamine resulted in maximum substitution of 65% with VBC and 19% with VBC:Sty(18:82). Tributylamine gave 75% substitution with the VBC support.

Because the phenoxide resins made by the two step method may retain hydroxide ions, a control was run to see if a trimethylammonium hydroxide resin (CS3-232) can react with benzyl chloride. It was found that the supported hydroxide does lead to a yield of 51% benzyl alcohol within 2 hours. In order to prevent this side reaction, the one step method was used to synthesize all phenoxide resins; their characterization is summarized in Tables 2.4-2.9. Conversion of the chloride to the substituted phenoxide ion was found to be influenced by the type of ammonium group immobilized on the resin. As the length of the trialkyl group increased from methyl to butyl to hexyl, the maximum percent conversion decreased from 100% to 32% to 0% when eluting with sodium para-nitrophenoxide. Because of the low degree of functionalization with the butyl and hexyl

Table 2.2
Characterization of benzyltrialkylammonium chloride resins[a]

Resin	Support	Pore Type	Trialkyl	Percent Solids	Nitrogen Capacity (mmol / g) [b]	Theoretical Capacity (mmol / g)	Percent Functionalization
CS3-220	VBC	Gel	Methyl	20.88	4.12	4.52	91.1
CS3-221	VBC	Gel	Hexyl	77.17	1.73	3.61	47.9
CS4-078	VBC	MR	Butyl	24.48	2.02	2.69	75.1
CS4-021	VBC	MR	Hexyl	31.38	1.49	2.28	65.3
Amberlite IRA-900	chloromethylated polystyrene	MR	Methyl	N/A	4.12	4.58	90.0
CS4-018	VBC:Sty (18:82)	MR	Methyl	27.21	0.50	1.33	37.6
CS4-019	VBC:Sty (18:82)	MR	Hexyl	21.54	0.20	1.04	19.2

[a] All resins except the Amberlite IRA-900 are beads between 150 and 250 μm in diameter.

[b] Nitrogen elemental analysis is accurate to +/- 0.2 mmol / g.

Table 2.3
Characterization of benzyltrimethylammonium chloride resins[a]

Resin	Support	Percent Solids	Nitrogen Capacity (mmol / g) [b]	Theoretical Capacity (mmol / g)	Percent Functionalization
CS4-020	VBC	19.47	3.54	4.37	81.0
CS4-060	VBC	19.98	3.60	4.37	82.4
CS4-061	VBC	20.07	3.69	4.37	84.4
CS4-195	VBC	35.58	3.64	4.37	83.3
CS4-243	VBC	22.39	3.78	4.37	86.5
CS5-021	VBC	24.39	3.76	4.37	86.0
CS5-068	VBC	24.55	3.63	4.37	83.1
CS5-069	VBC	23.25	3.83	4.37	87.6
CS4-177	VBC:Sty	15.94	2.68	2.92	91.8
CS5-023	VBC:Sty	35.28	2.76	2.92	94.5
CS4-109	VBC:MMA	24.60	2.39	2.94	81.3
CS4-176	VBC:MMA	25.19	2.33	2.94	79.2
CS5-028	VBC:MMA	35.28	2.76	2.94	93.9

[a] All resins are macroporous.

[b] Nitrogen elemental analysis is accurate to +/- 0.2 mmol / g.

Table 2.4
Characterization of benzyltrialkylammonium p-nitrophenoxide resins

Precursor Copolymer	Resin	Support	Pore Type	Trialkyl	p-Nitrophenoxide Capacity (mmol / g) [a]	Theoretical Capacity (mmol / g)	Percent Functional-ization
CS3-220	CS3-239	VBC	Gel	Methyl	2.02[b]	3.12	64.7
CS3-220	CS3-241	VBC	Gel	Methyl	2.16[b]	3.12	69.2
CS3-220	CS3-243	VBC	Gel	Methyl	2.28[b]	2.12	73.1
CS3-221	CS4-006	VBC	Gel	Hexyl	0.00	1.87	0.00
CS4-078	CS4-090	VBC	MR	Butyl	0.61	2.06	29.6
CS4-078	CS4-097	VBC	MR	Butyl	0.65	2.06	31.5
CS4-021	CS4-032	VBC	MR	Hexyl	0.01	1.00	0.01
N/A	CS3-259	IRA-900	MR	Methyl	2.71	2.88	94.1

[a] Nitrophenoxide loading analysis is accurate to +/- 0.03 mmol / g.

[b] The p-nitrophenoxide capacity was calculated from the nitrogen elemental analysis of this resin.

Table 2.5
Characterization of benzyltrimethylammonium p-nitrophenoxide resins

Precursor Copolymer	Resin	Support	p-Nitrophenoxide Capacity (mmol / g)[a]	Theoretical Capacity (mmol / g)	Percent Functional-ization
CS4-020	CS4-043	VBC	2.43	2.75	88.4
CS4-020	CS4-045	VBC	2.26	2.75	82.2
CS4-060	CS4-098	VBC	2.59	2.75	94.2
CS4-060	CS4-118	VBC	2.67	2.75	97.1
CS4-060	CS4-131	VBC	2.65	2.75	96.4
CS4-061	CS4-146	VBC	2.57	2.75	93.4
CS4-243	CS4-250	VBC	2.41	2.75	87.6
CS4-243	CS4-251	VBC	2.66	2.75	96.7
CS4-243	CS4-261	VBC	2.66	2.75	96.7
CS4-243	CS5-001	VBC	2.65	2.75	96.4
CS4-243	CS5-002	VBC	2.34	2.75	85.1
CS5-021	CS5-057	VBC	2.63	2.75	95.6
CS5-021	CS5-058	VBC	2.56	2.75	93.1
CS5-068	CS5-078	VBC	2.77	2.75	100
CS4-177	CS4-189	VBC:Sty	1.55	2.15	72.1
CS4-177	CS4-214	VBC:Sty	1.67	2.15	77.7
CS4-177	CS4-256	VBC:Sty	1.63	2.15	75.8
CS4-177	CS4-257	VBC:Sty	1.39	2.15	64.6
CS4-109	CS4-124	VBC:MMA	1.83	1.95	93.8
CS4-109	CS4-166	VBC:MMA	1.89	1.95	96.9
CS4-176	CS4-206	VBC:MMA	1.76	1.95	90.3
CS4-176	CS4-225	VBC:MMA	1.70	1.95	87.2
CS4-176	CS4-232	VBC:MMA	1.75	1.95	89.7
CS4-176	CS4-236	VBC:MMA	1.70	1.95	87.2
CS4-176	CS4-263	VBC:MMA	1.53	1.95	78.5
CS4-176	CS4-264	VBC:MMA	1.59	1.95	81.5

[a] Nitrophenoxide loading analysis is accurate to +/- 0.03 mmol / g.

Table 2.6
Characterization of benzyltrimethylammonium m-nitrophenoxide resins[a]

Precursor Copolymer	Resin	Support	m-Nitrophenoxide Capacity (mmol / g)[a]	Theoretical Capacity (mmol / g)	Percent Functional-ization
CS4-061	CS4-169	VBC	2.43	2.75	88.4
CS4-243	CS5-008	VBC	2.48	2.75	90.2
CS4-243	CS5-009	VBC	2.37	2.75	86.2
CS5-069	CS5-086	VBC	2.66	2.75	96.7
CS5-069	CS5-087	VBC	2.70	2.75	98.2
CS4-177	CS5-012	VBC:Sty	1.62	2.15	75.3
CS5-023	CS5-098	VBC:Sty	1.78	2.15	82.8
CS4-109	CS5-013	VBC:MMA	1.72	1.95	88.2
CS5-028	CS5-099	VBC:MMA	1.98	1.95	100

[a] Nitrophenoxide loading analysis is accurate to +/- 0.03 mmol / g.

Table 2.7
Characterization of benzyltrimethylammonium phenoxide resins

Precursor			Capacity (mmol / g)[a]				Percent
Copolymer	Resin	Support	Nitrogen Capacity	Theoretical Nitrogen	Chlorine Capacity	Theoretical Chlorine	Functional-ization[b]
CS4-060	CS4-105	VBC	2.99	3.14	0.26	0.49	95.2
CS4-061	CS4-133	VBC	2.97	3.14	-	0.49	94.6
CS4-243	CS5-024	VBC	3.10	3.14	1.68	0.49	98.7
CS5-021	CS5-032	VBC	2.96	3.14	0.44	0.49	94.3
CS5-068	CS5-075	VBC	2.84	3.14	0.47	0.49	90.4
CS5-068	CS5-076	VBC	3.07	3.14	0.33	0.49	97.8
CS5-068	CS5-077	VBC	2.99	3.14	0.35	0.49	95.2
CS5-069	CS5-105	VBC	2.97	3.14	0.35	0.49	94.6
CS5-023	CS5-033	VBC:Sty	2.24	2.38	0.39	0.16	94.1
CS5-023	CS5-106	VBC:Sty	2.28	2.38	0.35	0.16	95.8
CS4-109	CS4-167	VBC:MMA	2.04	2.14	-	0.42	95.3
CS5-028	CS5-034	VBC:MMA	2.20	2.14	0.56	0.42	100
CS5-028	CS5-107	VBC:MMA	2.24	2.14	0.35	0.42	100

[a] Nitrogen and chlorine elemental analyses are accurate to +/- 0.2 mmol / g.

[b] Percent functionalization is based on the nitrogen capacity.

Table 2.8
Characterization of benzyltrimethylammonium p-methylphenoxide resins

Precursor			Capacity (mmol / g)[a]				Percent
Copolymer	Resin	Support	Nitrogen Capacity	Theoretical Nitrogen	Chlorine Capacity	Theoretical Chlorine	Functional-ization[b]
CS4-060	CS4-104	VBC	2.67	2.87	0.29	0.45	93.0
CS4-061	CS4-139	VBC	2.81	2.87	-	0.45	97.9
CS5-021	CS5-035	VBC	2.52	2.87	0.41	0.45	87.8
CS5-021	CS5-054	VBC	2.96	2.87	-	0.45	100
CS5-021	CS5-055	VBC	2.80	2.87	0.35	0.45	97.6
CS5-021	CS5-056	VBC	2.68	2.87	0.33	0.45	93.4
CS5-069	CS5-091	VBC	2.77	2.87	-	0.45	96.5
CS5-069	CS5-092	VBC	2.72	2.87	0.36	0.45	94.8
CS5-023	CS5-036	VBC:Sty	2.12	2.22	0.35	0.15	95.5
CS5-023	CS5-093	VBC:Sty	1.85	2.22	0.32	0.15	83.3
CS4-109	CS4-191	VBC:MMA	1.86	2.01	-	0.39	92.5
CS5-028	CS5-037	VBC:MMA	2.16	2.01	0.49	0.39	100
CS5-028	CS5-094	VBC:MMA	2.15	2.01	0.32	0.39	100

[a] Nitrogen and chlorine elemental analyses are accurate to +/- 0.2 mmol / g.

[b] Percent functionalization is based on the nitrogen capacity.

Table 2.9
Characterization of benzyltrialkylammonium p-chlorophenoxide and p-methoxyphenoxide resins

Precursor Copolymer	Resin	Support	Trialkyl	para-Phenoxide	Nitrogen Capacity (mmol / g)[a]	Theoretical (mmol / g)	Percent Functionalization
CS4-060	CS4-108	VBC	Methyl	Cl	2.32	2.84	81.7
CS4-061	CS4-153	VBC	Methyl	Cl	3.19	2.84	100
CS4-195	CS4-200	VBC	Methyl	Cl	2.53	2.84	89.1
CS4-060	CS4-240	VBC	Methyl	Cl	2.87	2.84	100
CS4-061	CS4-242	VBC	Methyl	Cl	2.57	2.84	90.5
CS4-061	CS4-070	VBC	Methyl	OCH_3	2.36	3.01	78.4

[a] Nitrogen and chlorine elemental analyses are is accurate to +/- 0.2 mmol / g.

resins, neither of these resins was0 used in the kinetic studies.

Reaction conditions

To determine the reaction conditions needed to study the kinetics of the Williamson ether synthesis, a series of small scale reactions with the VBC supported benzyltrimethylammonium p-nitrophenoxide resin were performed in toluene (Table 2.10). The results found the reaction rate to be significantly influenced by the porosity of the resin. The initial four reactions with microporous beads found little or no reaction to occur within one day. This limitation was obviated by using macroporous resin.

The enhanced reactivity of benzyl bromide over benzyl chloride is demonstrated in comparing runs 04-004 and 04-005 of Table 2.10. The reactivity of benzyl bromide was ideal for establishing reaction conditions at room temperature. However, a small side product detected in the benzyl bromide reactions was identified as benzyl chloride. Two experimental controls determined that benzyl chloride can be formed by a halide exchange of chloride ions on a resin with benzyl bromide (Table 2.11). In order to prevent this side reaction from interfering with the synthesis of the ether, an aryl chloride must be used as the halide. The last set of small scale reactions, runs 04-005 through 04-095 in Table 2.10, were used to determined the ideal reaction concentrations to study the Williamson ether synthesis.

Preliminary reactions were used to evaluate the reactivity of six different phenoxides on the VBC supported benzyltrimethylammonium resin: p-nitrophenoxide, m-nitrophenoxide, p-chlorophenoxide, phenoxide, p-methylphenoxide, and p-methoxyphenoxide. Of these six, only the p-methoxyphenoxide resin was found to

Table 2.10
Reaction condition controls using benzyltrimethylammonium p-nitrophenoxide resins in toluene[a]

Run	Resin	Pore Type	RX	Conc. RX (M)	Phenoxide :RX Ratio	Temp. (°C)	Percent RX Conversion
03-256	CS3-243	Gel	BzCl	0.062	1 : 0.34	RT	0% @ 94 h
03-263	CS3-241	Gel	BzCl	0.071	1 : 0.38	RT	0 % @ 24 h
03-264	CS3-241	Gel	BzBr	0.098	1 : 0.52	RT	0% @ 22.5 h
03-267	CS3-241	Gel	CH_3I	0.087	1 : 0.43	RT	5% @ 16.5 h
04-001	CS3-259	MR	BzBr	0.068	1 : 0.37	RT	96% @ 23.5 h
04-002	CS3-259	MR	BzBr	0.58	1 : 3.1	RT	51% @ 24 h
04-004	CS3-259	MR	BzBr	0.26	1 : 2.0	RT	61% @ 25.3 h
04-005	CS3-259	MR	BzCl	0.25	1 : 2.0	RT	5% @ 20.1h
04-007	CS3-259	MR	BzCl	0.50	1 : 4.0	RT	6% @ 26h
04-042	CS3-259	MR	BzCl	0.50	1 : 5.0	RT	0% @ 25h
04-047	CS3-259	MR	BzCl	1.0	1 : 2.0	RT	19% @ 27h
04-050	CS3-259	MR	BzCl	1.5	1 : 3.0	RT	17% @ 22h
04-055	CS3-259	MR	BzCl	0.11	1 : 1.0	50	26% @ 20.6h
04-058	CS3-259	MR	BzCl	0.41	1 : 1.0	75	92% @ 25h
04-069	CS4-045	MR	BzCl	0.20	1 : 1.0	75	79% @ 23.5h
04-072	CS4-045	MR	BzCl	0.22	1 : 1.0	75	77% @ 23.5h
04-091	CS4-043	MR	BzCl	0.049	1 : 1.0	75	24% @ 22.7h
04-095	CS4-043	MR	BzCl	0.079	1 : 1.0	75	40% @ 20h

[a] All reaction were performed using the small scale reaction procedure.

Table 2.11
Side-reaction controls using benzyltrimethylammonium resins in toluene[a]

Run	Resin	Pore Size	Anion on Resin	RX	Conc. RX (M)	Resin:RX Ratio	Temp. (°C)	Product Detected[b]
03-235	CS3-232	Gel	$^-$OH	BzCl	2.10	1 : 3.0	50	BzOH
04-016	CS3-220	Gel	$^-$Cl	BzBr	0.25	1 : 2.2	RT	BzCl
04-010	Amberlite IRA-900	MR	$^-$Cl	BzBr	0.36	1 : 2.9	RT	BzCl

[a] All reaction were performed using the small scale reaction procedure.

[b] Products were identified by comparing the product's GC/FID retention time with a standard.

produce more than one product (Table 2.12). ^{1}H NMR analysis of the isolated product from the reactions with p-nitrophenoxide, m-nitrophenoxide, phenoxide, and p-methylphenoxide resins identified each product as the expected ether. No solvolysis or C-alkylated products were detected.

The reaction rate of the Williamson ether synthesis was monitored by measuring the decrease in benzyl chloride concentration during the course of the reaction. The initial kinetic studies at 75 °C with various substituted phenoxide supports showed the kinetics to be non-reproducible. As summarized in Tables 2.13 and 2.14 and Figures 2.6 and 2.7, reaction rates could not always be duplicated. When the reaction temperature was lowered from 75 to 65 °C, the standard deviation error of the determined initial reaction rate decreased from 93% to 2.1% with the VBC p-nitrophenoxide resin in toluene (Tables 2.13 and 2.15). All kinetic studies were performed at 65 °C to prevent evaporation of solvent and enable reproducibility. Differences in the reaction rate of the phenoxide resins were determined by monitoring the benzyl chloride concentration. Because the reaction equilibrium after 72 hours, the benzyl chloride concentration was monitored during the first 5.5 hours of the reaction for convenience.

Kinetic study

The reaction rates of twelve different resins were measured in duplicate (Figure 2.8). These twelve resins consisted of four different substituted phenoxides (p-nitrophenoxide, m-nitrophenoxide, phenoxide, and p-methylphenoxide) each immobilized on three different supports (VBC, VBC:Sty, and VBC:MMA). The VBC:Sty(18:82) support was not studied further because of volume of resin required

Table 2.12
Side reactions with benzyltrimethylammonium
p-methoxyphenoxide resins in toluene[a]

Run	Resin	Conc. BzBr (M)	Resin:BzBr Ratio	Temperature (°C)	Products Detected
04-064	CS4-033	0.4	1 : 1	75	5
04-092	CS4-070	0.4	1 : 2	75	5

[a] All reaction were performed using the small scale reaction procedure.

Table 2.13
Non-reproducible data using benzyltrimethylammonium p-nitrophenoxide resins in toluene

Run	Resin	Support	Initial Rate ($1x10^5$ $M \cdot s^{-1}$)	Percent BzCl Conversion[b]
04-136	CS4-118	VBC	0.108	20.3
04-144	CS4-131	VBC	0.160	20.7
04-148	CS4-146	VBC	0.200	22.0
04-186	CS4-146	VBC	0.692	-
04-194	CS4-189	VBC:Sty	1.46	62.8
04-196	CS4-189	VBC:Sty	0.650	56.9
04-217	CS4-214	VBC:Sty	0.507	50.2
04-221	CS4-214	VBC:Sty	0.527	50.7
04-175	CS4-166	VBC:MMA	1.28	75.4
04-178	CS4-166	VBC:MMA	1.37	76.2
04-209	CS4-206	VBC:MMA	1.44	60.9
04-212	CS4-166	VBC:MMA	1.36	-

[a] Reaction temperature was 75 °C.

[b] Percent conversion determined at 5.5 h into the reaction.

Table 2.14
Non-reproducible data using benzyltrimethylammonium [X]phenoxide resins in toluene[a]

Run	Resin	Support	X	Initial Rate ($1x10^5$ $M \cdot s^{-1}$)	Percent BzCl Conversion[b]
04-184	CS4-169	VBC	m-NO_2	2.34	64.3
04-150	CS4-133	VBC	p-H	2.02	-
04-152	CS4-133	VBC	p-H	2.22	50.7
04-165	CS4-153	VBC	p-Cl	4.19	50.9
04-168	CS4-153	VBC	p-Cl	3.36	45.1
04-213	CS4-200	VBC	p-Cl	3.69	64.0
04-222	CS4-200	VBC	p-Cl	2.17	51.2
04-157	CS4-139	VBC	p-CH_3	4.19	63.4
04-160	CS4-139	VBC	p-CH_3	3.36	59.3
04-188	CS4-167	VBC:MMA	p-H	13.3	81.1
04-190	CS4-167	VBC:MMA	p-H	14.7	80.7
04-202	CS4-191	VBC:MMA	p-CH_3	10.4	-
04-203	CS4-191	VBC:MMA	p-CH_3	11.3	80.0

[a] Reaction temperature was 75 °C.

[b] Percent conversion determined at 5.5 h into the reaction.

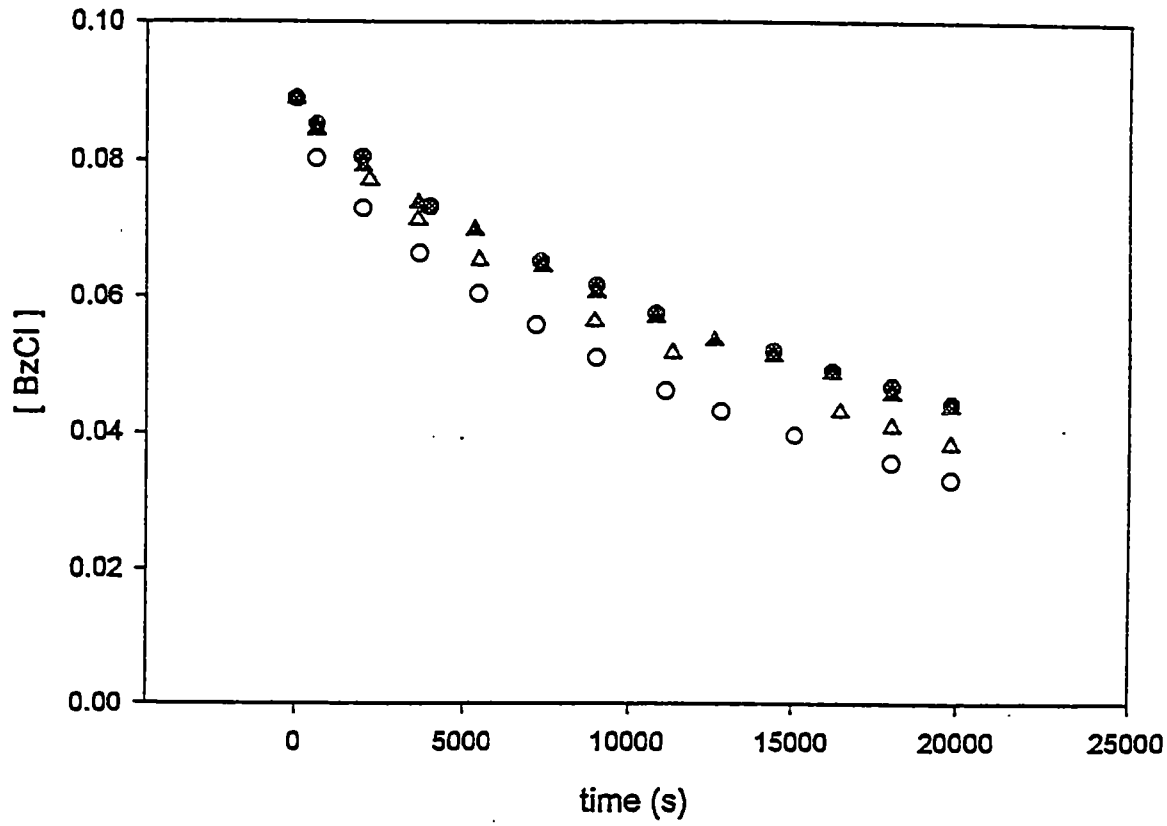


Figure 2.6. Non-reproducible data using VBC:Sty supported benzyltrimethylammonium p-Nitrophenoxide resins

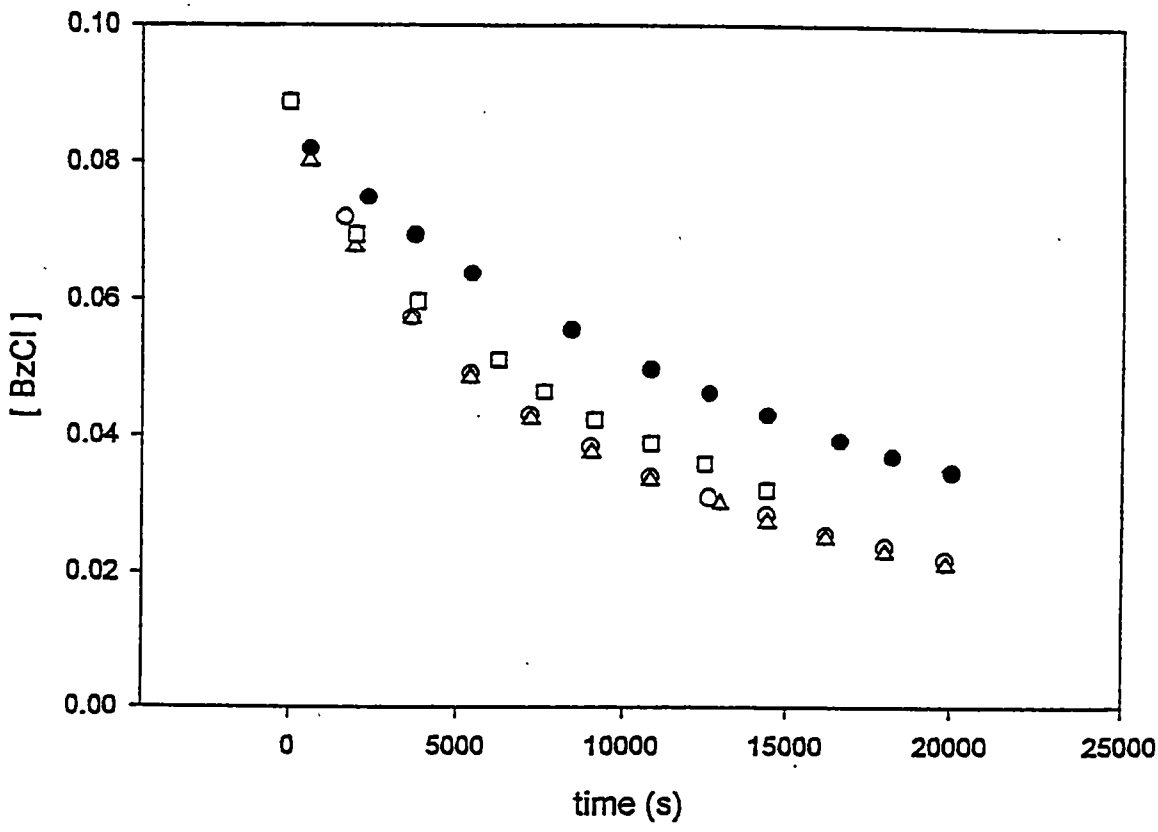


Figure 2.7. Non-reproducible data using VBC:MMA supported benzyltrimethylammonium p-Nitrophenoxide resins

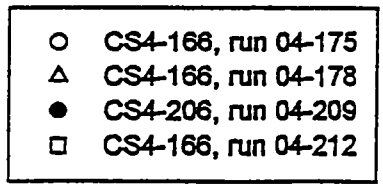
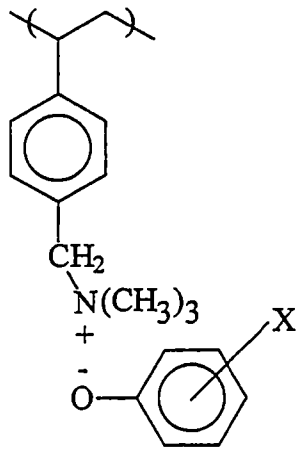


Table 2.15
Williamson ether synthesis using benzyltrimethylammonium p-nitrophenoxide resins[a]

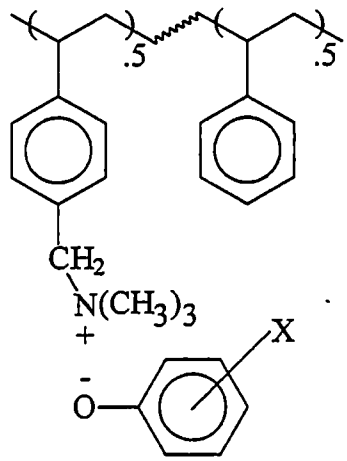
Run	Resin	Support	Solvent	Initial Rate ($1x10^5$ $M \cdot s^{-1}$)	Percent BzCl Conversion[b]
05-070	CS5-058	VBC	Toluene	0.0753	14.4
05-081	CS5-078	VBC	Toluene	0.0776	16.0
04-254	CS4-250	VBC	Ethanol	0.313	43.3
04-255	CS4-251	VBC	Ethanol	0.273	38.4
04-266	CS4-261	VBC	Ethanol	0.290	40.8
04-256	CS4-256	VBC:Sty	Ethanol	0.385	46.2
04-257	CS4-257	VBC:Sty	Ethanol	0.452	51.9
04-263	CS4-263	VBC:MMA	Ethanol	0.543	50.8
04-264	CS4-264	VBC:MMA	Ethanol	0.638	47.9

[a] Reaction temperature was 65 °C.

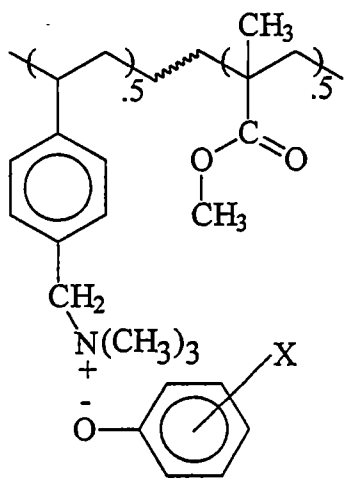
[b] Percent conversion determined at 5.5 h into the reaction.



VBC



VBC:Sty



VBC:MMA

X = p-NO_2, m-NO_2, H, or p-CH_3

Figure 2.8. Twelve phenoxide resins studied

exceeded the volume of solvent used. The influence of ion solvation on the reaction rate was studied by using either ethanol or toluene as the solvent.

The reaction rate and percent benzyl chloride conversion for each reaction are listed in Table 2.15 - 2.18. The average initial rates of the twelve resins are summarized in Table 2.19. An overview of these data reveals one common trend. Regardless of the support or solvent used, the rate of the reaction increases as the meta or para group of the substituted phenoxide becomes more electron-donating.

Table 2.15 - 2.18 compare the reaction rates of the three resins containing the same phenoxide. No trend was identified by comparing the VBC, VBC:Sty, and VBC:MMA supported reactions in ethanol. A comparison of the VBC reactions in ethanol and toluene found the ethanol reactions to be faster with strong electron-withdrawing substituents on the phenoxide. The VBC supported p-nitrophenoxide reaction in ethanol was an average of 3.8 times faster than the same reaction in toluene (Table 2.15). The VBC m-nitrophenoxide supported reaction was 1.7 times faster in ethanol than in toluene (Table 2.16). When the anion was changed to the phenoxide and p-methylphenoxide (Tables 2.17 and 2.18), the initial rate of the VBC reaction in ethanol was only 1.1 times faster than the toluene reaction.

To insure that accessibility of the reagents into the beads was not a rate limiting factor, several experimental controls were performed (Table 2.20 and Figure 2.9). The results of these controls determined no change in the reaction rate by increasing the stir speed or decreasing the bead size. Therefore benzyl chloride accessibility into the beads was not a rate limiting factor. The ability of the solvent to solvate the polymers was

Table 2.16
Williamson ether synthesis using benzyltrimethylammonium m-nitrophenoxide resins[a]

Run	Resin	Support	Solvent	Initial Rate ($1x10^5$ $M \cdot s^{-1}$)	Percent BzCl Conversion[b]
05-090	CS5-086	VBC	Toluene	0.902	58.2
05-095	CS5-087	VBC	Toluene	0.799	56.7
05-011	CS5-008	VBC	Ethanol	1.53	78.3
05-071	CS5-009	VBC	Ethanol	1.34	77.8
05-012	CS5-012	VBC:Sty	Ethanol	1.65	81.8
05-098	CS5-098	VBC:Sty	Ethanol	1.89	-
05-013	CS5-013	VBC:MMA	Ethanol	1.43	77.6
05-099	CS5-099	VBC:MMA	Ethanol	1.48	77.9

[a] Reaction temperature was 65 °C.

[b] Percent conversion determined at 5.5 h into the reaction.

Table 2.17
Williamson ether synthesis using benzyltrimethylammonium phenoxide resins[a]

Run	Resin	Support	Solvent	Initial Rate ($1x10^5$ $M \cdot s^{-1}$)	Percent BzCl Conversion[b]
05-100	CS5-076	VBC	Toluene	2.39	50.5
05-101	CS5-077	VBC	Toluene	2.00	-
05-032	CS5-032	VBC	Ethanol	2.50	78.2
05-117	CS5-105	VBC	Ethanol	2.32	-
05-047	CS5-033	VBC:Sty	Ethanol	2.29	77.1
05-119	CS5-106	VBC:Sty	Ethanol	2.53	-
05-050	CS5-034	VBC:MMA	Ethanol	2.20	74.6
05-120	CS5-107	VBC:MMA	Ethanol	2.48	-

[a] Reaction temperature was 65 °C.

[b] Percent conversion determined at 5.5 h into the reaction.

Table 2.18
Williamson ether synthesis using benzyltrimethylammonium p-methylphenoxide resins[a]

Run	Resin	Support	Solvent	Initial Rate ($1x10^5$ $M \cdot s^{-1}$)	Percent BzCl Conversion[b]
05-085	CS5-055	VBC	Toluene	2.42	49.3
05-111	CS5-092	VBC	Toluene	2.25	56.6
05-041	CS5-035	VBC	Ethanol	2.55	75.4
05-073	CS5-056	VBC	Ethanol	2.42	67.9
05-043	CS5-036	VBC:Sty	Ethanol	2.60	71.2
05-112	CS5-093	VBC:Sty	Ethanol	2.82	-
05-044	CS5-037	VBC:MMA	Ethanol	2.68	76.4
05-113	CS5-094	VBC:MMA	Ethanol	2.90	-

[a] Reaction temperature was 65 °C.

[b] Percent conversion determined at 5.5 h into the reaction.

Table 2.19
Williamson ether synthesis Hammett data

Support	Solvent	[X]phenoxide	Average Initial Rate ($1x10^5$ $M \cdot s^{-1}$)	log $[r_{i,x} / r_{i,H}]$	σ
VBC	Toluene	p-NO_2	**0.0765** +/- 0.0016	**-1.46** +/- 0.06	**1.27**
VBC	Toluene	m-NO_2	**0.851** +/- 0.073	**-0.412** +/- 0.06	**0.74**
VBC	Toluene	p-H	**2.20** +/- 0.27	**0** +/- 0.06	**0**
VBC	Toluene	p-CH_3	**2.34** +/- 0.12	**0.027** +/- 0.06	**-0.17**
VBC	Ethanol	p-NO_2	**0.292** +/- 0.020	**-0.916** +/- 0.04	**1.27**
VBC	Ethanol	m-NO_2	**1.43** +/- 0.13	**-0.225** +/- 0.04	**0.74**
VBC	Ethanol	p-H	**2.41** +/- 0.13	**0** +/- 0.04	**0**
VBC	Ethanol	p-CH_3	**2.49** +/- 0.09	**0.014** +/- 0.04	**-0.17**
VBC:Sty	Ethanol	p-NO_2	**0.419** +/- 0.049	**-0.760** +/- 0.05	**1.27**
VBC:Sty	Ethanol	m-NO_2	**1.77** +/- 0.17	**-0.133** +/- 0.05	**0.74**
VBC:Sty	Ethanol	p-H	**2.41** +/- 0.17	**0** +/- 0.05	**0**
VBC:Sty	Ethanol	p-CH_3	**2.71** +/- 0.16	**0.0508** +/- 0.05	**-0.17**
VBC:MMA	Ethanol	p-NO_2	**0.590** +/- 0.067	**-0.598** +/- 0.05	**1.27**
VBC:MMA	Ethanol	m-NO_2	**1.46** +/- 0.03	**-0.206** +/- 0.05	**0.74**
VBC:MMA	Ethanol	p-H	**2.34** +/- 0.20	**0** +/- 0.05	**0**
VBC:MMA	Ethanol	p-CH_3	**2.79** +/- 0.16	**0.0761** +/- 0.05	**-0.17**

Table 2.20
Accessibility controls with VBC supported benzyltrimethylammonium p-nitrophenoxide resins in ethanol

Run	Resin	Bead Size (mm)	Stir Speed (RPM)	Initial Rate ($1x10^5$ $M \cdot s^{-1}$)	Percent BzCl Conversion[b]
04-254 04-255 04-266	CS4-250 CS4-251 CS4-261	0.15-0.25	352	**0.292**[c] +/- 0.020	**40.8**[c] +/- 2.5
05-004	CS5-001	0.15-0.25	651	0.297	40.7
05-007	CS5-002	<< 0.15[d]	352	0.301	43.4

[a] Reaction temperature was 75 °C.

[b] Percent conversion determined at 5.5 h into the reaction.

[c] Average value of three reactions.

[d] Resin was crushed into a powder with a mortar and pestle.

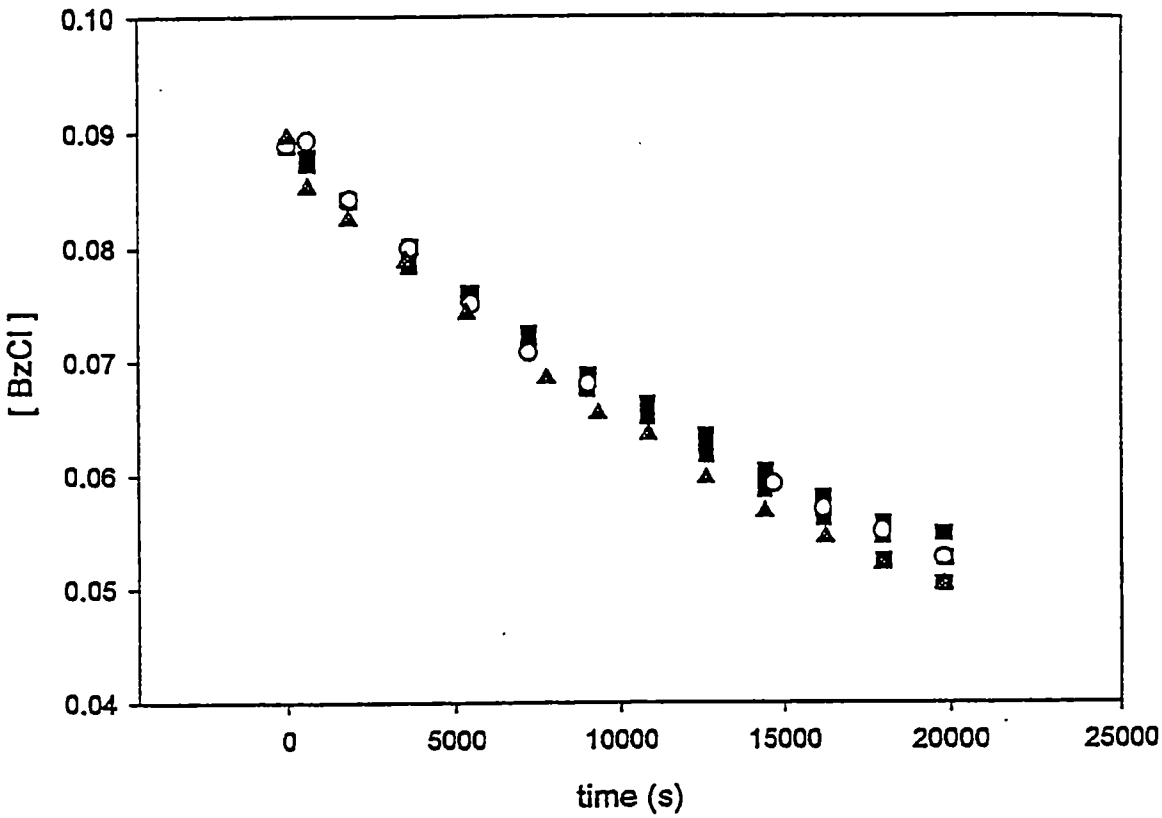
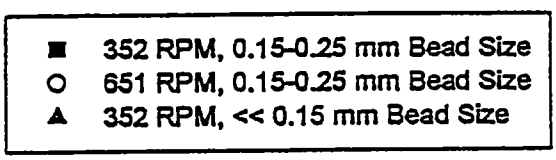


Figure 2. 9. Accessibility Controls with VBC p-Nitrophenoxide in Ethanol at 65°C



measured and found toluene unable to swell the VBC resins (Table 2.21). Ethanol was able to swell the VBC:Sty and VBC:MMA resins more than the VBC resins.

Hammett analysis

Using the Hammett equation, $\log (k_X / k_H) = \rho\sigma$, the influence of the nucleophile electron density on a reaction mechanism can be evaluated. An ideal Hammett study of the Williamson ether synthesis would entail determining the rate constant for each substituted phenoxide reaction. Because the polymer-supported reaction is a heterogenous mixture, the rate constant could not be determined by a simple second order rate equation (2) which is based on a homogenous system.[35-39] An attempt was made

$$\text{rate} = k\,[\text{Resin}]^a\,[\text{BzCl}]^b \qquad (2)$$

to determine the pseudo-first order rate constant where the "concentration" of the

$$\text{rate} = k^{\Psi}\,[\text{BzCl}]^b \qquad (3)$$

$$\text{when } k^{\Psi} = k\,[\text{Resin}]^a$$

substituted phenoxide resin is held constant during the course of the reaction (3). Unfortunately, the required 100:1 ratio of phenoxide to benzyl chloride resulted in reagent concentrations that were below the detection limits of the GC.

Although a rate constant for the polymer-supported reaction could not be determined, the (k_X / k_H) ratio was calculated from the initial rate values as described in Figure 2.10. The initial rate ratio, $(r_{i,X} / r_{i,H})$, for each resin is reported in Table 2.19. Figure 2.11 is the Hammett plot for the VBC support in ethanol and toluene. Both reaction conditions produce non-linear Hammett correlations. The toluene reaction

Table 2.21
Swelling ratios of [X]phenoxide resins

			Swelling Ratio	
Resin	**Support**	**X**	**Ethanol**	**Toluene**
CS5-058	VBC	p-NO_2	1.3	1.0
CS5-086	VBC	m-NO_2	1.5	1.0
CS5-032	VBC	p-H	1.5	1.1
CS5-035	VBC	p-CH_3	1.4	1.0
CS4-256	VBC:Sty	p-NO_2	1.7	-
CS5-098	VBC:Sty	m-NO_2	1.7	-
CS5-033	VBC:Sty	p-H	2.0	-
CS5-036	VBC:Sty	p-CH_3	1.8	-
CS4-263	VBC:MMA	p-NO_2	2.0	-
CS5-099	VBC:MMA	m-NO_2	1.9	-
CS5-034	VBC:MMA	p-H	1.8	-
CS5-037	VBC:MMA	p-CH_3	1.7	-

Reaction rate equation: $$\text{Rate} = k\,[\text{Resin}]^a\,[\text{BzCl}]^b \quad (1)$$

At t = 0 : $$\text{Initial Rate} = k\,[\text{Resin}]_o^a\,[\text{BzCl}]_o^b \quad (2)$$

Define r_i : $$r_i = k\,[\text{Resin}]_o^a\,[\text{BzCl}]_o^b \quad (3)$$

For [X]phenoxide: $$r_{i,x} = k_x\,[\text{Resin}]_{o,x}^a\,[\text{BzCl}]_{o,x}^b \quad (4)$$

Rate ratio with x = H for $r_{i,H}$: $$\frac{r_{i,x}}{r_{i,H}} = \frac{k_x\,[\text{Resin}]_{o,x}^a\,[\text{BzCl}]_{o,x}^b}{k_H\,[\text{Resin}]_{o,H}^a\,[\text{BzCl}]_{o,H}^b} \quad (5)$$

If $[\text{Resin}]_{o,x} = [\text{Resin}]_{o,H}$ and $[\text{BzCl}]_{o,x} = [\text{BzCl}]_{o,H}$, then: $$\frac{r_{i,x}}{r_{i,H}} = \frac{k_x}{k_H} \quad (6)$$

Hammett equation: $$\log (k_x / k_H) = \rho\sigma \quad (7)$$

Combine equations 6 and 7 : $$\log (r_{i,x} / r_{i,H}) = \rho\sigma \quad (8)$$

Figure 2.10. Calculating the Hammett rate constant ratio from the initial rate data

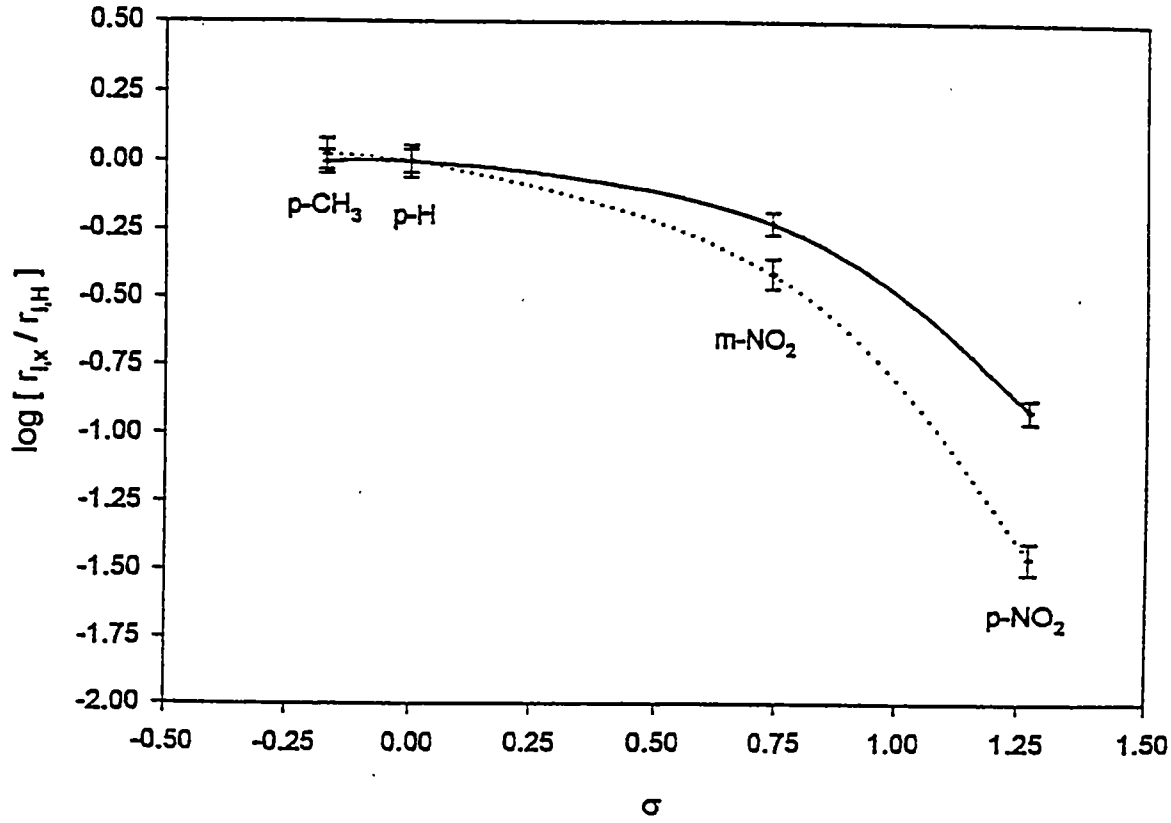


Figure 2.11 Hammett Plot of VBC Support in Ethanol at 65°C

clearly exhibits a larger negative slope than the ethanol reaction. This non-linear Hammett correlation also exists with the VBC:Sty and the VBC:MMA supports (Figure 2.12 and 2.13). A comparison of the VBC, VBC:Sty, and VBC:MMA reactions in ethanol finds overlap between sigma -0.17 and 0.74 of the Hammett plot (Figure 2.14). This overlap then separates as it approaches sigma 1.27. In this strong electron withdrawing region of the plot, the slope of the line becomes less negative as the support changes from VBC to VBC:Sty to VBC:MMA.

DISCUSSION

Non-linear Hammett correlations

An investigation of the Williamson ether synthesis with a polymer-supported benzyltrimethylammonium phenoxide showed that the reaction followed a non-linear Hammett correlation regardless of solvent or polymer structure. As predicted by the Hammett equation previously discussed, the negative slope of the Hammett plots indicate the reaction rate is decreased when the electron density at the phenoxide oxygen is depleted by the ring substituents. Hammett studies of substituted phenoxides in the Williamson ether synthesis have been studied by a number of authors. Reactions in water,[35] methanol,[36] ethanol,[37] 50% aqueous acetone,[38] and nitrobenzene:DMF (60:40)[39] were found to produce negative ρ values. This is interesting because regardless of substituted phenoxide, halide, temperature, and alkali cation, all of these reported reactions produced a linear Hammett relationship.

Reactions which exhibit concave downward Hammett plots have been reported

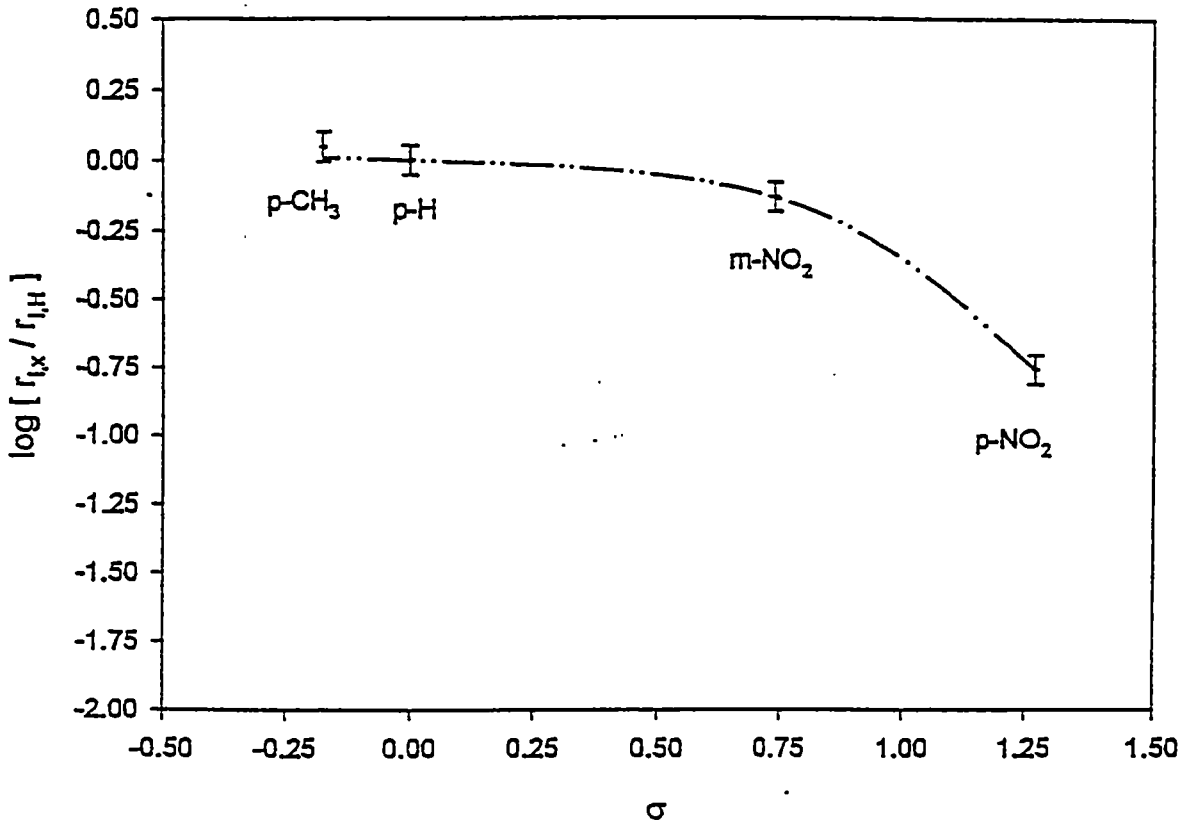


Figure 2.12. Hammett Plot of VBC:Sty Support in Ethanol at 65°C

VBC:Sty Support

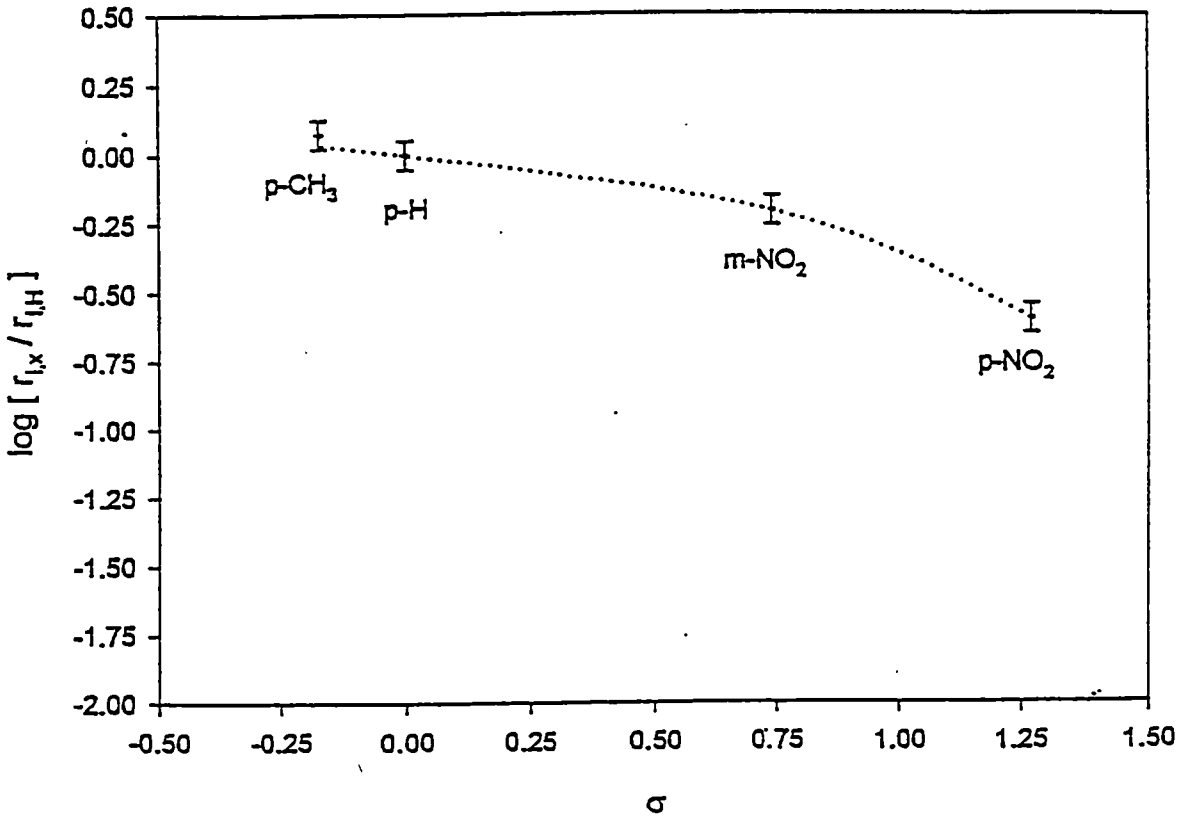


Figure 2.13. Hammett Plot of VBC:MMA Support in Ethanol at 65°C

VBC:MMA Support

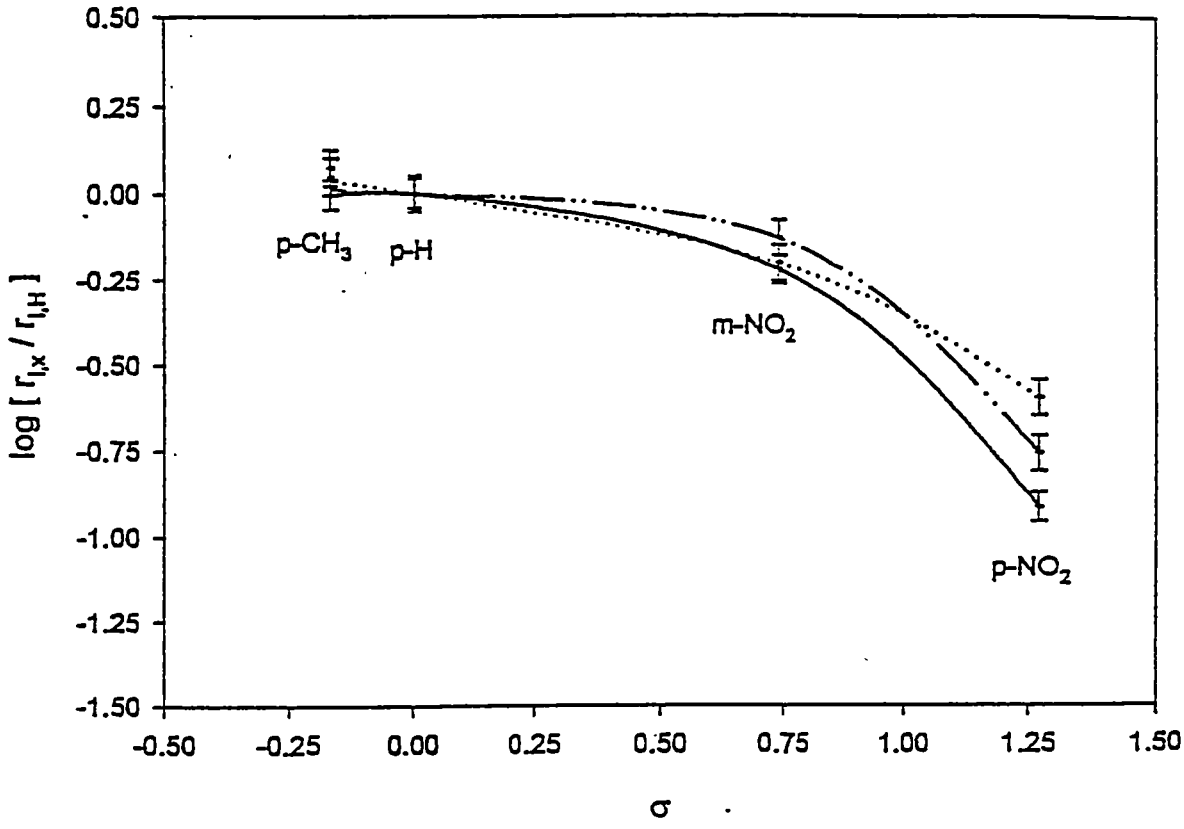


Figure 2.14. Hammett Plot of VBC, VBC:Sty, and VBC:MMA Supports in Ethanol at 65°C

and are well documented in the literature.[40] These non-linear Hammett correlations have been observed in the acid hydrolysis of substituted amides,[41] the decomposition of benzenediazonium salts,[42] and the hydrolysis of Schiff bases[43] to name a few. As in each of these examples, Hammett plots that concave downward are generally due to a change in the rate determining step caused by the ring substituent. For example, Anderson and Jencks concluded that the non-linear correlation of aromatic semicarbazone formation from substituted benzaldehydes was due to a shift in the rate limiting step from the addition to the dehydration step.[44]

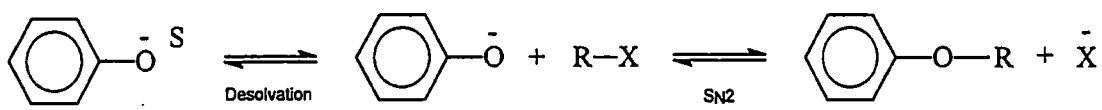
It is important to mention that a change in the reaction mechanism can also result in a non-linear Hammett correlation. However, these Hammett plots tend to form curves that concave upward.[40] If a change in the reaction mechanism of the Williamson ether synthesis was possible, then a product other than the expected ether should have been detected. Because solvolysis and carbon alkylated products have been reported in the Williamson ether synthesis,[29] the reaction products were isolated to identify their chemical structure. The results of this analysis found only the benzyl phenyl ether produced in the four different etherifications studied.

If the non-linear Hammett correlation of the Williamson ether synthesis is not due to a change in the reaction mechanism, then it must be due to a change in the rate limiting step. This is intriguing since the reaction mechanism only involves a single-step nucleophilic displacement as represented in Figure 2.2.[29] A change in the rate limiting step would require an additional reaction step before or after the S_N2 displacement transition state. This type of unexpected phenomena has been reported in mechanistic

studies of aqueous transesterification reactions. Several authors have reported that the nucleophilic reactivity of alkoxides is different than phenoxides in the transesterification of carboxylic esters.[45-51] Although the two types of nucleophiles followed a linear correlation separately, the slopes of the two regions do not agree. Most importantly, the larger slope of the phenoxide region indicates that the alkoxides should be more reactive than experimentally determined. Jencks and coworkers were the first to theorize that this reduced reactivity of the alkoxides is due to an additional rate limiting process that does not influence the phenoxides.[52] Because the electron density of the oxygen anion is more localized on the alkoxide, Jencks theorized that the energy of ion solvation is greater than the solvation of the delocalized phenoxide anion. This theory was later supported by the a comparison of alkoxide and phenoxide basicity in the gas phase and water.[53] Thus, because of a larger energy of desolvation with the alkoxide anion, the rate limiting step of the alkoxide reactions could be the desolvation of the anion instead of the addition-elimination process.

Jencks theory of ion desolvation as a potential rate limiting process still influences the theories of ionic mechanisms today.[54] It is plausible that a desolvation process could occur before nucleophilic attack in the Williamson ether synthesis, and that the non-linear correlation could be due to a change in the rate limiting step from nucleophilic attack to the desolvation process of the anion (Figure 2.15). However, all of the Williamson ether Hammett studies in the literature exhibit linear correlations and do not support this theory.

The non-linear correlation of VBC reaction in toluene suggests the presence of



S = Solvent molecule(s)

Figure 2.15. Desolvation vs. S_N2 rate limiting step

contact ion pair formation in this non-polar solvent. Whenever a salt is dissolved, an equilibrium between the dissociated ions and contact ion pairs is established. Dissociated ions are formed when the anion and cation are separated by a solvent cage around each ion, while contact ion pairs are the result of direct contact between the anion and cation. The dissociation constants of phenoxides in a wide range of polar aprotic solvents have been studied. The ionization constants for tetramethylammonium picrate in ethylene dichloride ($\epsilon = 10.23$), acetone ($\epsilon = 20.47$) and nitrobenzene ($\epsilon = 34.5$) are 0.32×10^{-4}, 112.0×10^{-4}, and 400×10^{-4} at 25 °C.[55] None of the polar solvents enabled significant dissociation of this highly delocalized phenoxide. The trend proves that the dissociation of tetramethylammonium picrate decreased as the dielectric constant (ϵ) of the solvent decreased. Because the dielectric constant of toluene is 2.379 at 25 °C,[56] the trend predicts that ionization constant for toluene will be significantly less than that of ethylene dichloride. Therefore, the dissociation equilibrium of the VBC supported phenoxides in toluene favors contact ion pair formation.

The Hammett relationship between the dissociation constants of phenoxides and ring substituents has been reported. Szczecinski's study of 5-substituted sodium 2-methylphenoxides in DMSO found the dimerization constants to exhibit a linear Hammett correlation, while the dissociation constants produced a non-linear curve.[57] Szczecinski concluded that the strong curvature between sigma values 0.0 and 0.3 was due to a significant shift in the ionization equilibrium. We propose that the non-linear Hammett correlation of the VBC supported reaction in toluene is due to the same shift in the equilibrium between contact ion pairs and solvent separated ion pairs. Szczecinski's

results predict that for phenoxides with electron donating substituents, $\sigma > 0.0$, the rate limiting step would be ion pair dissociation, and phenoxides with strong electron withdrawing substituents, $\sigma > 0.3$, the rate limiting step is nucleophilic attack (Figure 2.16). It is not clear if the polymer-supported Hammett data consist of a concave curve or two linear lines. Attempts to add more data points to the Hammett plots were not possible due to synthetic or experimental limitations with p-methoxyphenoxide, p-chlorophenoxide, p-cyanophenoxide and p-formylphenoxide.

Although the Hammett correlations of the polymer-supported phenoxide reactions in ethanol are non-linear, contact ion pair formation was not expected in this hydrogen bonding solvent. Because polar protic solvents readily solvate anions and cations, the ionization equilibrium is often shifted to favor dissociation. This shift is due to the ability of the solvent to solvate the anion through hydrogen bonding, and to solvate the cations through complexation with the solvent's lone pair electrons.[58] For example, the pKa of phenol in water and DMSO are 10.0 and 18.0 respectively. The degree of phenol dissociation in DMSO is lower due to the polar aprotic solvent's inability to hydrogen bond with the anion.[59]

The dissociation equilibrium of the trialkylammonium phenoxide is also influenced by the ionic strength of the solution. As the concentration of the salt is increased, the number of collisions between the anion and cation is increased, and the dissociation equilibrium is shifted to contact ion pair formation. Newton and Arcand demonstrated this in their study of aqueous cerous sulfate solutions.[60] When the ionic strength of the solution was increased from 0.2 to 2.0 M, the concentration of solvated

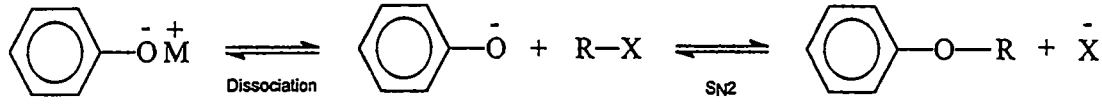


Figure 2.16. Dissociation vs. S_N2 rate limiting step

cerous ions decreased in conjunction with an increase in the concentration of cerous sulfate contact ion pairs.

We theorize that with the polymer-supported phenoxide and p-methylphenoxide in ethanol, an equilibrium shift to contact ion pair formation has occurred due to a localized concentration effect. Because the ammonium phenoxides are confined to a small volume by the polymer backbone, the resulting ionic matrix resembles that of a highly concentrated salt solution. This localized concentration effect of polymer-supported reagents has been reported by a number of authors.[61-63] For example, Ancillotti and coworkers have reported that a macroporous sulfonic acid resin exhibits a higher reactivity than p-toluenesulfonic acid in the addition of alcohols to tertiary olefins.[64] They attribute this enhanced kinetics to the high concentration of sulfonic acid groups inside the polymer bead. In a recent review of polymer-supported reagents, Hodge stated that for a highly crosslinked macroporous support with a loading of 0.5 mmol g^{-1}, the concentration of reactive sites can equal or exceed 1.0 M.[65] The minimum loading of VBC, VBC:Sty, and VBC:MMA supports were 2.4, 1.4, and 1.5 mmol g^{-1}.

Microenvironment effect

The variation in the initial rates with the supported p-nitrophenoxide in ethanol shows that the polarity of the local environment can influence the rate limiting step of nucleophilic attack. The VBC and VBC:Sty both contain the benzyltrimethylammonium p-nitrophenoxide repeating unit, but the VBC resin is fully functionalized while the VBC:Sty is less polar and 50% of the backbone contains reactive sites. By comparing the VBC and VBC:Sty supports, the results indicate that the reaction rate increased by a

factor of 1.4 due to a less polar matrix. This result can be explained by the Hughes-Ingold theory of solvent effects.[66] Because the transition state is less polar than the reactants due to charge dispersal, a more polar environment will lower the reactant free energy, increase activation energy of the reaction, and thus decrease the reaction rate. Panigrahi and Sinha came to the same conclusion in their kinetic study of the reaction between sodium phenoxide and allyl chloride in various solvents.[39] By comparing the second order rate constant of the reactions in methanol ($\epsilon = 32.6$) and ethanol ($\epsilon = 24.3$), they found the reaction rate to increase by a factor of 2.9 as the dielectric constant decreased.

The matrix of the VBC:Sty and VBC:MMA supported p-nitrophenoxide is similar in the fact that 50% of the polymer repeating units contain reactive sites. The remaining monomer units are either styrene or methyl methacrylate as described by the resin name. Because methyl methacrylate is polar and styrene is non-polar, the VBC:MMA polymer matrix is more polar than VBC:Sty. Therefore, the reaction rate of the p-nitrophenoxide polymers was expected to follow the trend VBC < VBC:MMA < VBC:Sty as predicted by the theory of solvent effects. Although the VBC:MMA reaction was 2 times faster than the VBC reaction, the VBC:MMA reaction was also 1.4 times faster than VBC:Sty. This deviation from the Hughes-Ingold theory could be due solvation of the anion by the methyl methacrylate portion of the polymer. Because the anion can be solvated by the methyl methacrylate moiety through an ion-dipole interaction, the energy of desolvation will be less than the anion solvated by ethanol through hydrogen bonding. Panigrahi and Sinha have reported that the phenoxide anions are more reactive in polar aprotic solvent

than in polar protic solvents.[39] They found the reaction between sodium phenoxide and allyl chloride in DMF ($\epsilon = 36.7$) to be 654 times faster than the same reaction in methanol ($\epsilon = 32.6$). Their conclusion was the same as ours, that the phenoxide reactivity is increased when the degree of anion solvation through hydrogen bonding is decreased.

The initial rates of the supported p-methylphenoxide and phenoxide in ethanol were not influenced by the polarity of polymer-support. These results establish that the microenvironment had no influence on the rate limiting step of ion pair dissociation with contact ion pairs.

CONCLUSION

A Hammett study of a polymer-supported benzyltrimethylammonium phenoxide, used in the Williamson ether synthesis, discovered a change in the rate limiting step to occur between sigma -0.17 and 1.27. It is proposed that a change in the rate limiting step from ion-pair dissociation to nucleophilic attack could result from the increased delocalization of the phenoxide electron density. Variations in the polymer microenvironment did not alter the rate of ion-pair dissociation, but did influence the activation energy of nucleophilic attack. These results suggest that the polarity of the localized environment can be tailored to enhance the reaction kinetics.

Chapter 3

THE APPLICATION OF POLYMER-SUPPORTED PHOSPHINE RESINS IN THE MITSUNOBU ETHERIFICATION REACTION

INTRODUCTION

Since its discovery in 1967, the Mitsunobu reaction has become a versatile method to alkylate carboxylic acids,[67-68] phenols,[69-70] phosphoric esters,[71] imides,[72-73] and cyano-compounds.[74] The clean stereochemical inversion and mild reaction conditions have made this reaction useful in the synthesis of multi-functional natural products[75] and combinatorial applications.[76-78] Examples of how this reaction enables the coupling of an alcohol and an acidic reagent are illustrated in Figures 3.1 and 3.2.

One limitation of the Mitsunobu reaction is that the acid must be highly acidic for satisfactory alkylation to occur. The product yield is significantly decreased when the pKa of the acid is between 11 and 13.[79] With these weaker acids, competition between the acid and alcohol for deprotonation by the phosphine-DEAD adduct may occur. If the alcohol is deprotonated first, then the Mitsunobu reaction is believed to proceed through a second mechanism to form an alkylated hydrazine and possibly other byproducts (Figures 3.3 and 3.4) Several attempts have been made to improve the yield when working in this pKa region. Research into new Mitsunobu reagents has found tributylphosphine and 1,1'-(azodicarbonyl)dipiperdine to successfully alkylate acids with pKas larger than 11.[79] Later work with cyanomethylenetributylphosphorane was found to provide high yields

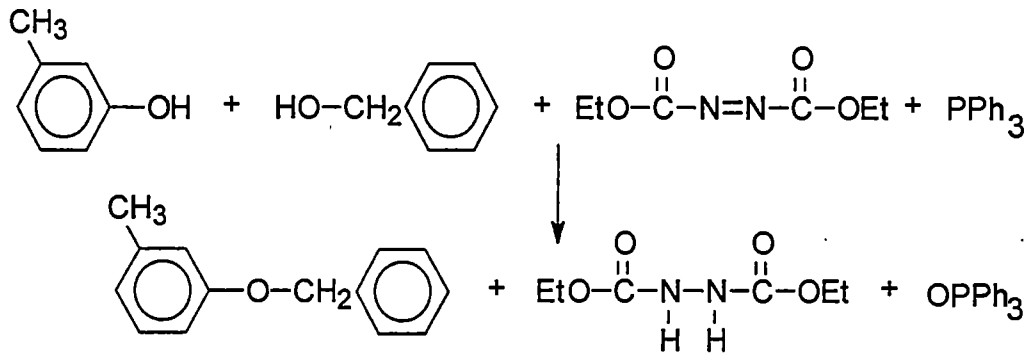


Figure 3.1. Mitsunobu etherification of m-cresol and benzyl alcohol

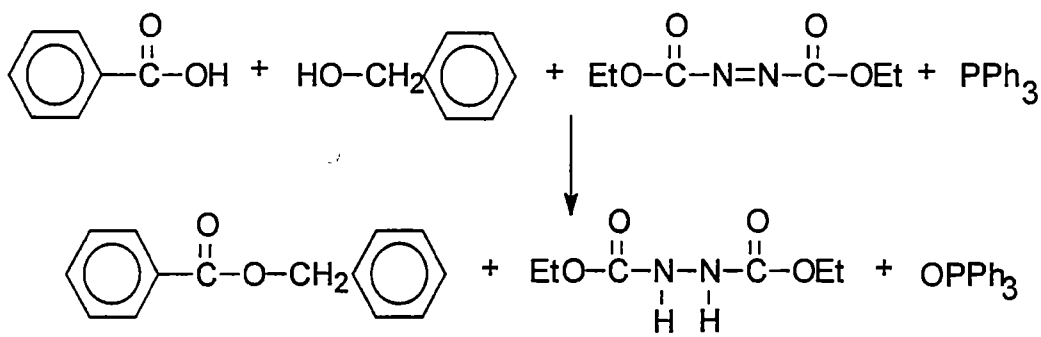


Figure 3.2. Mitsunobu esterification of benzoic acid and benzyl alcohol

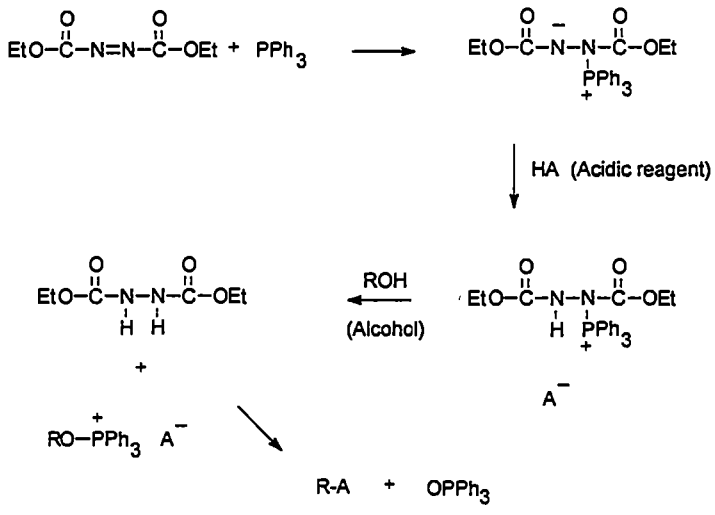


Figure 3.3. Mechanism of the Mitsunobu reaction

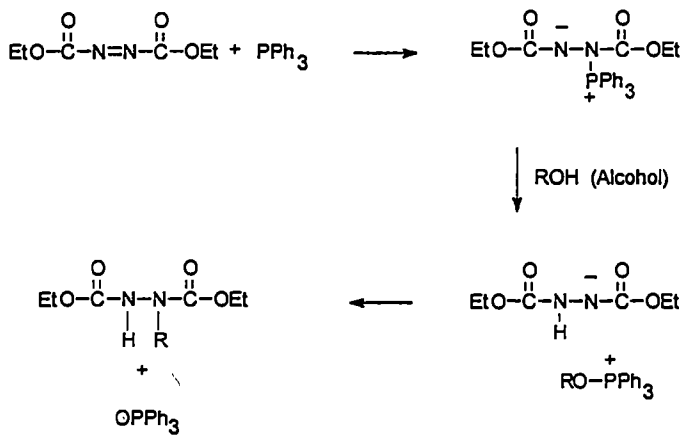


Figure 3.4. Mechanism of the alkylated hydrazine side-reaction

with compounds having pKa values up to 12.[80] Recent work with polymer-supported phosphines determined that a hydrophobic environment surrounding the active site profoundly reduces the degree of side reactions when alkylating benzoic acid (pKa = 4.2) with benzyl alcohol.[81]

The focus of this research is to study the Mitsunobu reaction with polymer-supported phosphines and compounds with a pKa of 10. A series of polymer-supported phosphines (Figure 3.5) were synthesized to evaluate the microenvironmental effect on the Mitsunobu etherification of m-cresol (pKa = 10.01) with benzyl alcohol (Figure 3.1). The reaction rates and yields of the phosphine resins were compared with their small molecule analogue. The results of the Mitsunobu etherification were compared with the reported esterification work using polymer-supported phosphines[81] (Figure 3.2).

EXPERIMENTAL

Synthesis of Phosphine Resins

Copolymer starting material was synthesized by the suspension copolymerization of vinylbenzyl chloride (VBC) and divinylbenzene (DVB). The polarity of the copolymer's microenvironment was adjusted by the addition of a third monomer to the copolymerization. Methyl methacrylate (MMA) and styrene (Sty) were used to change the polarity of the copolymer. The compositions of the various copolymers synthesized are summarized in Table 3.1.

Copolymer was sieved using USA standard testing sieves, and only microporous beads with a diameter between 0.25 to 0.425 mm were converted to the phosphine resin.

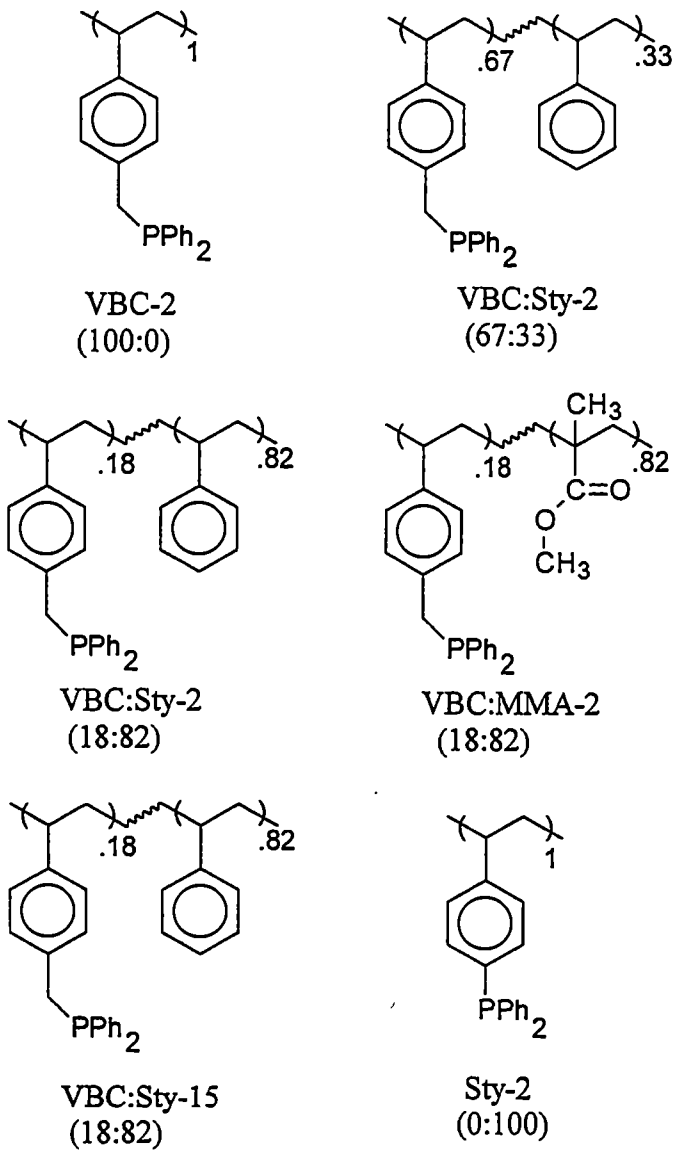


Figure 3.5. Structures of polymer-supported phosphines

Table 3.1
Composition of copolymer starting material

Copolymer	Support	%DVB[a]	Mole % of Monomers[b]		
			VBC	Styrene	MMA
CS3-084	VBC-2 (100:0)	2	100	0	0
CS3-085	VBC:Sty-2 (67:33)	2	67	33	0
CS3-064	VBC:Sty-2 (18:82)	2	18	82	0
CS3-198	VBC:Sty-15 (18:82)	15	18	82	0
CS3-143	Sty-2 (0:100)	2	0	100	0
CS3-101	VBC:MMA-2 (18:82)	2	18	0	82

[a] The weight percent of divinylbenzene (DVB) indicates the amount of cross-linking agent used to make the polymers insoluble.

[b] Mole percent of monomer repeating units excludes the cross-linking agent used.

Poly(vinylbenzyl chloride) beads were reacted with lithium diphenylphosphide to form the phosphine resin (Figure 3.6). Poly(styrene) beads were converted to the phosphine first by bromination and then reaction with lithium diphenylphosphide (Figure 3.7). Details of the phosphine resin synthesis and characterization techniques are provided in the Experimental section of this dissertation.

General Procedure for the Mitsunobu Reaction

Into a 100 ml three-neck roundbottom flask, 11.25 mmol m-cresol, 7.5 mmol phosphine reagent, 75 ml anhydrous tetrahydrofuran (THF), and 7.5 mmol dry benzyl alcohol were added. Under an argon atmosphere, the flask was placed in a water bath held at 25°C, and the mixture stirred at 252 rpm to enable mass transfer effects. The etherification reaction was started by the addition of 12.7 mmol of diethyl azodicarboxylate (DEAD). The reaction rate was monitored by microliter samples analyzed by gas chromatography (GC). Reactant and product concentrations were determined from the integrated data using THF as an internal standard. To perform the esterification reaction, the same procedure was followed except for the amount of two reagents: 7.5 mmol benzoic acid and 15 mmol phosphine reagent. The details of the GC analysis and concentration calculations are provided in the Experimental section of this dissertation.

Characterization of ether product

Benzyl 3-methylphenyl ether ^{1}H NMR: δ 2.28(s, 3H), δ 4.99(s, 2H), δ 6.72 (d, 3H), δ 7.06-7.39(m, 6H). MS: 198.1 m/z (198.28 expected)

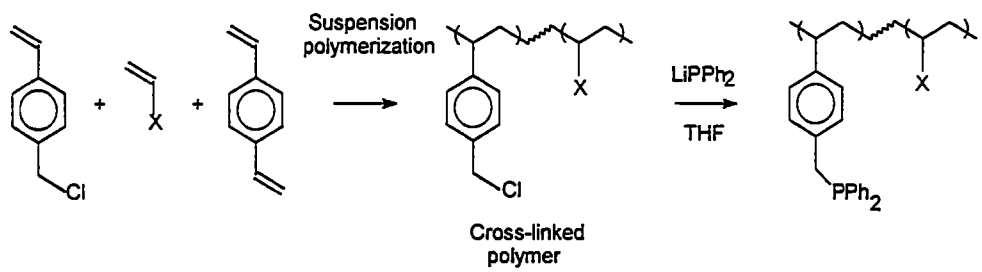


Figure 3.6. Synthesis of poly(vinylbenzyldiphenylphosphine) supports

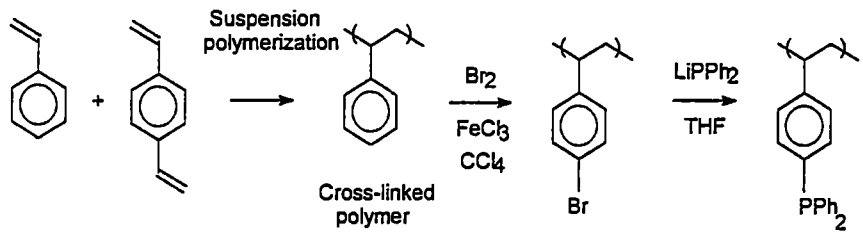


Figure 3.7. Synthesis of poly(styrenediphenylphosphine) support

RESULTS

Characterization

The poly(vinylbenzyldiphenylphosphine) supports, VBC-2(100:0), VBC:Sty-2(67:33), VBC:Sty-2(18:82), VBC:Sty-15(18:82), and VBC:MMA-2(18:82), are not direct analogues of triphenylphosphine, but can be easily synthesized from poly(vinylbenzyl chloride). The degree of phosphine loading and microenvironment was mainly controlled by the mole ratio of the monomers. The elemental analysis of the phosphine resins (Table 3.2) determined greater than 90% conversion of the halide to the phosphine for all of the supports except VBC:Sty-15(18:82) and VBC:MMA-2(18:82). The conversions for these two resins were 63% and 79% respectively. The Sty-2(0:100) support, or poly(styrenediphenylphosphine), is a structural analog of the soluble reagent. Control of the phosphine loading with the Sty support was not as readily accomplished as with the VBC supports. Although the bromination of the copolymer was limited to a 40% yield, 96% of the brominated poly(styrene) was converted to the phosphine.

Etherification Reaction Conditions

A comparison of the Mitsunobu etherification and esterification reactions determined a significant decrease in the ether yield as predicted by the literature.[79] Using triphenylphosphine, the etherification and esterification reactions produced yields of 1.6% and 85.3% respectfully. GC analysis of the etherification reaction identified one significant byproduct of approximately 74% yield. This major byproduct was identified as the alkylated hydrazine by comparing the GC retention time of the unknown with the retention time of a synthesized standard (CS3-251). The ether product was isolated and

Table 3.2
Characterization of phosphine resins

Resin	Support	Capacity (mmol / g) Phosphorus[a]	Capacity (mmol / g) Theoretical	Percent Functionalization
CS3-095	VBC-2 (100:0)	2.95	3.23	91.3
CS3-209	VBC:Sty-2 (67:33)	2.58	2.75	93.8
CS3-090	VBC:Sty-2 (18:82)	1.15	1.27	90.5
CS3-203	VBC:Sty-15 (18:82)	0.62	0.98	63.3
CS3-153	Sty-2 (0:100)	2.10	2.19	96.0
CS3-141	VBC:MMA-2 (18:82)	0.99	1.26	78.6

[a] Phosphorus elemental analysis is accurate to +/- 0.2 mmol / g.

identified by ^{1}H NMR and MS analysis as benzyl 3-methylphenyl ether.

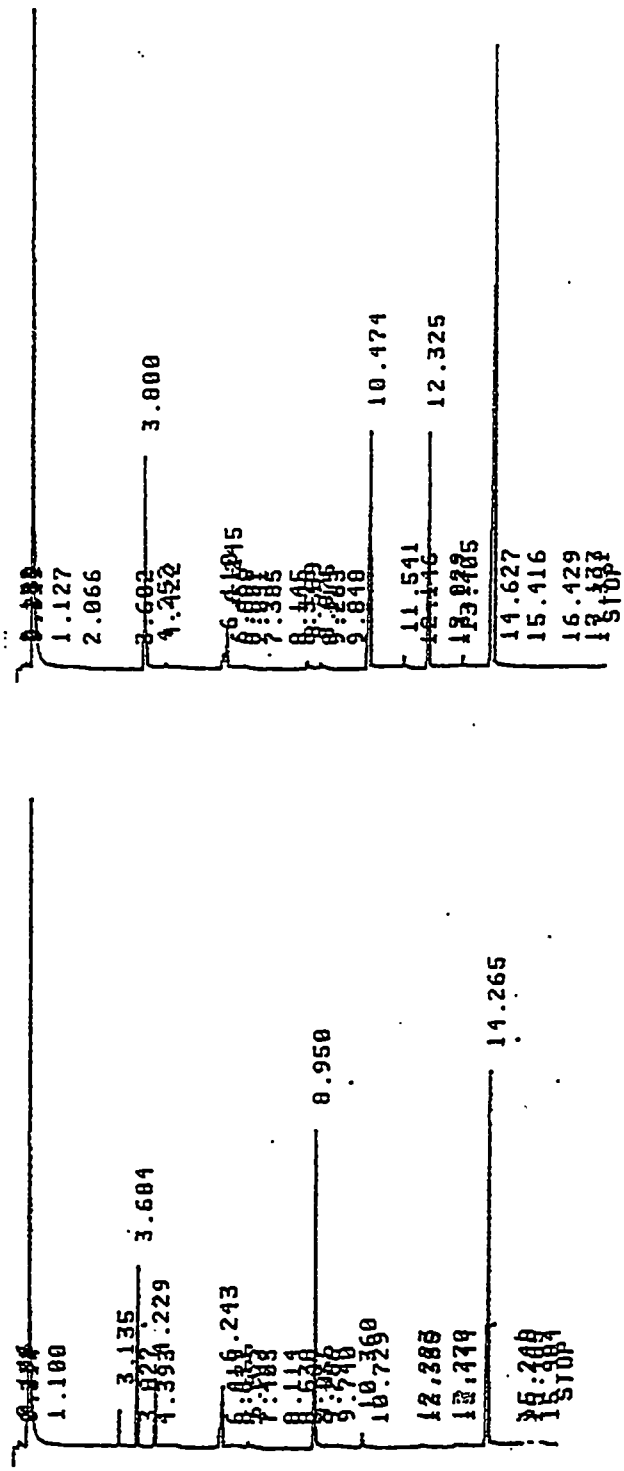
In an attempt to minimize the formation of the alkylated hydrazine product, several reactant concentrations were evaluated (Table 3.3). The results determined excess adduct formation and low m-cresol concentration to favor the alkylated hydrazine mechanism. A benzyl alcohol : m-cresol : phosphine : DEAD ratio of 1 : 1.5 : 1 : 1.7 was determined to maximize the ether yield while still maintaining one equivalent of the alcohol or acid (Figure 3.8).

The results of experimental controls with Sty-2(0:100) and VBC:MMA-2(18:82) proved accessibility of reagents into the polymer not to influence the ether yield (Table 3.4). The accessibility of reagents into the beads was also determined not to be a rate limiting factor in the Mitsunobu esterification[81]. The esterification reaction with Sty-2(0:100) beads between 0.25 and 0.425 mm in diameter was identical to the reaction with beads between 0.075 and 0.15 mm. The ability of the solvent to solvate the phosphine resins was measured and THF was found to swell most of the resins by a factor of two (Table 3.5).

It has been reported that changing the solvent from THF to N-methylmorpholine (NMM) can improve the yield of the Mitsunobu etherification[76]. The results of an etherification with VBC-2(100:0) in NMM determined the solvent to decrease the percent yield (Table 3.6). The influence of the reaction temperature was evaluated at 0 and 25^{0}C (Table 3.6). The results of the reactions with VBC:Sty-2(18:82) determined that increasing the temperature by 25 degrees improved the yield from 17 to 24%.

Table 3.3
Reaction condition controls using triphenylphosphine and a phosphine resin

Reactant Ratio				Percent Yield of Ether	
Benzyl alcohol	**m-Cresol**	**$RPPh_2$**	**DEAD**	**PPh_3**	**VBC:Sty-2 (18:82)**
1	1	2	1.7	1.6	23.6
1	1	1	1.7	58.6	15.5
1	1	1	1.5	62.0	-
1	1.5	1	1.7	74.5	20.8



Retention Time of Compound	Compound
~3.1	Benzyl alcohol
~3.7	m-Cresol
~4.2	DEAD
~6.2	Hydrazine product
~8.9	Ether product
~10.4	Alkylated hydrazine product
~12.3	Triphenyl-phosphine
~14.3	Triphenyl-phosphineoxide

Figure 3.8. GC analysis of the Mitsunobu etherification with triphenylphosphine at different reagent ratios (top: reagent ratio 1:1:2:1.7, bottom: reagent ratio 1:1.5:1:1.7).

Table 3.4
Etherification accessibility controls

Run	Resin	Bead Size (mm)	% Yield
3-165	Sty-2 (0:100)	0.25 - 0.425	43.7
3-169	Sty-2 (0:100)	<< 0.15[a]	41.0
3-149	VBC:MMA-2 (18:82)	0.25 - 0.425	0
3-162	VBC:MMA-2 (18:82)	<< 0.15[a]	0

[a] Resin was crushed into a powder with a mortar and pestle.

Table 3.5
Swelling ratio of phosphine resins in THF

Support	Swelling Ratio
VBC-2 (100:0)	2.0
VBC:Sty-2 (67:33)	2.3
VBC:Sty-2 (18:82)	2.8
VBC:Sty-15 (18:82)	1.5
VBC:MMA-2 (18:82)	1.9
Sty-2 (0:100)	3.1

Table 3.6
Etherification reactions using a different solvent or temperature

Run	Resin	Solvent	Temperature (°C)	% Yield
3-142	VBC-2[a] (100:0)	THF	25	11.0
3-163	VBC-2[a] (100:0)	NMM	25	2.2
3-098	VBC:Sty-2[b] (18:82)	THF	25	23.6
3-099	VBC:Sty-2[b] (18:82)	THF	0	16.7

[a] Alcohol:Phenol:Phosphine:DEAD ratio was 1 : 1.5 : 1 : 1.7.

[b] Alcohol:Phenol:Phosphine:DEAD ratio was 1 : 1 : 2 : 1.7.

Mitsunobu Etherification

The reactant and product concentrations were monitored by GC during the first 24 hours of the reaction to ensure equilibrium was reached. Figure 3.9 illustrates the ether yield as a function of time with triphenylphosphine and the phosphine resins. Table 3.7 compares the percent ether yield with the percent yield of alkylated hydrizine and the amount of benzyl alcohol consumed. Figure 3.9 clearly indicates that the faster the reaction rate the greater the ether yield. Triphenyphosphine enabled the largest ether yield of 74.5%. The fastest reaction with a phosphine resin, the fully functionalized Sty-2(0:100), produced only 43.7% of the ether. This yield was 2 times greater than any of the yields with the VBC supported phosphines. As shown in Table 3.7, when the mole percent of phosphine ligand in the VBC support was increased from 18% to 67% to 100%, the product yield decreased from 20.8% to 14.9% to 11.0%. An increase in the degree of cross-linking from 2 to 15%, comparing VBC:Sty-2(18:82) and VBC:Sty-15(18:82), found the percent yield to significantly decrease. The VBC:MMA-2(18:82) resin was unable to produce the ether product.

The degree of side-product formation is depicted by comparing the percent alcohol conversion and the final yield (Table 3.7). Of all the phosphines studied, triphenylphosphine produced the purest product with 13% of the alcohol consumed used to produce the alkylated hydrizine. Unlike the triphenylphosphine reaction, all of the etherification reactions with the phosphine resins were found to produce more than one byproduct. This is represented by the fact that a comparison of the percent alcohol consumed with the percent yield of the ether and alkylated hydrizine does not mass

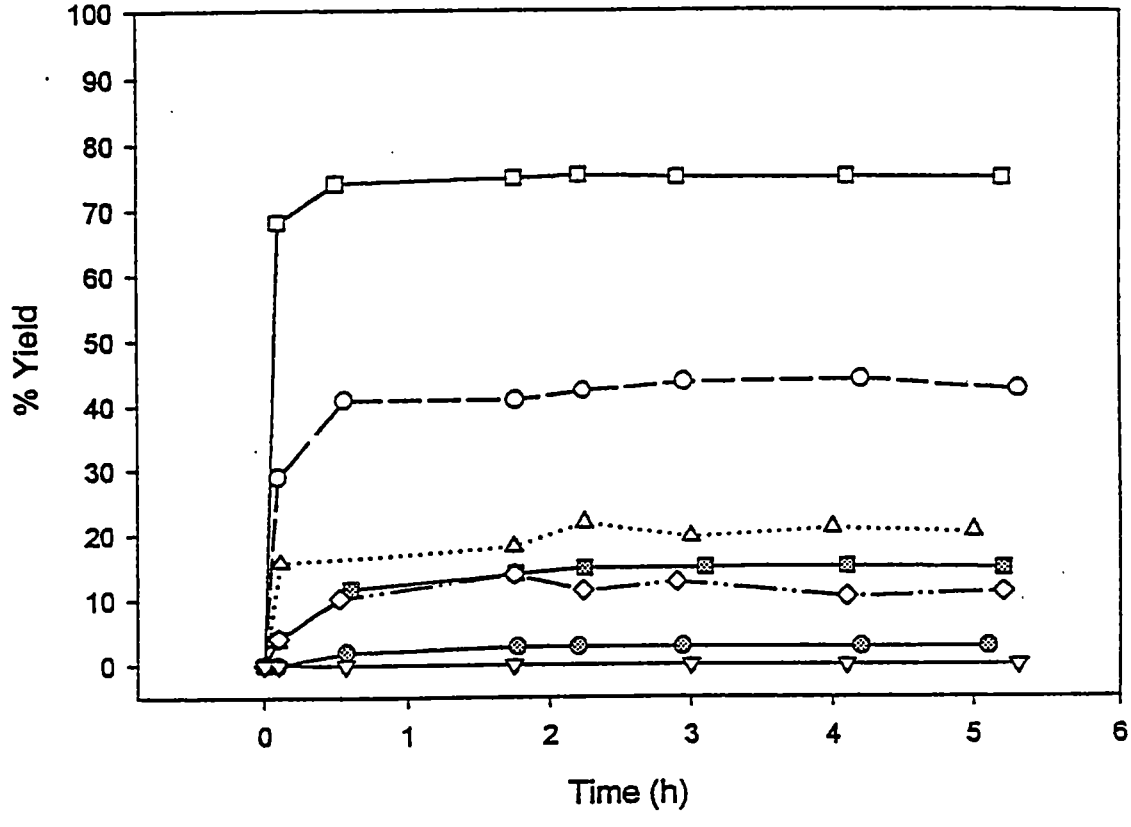


Figure 3.9. The Mitsunobu etherification with triphenylphosphine and polymer-supported phosphine resins

Table 3.7
Percent yield of benzyl 3-methylphenyl ether in the Mitsunobu etherification

Time (h)	PPh_3	Sty-2 (0:100)	VBC:Sty-2 (18:82)	VBC:Sty-2 (67:33)	VBC-2 (100:0)	VBC:Sty-15 (18:82)	VBC:MMA-2 (18:82)
0	0	0	0	0	0	0	0
0.1	68.2	29.0	15.7	4.1	4.2	2.0	0
24	74.5	43.7	20.8	14.9	11.0	2.8	0
% Alkylated hydrazine yield at 24 h	13[a]	14[a]	8.8[a]	16[a]	17[a]	11[a]	0
% Alcohol conversion at 24 h	87.1	84.3	70.4	62.2	61.6	22.3	30.0
Run	3-138	3-165	3-140	3-215	3-142	3-213	3-149

[a] Yield was estimated from the peak ratio of hydrazine to alkylated hydrazine detected by the GC.

balance. The byproducts formed in the polymer-supported reactions account for 30% to 100% of the alcohol consumed depending on the resin studied.

Mitsunobu Esterification

The results of the esterification reaction with benzoic acid demonstrated a relationship between reaction rate and product yield (Table 3.8), but with one important exception: although VBC:Sty-2(18:82) did not enable the fastest reaction, it did produce the largest ester yield of 95.1%. Similar to the etherification reaction, as the mole percent of phosphine ligands in the VBC support increased, the ester yield was found to decrease. The reaction rate order of esterification, PPh_3 ~ Sty-2(0:100) > VBC:Sty-2(18:82) > VBC-2(100:0) > VBC:MMA-2(18:82), is almost identical to the etherification reaction. The only variation is that the esterification with PPh_3 and Sty-2(0:100) was too fast to distinguish a difference in the rates.

The degree of side-product formation in the esterification was significantly lower than the etherification reaction. Except for VBC:MMA-2(18:82), the maximum amount of benzyl alcohol consumed to form side-products was 17% in the esterification, as compared to 51% in the etherification. The VBC:MMA-2(18:82) resin consumed approximately 31% excess alcohol in both reactions. The VBC:Sty-2(18:82) resin produced the purest ester product with only 2.3% of the alcohol consumed used to produce side-products.

DISCUSSION

Hughes and coworkers study of the Mitsunobu reaction determined the S_N2

Table 3.8
Percent yield of benzyl benzoate in the Mitsunobu esterification[a]

Time (h)	PPh_3	Sty-2 (0:100)	VBC:Sty-2 (18:82)	VBC-2 (100:0)	VBC:MMA-2 (18:82)
0	0	0	0	0	0
0.1	85.3	84.6	83.1	27.3	0
24	85.3	84.6	95.1	79.8	15.9
% Alcohol conversion at 24 h	100	100	97.4	96.6	47.8

[a] Esterification results provided by Dr. Dorothy H.J. Miller.

displacement of the oxyphosphonium cation by the carboxylate anion to be the rate limiting step when the pKa of the acid is similar to acetic acid (pKa = 4.75), and the concentration ratio of acid to conjugate base is less than or equal to one.[82] Although the rate limiting step for reactions with weaker acids has not been determined, deprotonation of the alcohol or acidic reagent by the adduct is believed to determine the reaction pathway.[79] The results of the Mitsunobu etherification reaction indicate that reaction rate and product yield are directly related. Because of the competing reaction mechanisms, a high ether yield is only possible if deprotonation of m-cresol by the adduct is faster than the deprotonation of benzyl alcohol. If this conclusion is correct, then the phosphine must be the limiting reagent in the Mitsunobu etherification. GC analysis of the etherification with triphenylphosphine determined that consumption of the phosphine and the end of the reaction coincide. Analysis of the esterification products showed the alkylated hydrazine byproduct to be absent. Because of the lower pKa value of the acid in the esterification, deprotonation of benzoic acid is favored and thus would prevent this side reaction from occurring. These results agree with the reported influence of the acid pKa on the reaction mechanism discussed earlier.

The electronic structure of the phosphine was determined to significantly influence the reaction rate. In both the esterification and etherification reactions, the reaction rate of fully functionalized poly(styrenediphenylphosphine), Sty-2(0:100), was faster than the fully functionalized poly(vinylbenzyldiphenylphosphine), VBC-2(100:0). This phenomenon is consistent with Hughes' study of the Mitsunobu reaction where increasing electron-withdrawing substituents of the phosphine increased the reaction

rate.[82] The Hammett sigma constants of benzyl and phenyl verify the VBC-2(100:0) benzyl group to be more electron donating than the Sty-2(0:100) styrene group. (σ_m/σ_p values for benzyl are -0.08/-0.09 and 0.06/-0.01 for phenyl.)[83]

The influence of the local environment surrounding the active sites of the phosphine resin was evaluated by diluting the copolymer with polar and non-polar monomer units. The results of both the esterification and etherification reactions with VBC:MMA-2(18:82) showed that a polymer-bound phosphine surrounded by ester ligands hinders product formation. To contrast this hydrophilic environment, the VBC:Sty-2(18:82) was synthesized using the same molar substitution ratio, but with the ester groups replaced with phenyl rings. The results of VBC:Sty-2(18:82) reactions showed that it not only produced a higher yields than the VBC:MMA-2(18:82), but it also produced more ester and ether faster than any of the VBC supported phosphines. A comparison of the Mitsunobu reactions with the partially and fully functionalized poly(vinylbenzyldiphenylphosphine) showed that the reaction rate decreased when the phosphine neighboring groups were changed from the phenyl rings of VBC:Sty-2(18:82) to the benzyldiphenylphosphine groups of VBC-2(100:0). These results prove that the polarity of the phosphine neighboring groups profoundly influences the reaction kinetics. In both examples, the reaction kinetics were enhanced when the polymer's microenvironment became more hydrophobic in nature. It is proposed that this increased reactivity is due to the destabilization of ionic intermediates with a localized non-polar environment. This microenvironmental effect is identical to the Hughes-Ingold theory of solvent effects in nucleophilic substitution reactions.[84] As in the Mitsunobu reaction,

increasing the polarity of the solvent will increase the solvation of the ionic intermediates and lower the reactant free energy. This decrease in free energy would cause an increase the activation energy of the reaction and decrease the reaction rate. Two reported examples of this solvent effect are the alkaline hydrolysis of ethyl iodide in aqueous ethanol,[85] and the bromide exchange between lithium bromide and n-butyl bromide in acetone.[86] In both studies, the reaction rate was found to decrease as the polarity of the solvent was increased by adding water.

Although the electronic and microenvironment of the polymer-supported phosphine could be altered to improve the yields of both Mitsunobu reactions, the etherification yield with the phosphine resins was significantly lower than with triphenylphosphine. This difference can be attributed to the side-products produced only by the polymer-supported phosphines. In an attempt to improve the reactivity of a phosphine resin, the degree of cross-linking of a partially functionalized resin was increased from 2 to 15% DVB. Increasing the rigidity of this polymer should increase the hydrophobic nature of the microenvironment by limiting neighboring group mobility. The influence of cross-linking on the mobility of the polymer chains was measured by the swelling ratios, with VBC:Sty-15(18:82) swelling half as much as VBC:Sty-2(18:82). A comparison of reactions with VBC:Sty-2(18:82) and VBC:Sty-15(18:82) showed that increasing the degree of cross-linking decreased the percent yield from 20.8% to 2.8%. It is believed that this reduced yield is caused by the steric hindrance of polymer chain overlap in the highly rigid structure of VBC:Sty-15(18:82). This type of steric hindrance has also been reported in the hydrogenation of alkenes using polymer-supported

rhodium(I) catalyst.[87] Grubbs and Kroll found that, unlike the soluble catalyst, the rate of hydrogenation with the polymer-support was dependent on the molecular size of the alkenes. The hydrogenation with 1-hexene, octadecene, cyclohexene, cyclooctene, cyclodecene, and Δ^2-cholestene showed that the high degree of crosslinking within the polymer was sterically hindering the reaction.

The influence of solvent basicity on the etherification yield was evaluated. It has been reported that the use of NMM in the Mitsunobu etherification can increase the product yield. Because the deprotonation of the alcohol or acidic reagent by the adduct is believed to determine the reaction pathway, the addition of a tertiary amine to the reaction should increase the degree the phenol dissociation and favor the ether product mechanism.[76] In contrast to this, the etherification with VBC-2(100:0) in THF produced 5 times more ether than in NMM. It is not clear what influence NMM had on the polymer-supported reaction.

CONCLUSION

Reactions with polymer-supported reagents are influenced by the local environment surrounding the active sites. Because the Mitsunobu reaction proceeds through ionic intermediates, a non-polar microenvironment was found to enhance the intermediates' reactivity and increase the rate of product formation. Attempts to optimize the yield of the etherification reaction by tailoring the microenvironment was complicated by the formation of side-products.

Chapter 4

IONIC ACCESSIBILITY OF SELECTIVE ION-EXCHANGE RESINS

INTRODUCTION

The selective removal of toxic metal ions from water is an important objective for many applications, including environmental remediation, the purification of industrial process waste and the isolation of precious metals from low grade ores.[88] Because many of these applications involve a complex mixture of toxic and benign ions, much research has been devoted to the design of polymer-supported reagents which are capable of ion selective complexation, exhibit rapid kinetics, and are applicable to a wide pH range.[89]

The commercially available sulfonic acid resin is one example of an ion-exchange resin with rapid kinetics (Figure 4.1). Although this resin has proven quite useful in applications requiring the complete removal of metal ions from a solution, the low metal ion selectivity of this resin makes it ineffective for selective metal ion extraction.[90]

For such applications, polymer-supported reagents with immobilized chelating ligands exhibit the required selectivity. For example, dithizone ligands immobilized onto poly(4-vinylpyridine) can selectively remove Hg(II) in the presence of Cd(II) and Zn(II)[91] (Figure 4.2), poly(glycidyl methacrylate)-supported pyrazole is capable of selective removal of Cu(II) from solutions containing Cd(II), Co(II), Ni(II) and Zn(II)[92], and polystyrene-supported 1-(2-aminoethyl)piperazine can selectively remove Au(III) and

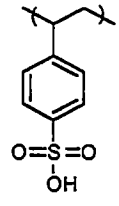


Figure 4.1 Non-selective sulfonic acid ion-exchange resin

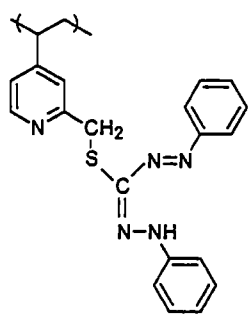


Figure 4.2 Ion selective dithizone resin

Pd(II) from solutions containing Cu(II), Ni(II), and Fe(III).[93] Although these resins exhibit ion selectivity, chelating resins tend to be hydrophobic and require long contact times,[94] the use of non-aqueous solvents,[95] or very small particle size[96] to obtain high levels of complexation. These limitations often cause chelating resins to be undesirable for industrial applications.

Dual mechanism bifunctional polymers[97] (DMBP) are a novel class of resins that combine the desirable properties of ion-exchange and coordination resins. By the use of multiple ligands on the same polymer, selective complexation of the target metal ion is achieved with an ion selective ligand, while a non-selective ion-exchange ligand is used to increase the accessibility of all ions into the polymer matrix. Diphonix is the first commercially available resin developed using the DMBP model (Figure 4.3). This bifunctional sulfonic acid/diphosphonic acid resin can selectively and rapidly complex high levels of lanthanide and actinide ions in the presence of sodium.[98-99]

It is the goal of this work to further the understanding between the structural properties of the polymer-support and the rate of selective complexation in highly acidic solutions. Metal ion complexation with phosphonic acid resins tends to decreases when the pH of the solution decreases.[100-101] It was originally hypothesized that the amount of metal ions complexed decreased due to the increased competition by H^+ for the binding sites.[100] In a recent study by this research group, it was determined that hydration of the microporous polymer matrix is influenced by the acid concentration of the solution.[102] By measuring the solution uptake of a microporous and macroporous phosphonic acid resin in 0.0 N and 1.0 N nitric acid, the decrease in solvent uptake for the microporous resin

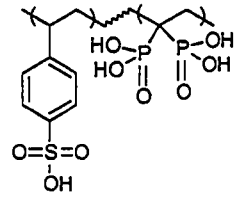


Figure 4.3 Diphonix, an ion selective DMBP

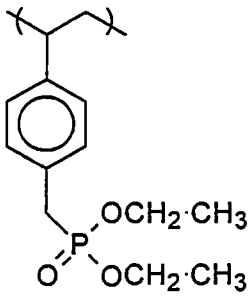
was determined to be 3.4 times larger than the macroporous resin. Therefore, a decrease in the solution pH results in a collapse of the polymer's microporous structure and a decrease in complexation due to limited ion accessibility into the polymer. This theory was applied in the study of polystyrene-support phosphinic acid resins with crosslinking agents of various flexibility.[103] Kinetic complexation studies determined that polymers with additional matrix flexibility were more susceptible to pore collapse in acidic solutions.

Preliminary work by this research group indicates that a polystyrene-supported phosphonic acid gel resin with 2 percent divinylbenzene crosslinking is more susceptible to pore collapse than a 5 percent crosslinked resin.[102] It is the focus of this work to evaluate further the influence of crosslinking on the complexation of Eu(III) with a polystyrene-supported diethyl phosphonate ester and phosphonic acid (Figure 4.4) The effect of the crosslink level, structure of the complexation ligand, and bifunctionality will be evaluated.

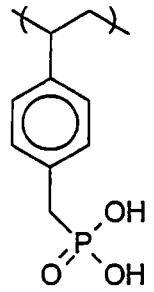
EXPERIMENTAL

Synthesis of ion-exchange resins

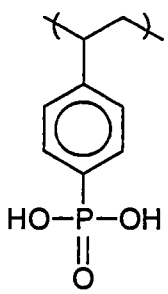
Copolymer starting material was synthesized by the suspension copolymerization of vinylbenzyl chloride (VBC) or styrene (Sty) with divinylbenzene (DVB). The resulting beads were sieved using USA standard testing sieves, and only microporous beads with a diameter between 0.25 to 0.425 mm were converted to the ion-exchange resin. The VBC supported diethyl phosphonate ester (VBC-PE) was immobilized by



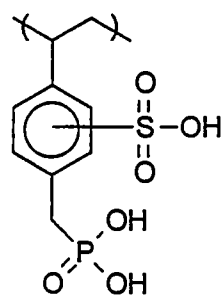
VBC-PE



VBC-PA



Sty-PA



VBC-PA/SA

Figure 4.4 Structures of ion-exchange resins

refluxing VBC copolymer in triethyl phosphite (Figure 4.5). The phosphonate ester was then hydrolyzed with concentrated HCl to form the phosphonic acid resin (VBC-PA). The polystyrene-supported phosphonic acid resin (Sty-PA) was synthesized by first reacting polystyrene with $AlCl_3$ in excess PCl_3, followed by hydrolysis, and then oxidation with HNO_3 (Figure 4.6). Unless stated otherwise, all of the bifunctional resins were synthesized by sulfonating the appropriate ester or acid resin with chlorosulfonic acid. All resins were characterized by percent solids (% solids = [weight of oven-dried resin / weight of wet resin]x100), phosphorus elemental, and acid capacity. The details of the ion-exchange resin synthesis and characterization techniques are provided in the Experimental section of this dissertation.

Metal Ion Studies

The ability of the ion-exchange resin to absorb Eu(III) ions was determined by contacting 0.1 mequiv of phosphorus ligands (based on phosphorus capacity) with 10 ml 10^{-4} $Eu(NO_3)$ in either 0.01 N, 0.10 N, 0.50 N, or 1.00 N HNO_3. The selectivity of the resins to absorb Eu(III) in the presence of excess sodium ions was determined by using $Eu(NO_3)$ solutions that contained 0.40 N $NaNO_3$. All resins were shaken for 24 h, and the Eu(III) concentration of the solution determined by atomic absorption. The results are reported in terms of percent complexed from the solution, and the distribution coefficient (D = mequiv M^{n+} on the resin per g_{resin} / mequiv M^{n+} in the solution per ml_{soln}). Distribution coefficient values for resins which absorb more than 99% Eu(III) were not calculated due to the insufficient accuracy of the atomic absorption technique.

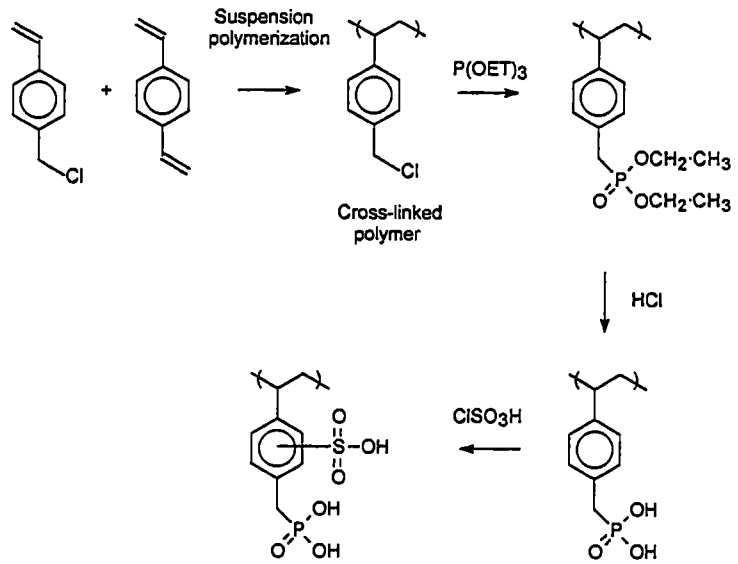


Figure 4.5 Synthesis of VBC-PE, VBC-PA, and VBC-PA/SA

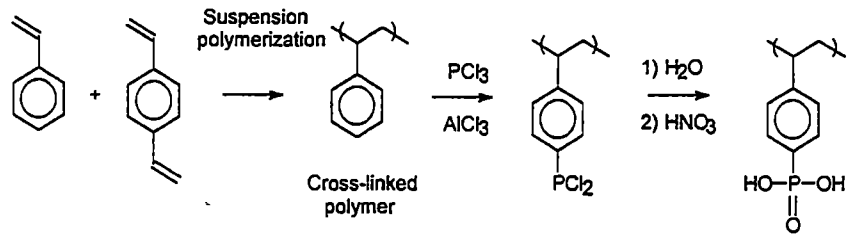


Figure 4.6 Synthesis of Sty-PA

RESULTS

Characterization

Characterization of the monofunctional ion-exchange resins showed that the degree of crosslinking influenced the amount of water solvating the resin (Tables 4.1-4.3). For all resins, the percent solids was found to increase as the percent DVB was increased. The percent functionalization was also influenced by the crosslink level. When the percent crosslinking of the styrene-supported phosphonic acid was increased from 8% to 12%, the degree of functionalization decreased from 90% to 73% (Table 4.3). The immobilization of the phosphonic acid onto the VBC support was not hindered by crosslink levels between 2% and 12% DVB. However, the hydrolysis of the 40% DVB phosphonate ester resin was incomplete as indicated by the low phosphorus:acid capacity ratio of CS2-049. (Table 4.2).

Sulfonation of the VBC phosphonic acid resin resulted in a 100% substitution of the sulfonic acid ligand onto the polymer backbone, and a lower percent solids than the monofunctional resin (Tables 4.2 & 4.4). The degree of sulfonation for each resin was determined by comparing the phosphorus:acid capacity ratio with the expected value of 1:3 as predicted by the structure. The 1:2 phosphorus:acid capacity ratio of the 25% crosslinked bifunctional resin (CS1-114) showed that the sulfonation with chlorosulfonic acid was unsuccessful. The 25% VBC phosphonic / sulfonic acid resin (VBC-PA/SA) was successfully synthesized by sulfonating the phosphonic acid resin with concentrated sulfuric acid (CS1-121). Because the phosphorus:acid ratio of this bifunctional resin was greater than 1:3, it is plausible that part of the crosslinking agent was also sulfonated in

Table 4.1
Characterization of VBC diethyl phosphonate ester resins (VBC-PE)

Resin	Percent DVB	Percent Solids	P Capacity[a] (mmol / g)	Theory (mmol / g)	Percent Functionalization
CS1-029	2	73.8	3.82	3.82	100
CS1-238	2	71.2	3.88	3.82	100
CS1-003	8	81.2	3.52	3.54	100
CS1-030	12	84.0	3.27	3.34	97.9

[a] Phosphorus elemental analysis is accurate to +/- 0.2 mmol / g.

Table 4.2
Characterization of VBC phosphonic acid resins (VBC-PA)

Resin	Percent DVB	Percent Solids	P Capacity[a] (mmol / g)	Theory (mmol / g)	Percent[b] Functional-ization	Acid Capacity[a] (mmol / g)	P : Acid Ratio
CS1-032	2	51.2	4.94	4.86	100	9.88	1 : 2.0
CS1-012	8	70.3	4.38	4.43	98.9	8.85	1 : 2.0
CS1-033	12	76.0	4.10	4.11	100	7.69	1 : 1.9
CS2-055	25	83.0	2.55	2.74	93.2	4.84	1 : 1.9
CS2-049	40	85.8	1.37	1.40	N/A[c]	1.06	1 : 0.77

[a] Phosphorus elemental and acid capacity analysis is accurate to +/- 0.2 mmol / g.

[b] Percent functionalization based on phosphorus capacity.

[c] Not applicable due to incomplete hydrolysis.

Table 4.3
Characterization of styrene phosphonic acid resins (Sty-PA)

Resin	Percent DVB	Percent Solids	P Capacity[a] (mmol / g)	Theory (mmol / g)	Percent[b] Functional-ization	Acid Capacity[a] (mmol / g)	P : Acid Ratio
CS1-052	2	20.4	4.83	5.28	91.4	10.77	1 : 2.2
CS1-090	2	36.6	5.10	5.28	96.5	10.31	1 : 2.0
CS1-050	8	56.2	4.49	4.92	91.3	9.25	1 : 2.1
CS1-172	8	55.5	4.43	4.92	90.0	9.35	1 : 2.1
CS1-110	12	68.7	3.42	4.66	73.4	7.10	1 : 2.1

[a] Phosphorus elemental and acid capacity analysis is accurate to +/- 0.2 mmol / g.

[b] Percent functionalization based on phosphorus capacity.

Table 4.4
Characterization of VBC phosphonic / sulfonic acid resins (VBC-PA/SA)

Resin	Percent DVB	Percent Solids	P Capacity[a] (mmol / g)	Theory (mmol / g)	Percent[b] Functional-ization	Acid Capacity[a] (mmol / g)	P : Acid Ratio
CS1-152	2	33.7	3.52	3.50	100	10.89	1 : 3.1
CS1-154	12	63.4	3.10	3.09	100	9.03	1 : 2.9
CS3-114	25	75.2	2.48	1.95	0	4.98	1 : 2.0
CS3-121	25	71.2	1.95	1.95	100	6.88	1 : 3.5

[a] Phosphorus elemental and acid capacity analysis is accurate to +/- 0.2 mmol / g.

[b] Percent functionalization based on phosphorus:acid ratio.

the reaction.

Attempts to synthesize a bifunctional phosphonate ester/sulfonic acid resin resulted in the undesired hydrolysis of the ester sites (Table 4.5). Even with a reduced reaction time of 3.5 h, or a lower chlorosulfonic acid concentration, the sulfur:acid capacity ratio of these resins was greater than 1:1. Attempts to synthesize a bifunctional polystyrene-supported phosphonic/sulfonic acid resin were also unsuccessful. As reported in Table 4.6, the phosphorus:acid ratio of 1:2 indicates no sulfonic acid ligands are present on the polymer. Sulfonation controls with a styrene-supported phosphinic acid resin showed that increasing the reaction temperature to 60^{0}C only yielded 19% sulfonation (Table 4.7).

Metal Ion Studies

Initial metal ion studies were performed with 2%, 8%, and 12% crosslinked monofunctional resins to evaluate the influence of crosslinking on the complexation of Eu(III) in highly acidic solutions. The percent Eu(III) complexed and distribution coefficients of these contact studies are listed in Table 4.8. Regardless of the percent DVB or acid concentration, VBC-PE complexed negligible amounts of Eu(III). The acid analog of the ester resin, VBC-PA, was found to quantitatively complex Eu(III) in 0.01 N and 0.10 N nitric acid. A significant decrease in the percent complexed was observed when the nitric acid concentration was increased to 0.50 N and 1.00 N. The percent complexed in 0.50 N and 1.00 N also decreased when the crosslink level increased from 8% to 12% DVB. The results with the styrene phosphonic acid resin were similar to the VBC phosphonic acid resin. However, Sty-PA complexed more Eu(III) in 0.50 N and

Table 4.5
Characterization of VBC diethyl phosphonate ester / sulfonic acid resins

	Percent	Percent	Capacity (mmol / g)			S : Acid
Resin	DVB	Solids	P[a]	S[b]	Acid[a]	Ratio
CS1-168	2	30.4	3.56	1.23	2.86	1 : 2.3
CS1-245	2	56.2	3.57	0.48	1.33	1 : 2.8

[a] Phosphorus elemental and acid capacity analysis is accurate to +/- 0.2 mmol / g.

[b] Sulfur elemental analysis was provided by Galbraith Laboratories, Inc.

Table 4.6
Characterization of styrene supported phosphonic / sulfonic acid resins

Resin	Percent DVB	Percent Solids	Capacity[a] (mmol / g) P	Capacity[a] (mmol / g) Acid	P : Acid Ratio
CS1-207	2	29.1	5.10	10.6	1 : 2.1
CS1-208	12	55.8	3.64	7.81	1 : 2.1

[a] Phosphorus elemental and acid capacity analysis is accurate to +/- 0.2 mmol / g.

Table 4.7
Sulfonation of styrene supported phosphinic acid resin

Resin	Reaction Temperature (^{0}C)	Percent Solids	P Capacity [a] (mmol / g)	Theory (mmol / g)	Percent[b] Functional-ization
CS1-220	0	35.0	5.23	4.00	0
CS1-241	60	32.0	4.90	4.00	19

[a] Phosphorus elemental and acid capacity analysis is accurate to +/- 0.2 mmol / g.

[b] Percent functionalization based on phosphorus capacity.

Table 4.8
Complexation of Eu(III) from 10^{-4} N $Eu(NO_3)_3$ / HNO_3 Solutions[a]

	0.01 N HNO_3	**0.10 N HNO_3**	**0.50 N HNO_3**	**1.00 N HNO_3**
VBC Diethyl Phosphonate Ester Resins (VBC-PE)				
2% DVB	2.92% (1.15)	0.53% (0.21)	2.96% (1.16)	4.89% (1.79)
8% DVB	0% (0)	6.61% (2.49)	3.99% (1.52)	4.54% (1.68)
12% DVB	0% (0)	5.20% (1.79)	1.78% (0.59)	0% (0)
VBC Phosphonic Acid Resins (VBC-PA)				
2% DVB	>99%	>99%	56.7% (64.8)	17.2% (10.3)
8% DVB	>99%	>99%	57.4% (59.2)	15.6% (8.08)
12% DVB	>99%	>99%	28.3% (13.1)	7% (3.3)
Styrene Phosphonic Acid Resins (Sty-PA)				
2% DVB	>99%	>99%	78.9% (190.)	40.2% (34.3)
8% DVB	>99%	>99%	81.5% (195.)	34.8% (24.0)
12% DVB	>99%	>99%	77.7% (113.)	39.1% (20.8)

[a] Percent complexed (Distribution coefficient values in parenthesis)

1.00 N nitric acid, and was not influenced by crosslinking.

Using these results as a preliminary evaluation, a series of experiments were designed to compare Eu(III) complexation of a monofunctional resin with its bifunctional analog. Due to synthetic limitations, metal ion studies of the bifunctional VBC phosphonate ester/sulfonic acid resin and styrene phosphonic/sulfonic acid resin could not be performed. A comparison of the monofunctional VBC-PA and bifunctional VBC-PA/SA is listed in Table 4.9. Because the 2% DVB and 8% DVB VBC-PA were found to complex the same amount of Eu(III), the 8% DVB resin was omitted from this study. Monofunctional and bifunctional resins with 25% and 40% DVB were added to this study to determine the influence of a highly rigid polymer matrix. However, due to the incomplete hydrolysis of the 40% DVB VBC-PA/SA, the 40% DVB resins could not be studied.

The percent Eu(III) complexed by VBC-PA was found to decrease when the percent crosslinking was increased from 12% to 25% in 0.01 N, 0.10 N and 0.50 N nitric acid (Table 4.9.). This decrease was not as significant in the 0.01 N matrix as it was in 0.10 N and 0.50 N nitric acid. Unlike the monofunctional resin, the percent complexed by the bifunctional resin was not influenced by the degree of crosslinking or the concentration of nitric acid. VBC-PA/SA quantitatively complexed the Eu(III) under nearly all conditions studied. In order to prove that the enhanced complexation of the bifunctional resin is not due to ion-exchange with the sulfonic acid ligand, contact studies were performed with solutions containing a large excess of sodium ions (1:12000). The results of the Eu(III) complexed in the presence of sodium, with the monofunctional and

Table 4.9
Complexation of Eu(III) from 10^{-4} N $Eu(NO_3)_3$ / HNO_3 Solutions[a]

	0.01 N HNO_3	**0.10 N HNO_3**	**0.50 N HNO_3**	**1.00 N HNO_3**
VBC Phosphonic Acid Resins (VBC-PA)				
2% DVB	>99%	>99%	56.7% (64.8)	17.2% (10.3)
12% DVB	>99%	>99%	28.3% (13.1)	7% (3.3)
25% DVB	91.6% (277.)	25.8% (8.80)	4% (1.1)	6% (1.7)
VBC Phosphonic / Sulfonic Acid Resins (VBC-PA/SA)				
2% DVB	>99%	>99%	98.5% (2350.)	95.3% (734.)
12% DVB	>99%	>99%	>99%	>99%
25% DVB	>99%	>99%	>99%	>99%

[a] Percent complexed (Distribution coefficient values in parenthesis)

bifunctional resins, are identical to the initial complexation results without sodium (Tables 4.9 and 4.10).

DISCUSSION

Diethyl phosphonate ester resin (VBC-PE)

The initial metal ion studies, with 2%, 8%, and 12% crosslinked monofunctional resins, determined the VBC-PA and Sty-PA to complex greater levels of Eu(III) than the VBC-PE (Table 4.8). These results illustrate the fact that phosphonate ester resins have different ion selectivity than phosphonic acid resins.[104] Research with immobilized phosphonate esters has determined that the length of the alkyl group influences the resin's metal ion affinity.[105] Contact studies with VBC-PE have shown that the diethyl phosphonate ester ligand complexes higher levels of Ag(I) than Hg(II) and Fe(III) (distribution coefficients in 1 N HNO_3 were 291, 9 and 2 respectfully). As the size of the alkyl ester group was increased from methyl to ethyl to butyl, the amount of Ag(I) complexed increased while the amount of Fe(III) decreased. The negligible amount of Eu(III) complexed by VBC-PE is also a result of limited metal ion accessibility into the polymer matrix. Recently reported work with polymer-supports of different porosity (macroporous beads and a foam column with an approximate porosity of 50% and 95% respectively) determined the pore structure to significantly influence ion accessibility.[106] Contact studies with diethyl phosphonate ester resins in 1 N HNO_3 found the macroporous resin to complex 4.90% Eu(III) after 24 hours, while the foam resin complexed 45.26%.

Table 4.10
Complexation of Eu(III) from 10^{-4} N $Eu(NO_3)_3$ / HNO_3 / 0.40 N $NaNO_3$ Solutions[a]

	0.01 N HNO_3	**0.10 N HNO_3**	**0.50 N HNO_3**	**1.00 N HNO_3**
VBC Phosphonic Acid Resins (VBC-PA)				
2% DVB	>99%	97.6% (2010.)	50.4% (50.2)	15.7% (9.2)
12% DVB	>99%	94.2% (670.)	26.0% (14.4)	6% (2.6)
25% DVB	81.1% (107.)	9% (2.5)	8% (2.3)	9% (2.6)
VBC Phosphonic / Sulfonic Acid Resins (VBC-PA/SA)				
2% DVB	>99%	>99%	>99%	92.7% (451.)
12% DVB	>99%	>99%	>99%	>99%
25% DVB	>99%	>99%	>99%	98.6% (1400.)

[a] Percent complexed (Distribution coefficient values in parenthesis)

Phosphonic acid resins (VBC-PA and Sty-PA)

The quantitative removal of Eu(III) with the phosphonic acid resins in 0.01 N and 0.10 N HNO_3 demonstrates that ion accessibility was not a limiting factor as with the phosphonate ester (Table 4.8). This difference can be explained by the hydrophilic nature of the two ligands. The greater hydrogen bonding capability of the phosphonic acid ligand increases the degree of polymer chain hydration, and increases the size of the microporous structure. As discussed previously, hydration of the polymer matrix is influenced by the normality of the acid solution.[102] When the nitric acid concentration was increased to 0.50 N and 1.00 N, the percent Eu(III) complexed decreased each time with VBC-PA and Sty-PA. This correlation between acid concentration and percent complexed is due to the collapse of the microporous structure as the solution pH is decreased.

The hydrophilicity of the polymer is also fundamental in the comparison of the VBC-PA and Sty-PA results. The percent solids of these resins indicates that the hydration of Sty-PA is greater than VBC-PA (Tables 4.2 - 4.3). The greater hydrophilicity of Sty-PA explains why increasing the degree of crosslinking from 8% to 12% did not influence the amount of Eu(III) complexed (Tables 4.8). Unlike Sty-PA, the less hydrophilic VBC-PA is more sensitive to pore collapse caused by an increase in the amount of hydrophobic crosslinking agent and matrix rigidity.

Monofunctional and bifunctional resins (VBC-PA and VBC-PA/SA)

The complexation of Eu(III) with monofunctional and bifunctional phosphonic acid resins is summarized in Table 4.9. Unlike the VBC-PA results, the VBC-PA/SA

quantitatively complexed Eu(III) regardless of acid concentration or degree of crosslinking. These results demonstrate the enhanced metal ion accessibility characteristic of dual mechanism bifunctional polymers. It is postulated that the sulfonic acid ligand of the VBC-PA/SA increases the degree of polymer hydration and enhances the complexation kinetics of the phosphonic acid ligand. The increased hydration of the bifunctional resin is evident by the smaller percent solids values of VBC-PA/SA (Tables 4.2 and 4.5).

In order to prove that the increased complexation of the VBC-PA/SA is due to enhanced metal ion accessibility, the contact studies were repeated using Eu(III) solutions containing excess sodium ions. If the enhanced complexation of the VBC-PA/SA was due to ion-exchange with the sulfonic acid ligands, then the complexation of Eu(III) should decrease due to the low metal ion selectivity of sulfonic acid.[90] The results of the $Eu(III)/Na^{+}$ metal ion study with VBC-PA and VBC-PA/SA were practically identical to the initial Eu(III) study (Tables 4.9 and 4.10). These results are characteristic of the phosphonic acid ligand which will complex transition and heavy metal ions in the presence of a large excess of alkali metal ions.[107] The increased hydration of the bifunctional resin enhanced metal ion accessibility and prevented the collapse of the microporous structure.

CONCLUSION

Increased crosslinking of a monofunctional phosphonic acid resin was unable to prevent pore collapse in highly acidic solutions. The inherent hydrophobicity of crosslink

levels between 12% and 25% DVB was determined to increase the matrix sensitivity to solution pH and decrease the amount of Eu(III) complexed. Pore collapse of the phosphonic acid resin was prevented by sulfonating the ion-exchange resin. In highly acidic solutions, the sulfonic acid ligand of the bifunctional resin provided an access mechanism for metal ions, and prevented collapse of the microporous structure. Selective ion complexation was enabled by the recognition mechanism of the phosphonic acid ligands which selectively coordinated Eu(III) ions once inside the polymer.

Chapter 5

EXPERIMENTAL PROCEDURES

All chemicals were used without further purification and were obtained from common chemical companies. Metal ion solutions and calibration standards were prepared using Class A glass pipettes and volumetric flasks.

SYNTHESIS

Copolymer synthesis

Polystyrene and poly(vinylbenzyl chloride) crosslinked beads were prepared by suspension polymerization. Poly(vinylbenzyl chloride) with 5 wt% divinylbenzene crosslinking and macroreticular pores was synthesized by the following technique. The aqueous phase was prepared by mixing 1.44 g gelatin dissolved in 158.25 ml distilled water with a second solution containing 9.495 g boric acid, 17.85 g poly(diallyldimethylammonium chloride), and 316.5 ml distilled water. The pH was adjusted to 10.3 using 50% sodium hydroxide, and moved to a 1 L three-neck round-bottom flask fitted with a condenser, nitrogen inlet and outlet, thermometer, and overhead stir apparatus. The organic phase was prepared by combining 134.95 g vinylbenzyl chloride, 13.55 g technical grade divinylbenzene (44.6% ethylstyrene impurity), 1.50 g benzoyl peroxide, and 150 g 4-methyl-2-pentanol (diluent). Oxygen was removed from the two phases by sparging the aqueous phase with nitrogen for 10 minutes, and the

organic phase for 5 minutes. The organic phase was then added to the round-bottom flask under a nitrogen sweep. To insure suspension formation, the two phases were mixed at 250 rpm for two minutes, allowed to separate, and the process repeated two more times. The reaction mixture was heated at rate of 7°C every 15 minutes until the temperature reacted 80°C, and then was held at this temperature for 10 h. After the reaction mixture had cooled to room temperature, the round-bottom was then fitted with a Dean Stark trap and 100 ml of distilled water added. The system was then refluxed for 6 h to remove the diluent. After cooling to room temperature, the resulting beads were washed with a pH 4 HCl solution, water, and then acetone. The beads were then extracted with toluene for 17 h, and dried before used.

Polystyrene with 5 wt% divinylbenzene crosslinking and macroreticular pores was synthesized using the same procedure. The only variations were that the organic phase contained styrene instead vinylbenzyl chloride, and the aqueous phase contained 0.9495 g boric acid with an adjusted pH of 10.0. Polymers with micropores were synthesized by omitting the diluent from the organic phase and increasing the amount of monomers and initiator by a factor of 2. After the 10 h polymerization, the gel beads were only refluxed for 2 h, and the Dean Stark trap with 100 ml of water was not required.

Washing of copolymer[81]

Copolymer used to synthesize the phosphine resins were first washed to remove surface impurities. The copolymer was placed in a round-bottom and washed for 30 min at 70°C with each of the following solutions: 1 N NaOH, 1 N HCl, 2 N NaOH:dioxane (1:2), 2 N HCl:dioxane (1:2), water and dimethylformamide. Solutions containing

poly(vinylbenzyl chloride) and NaOH were stirred at 25°C in order to prevent a reaction between the two. The copolymer was then washed at room temperature with the following solutions: 2 N HCl in methanol, H_2O, methanol, methanol:dichloromethane (1:3) and methanol:dichloromethane (1:10). The copolymer was then dried at 60°C under vacuum for 24 hours.

Synthesis of benzyltrialkylammonium chloride resins

Benzyltrimethylammonium chloride resins were synthesized by swelling 20 g of poly(vinylbenzyl chloride) beads in 25 wt% aq trimethylamine (100 ml) overnight in a 1 L round-bottom flask. A condenser, overhead stirrer, and 600 ml of 25 wt% aq trimethylamine were then added to the flask, and the mixture heated to reflux for 17 h. After cooling to room temperature, the resin was then washed with 1 N HCl and water. The resin was then moved to a column and conditioned with 1 L H_2O, 1N NaOH, H_2O, 1 N HCl, and H_2O with a 1 h elution time for each liter. The benzyltributylammonium chloride and benzyltrihexylammonium chloride resins were synthesized by a similar technique. The copolymer was first swollen in 200 ml of dioxane instead of the amine, and then a mixture of 40 ml dioxane, 20 ml water, and 200 ml of the appropriate amine was added and heated to reflux.

Synthesis of benzyltrialkylammonium phenoxide resins

All of the phenoxide resins were synthesized by eluting the anion-exchange resin (36 g) with several liters of a sodium phenolate solution. Both the p-nitrophenoxide and m-nitrophenoxide resins required a two hour elution with 2 L of a 0.10 N phenol / 0.095 N sodium hydroxide mixture. The phenoxide resin was eluted with 6 L of a 0.20 N

sodium phenoxide solution over 6 days. The p-methylphenoxide was eluted with 6 L of a 0.20 N p-cresol / 0.19 N sodium hydroxide mixture over 6 days. After the elution was complete, all resins were washed with 2 L of ethanol at a rate of 1 L/h, and vacuum dried overnight at 40°C.

Bromination of polystyrene beads[81]

Polystyrene divinylbenzene copolymer (24.85 g) was swollen in a round-bottom containing CCl_4 (250 ml) for 1 h. Anhydrous $FeCl_3$ (4.1 g) was added to round-bottom, and a solution of 6.5 ml Br_2 in 25 ml CCl_4 was placed in an addition funnel. The bromine solution was added dropwise to the round-bottom while stirring in the dark. After the mixture stirred overnight, the resin was then recovered by filtration, and washed with acetone until the unreacted bromine had been removed. The resin was then washed with a dioxane:water mixture (2:1), methyl ethyl ketone, and then vacuum dried at 65°C for 18 hours.

Synthesis of poly(vinylbenzyldiphenylphosphine) and poly(styrenediphenylphosphine) resins

A solution of chlorodiphenylphosphine (52.5 g) and THF (235 ml) was added dropwise through an addition funnel to a mixture of lithium metal (5.1 g) and THF (100 ml) under an argon atmosphere, and stirred for 24 h. In a second round-bottom, 20 g of poly(vinylbenzyl chloride) or brominated polystyrene was swollen in 200 ml THF for 1 h. Unreacted lithium metal in the first mixture was filtered off, the two solutions mixed, and stirred for 24 h under argon. The resin was then recovered by filtration, washed with THF, diethyl ether, 2:1 (v/v) THF:water, water, THF, toluene, and methanol (30 min stir

time each), and vacuum dried at 60^{0}C for 44 h.

Synthesis of diethyl phosphonate ester resins

Approximately 40 g of poly(vinylbenzyl chloride) beads were placed in a 500 ml three-neck round bottom flask fitted with an overhead stirrer, condenser and a stopper. A volume of 400 ml of triethyl phosphite was added and the mixture refluxed for 17 h. The solution was siphoned off and the beads washed 3 times with ethanol and water. The resin was then transferred to a fritted glass column and conditioned with 1 L elutions of water, 4 wt% NaOH, water, 4 wt% HCl and water (approximate flow rate of 1 L/h). The resin was then soxlet extracted with water for 17 h and reconditioned.

Synthesis of poly(vinylbenzyl chloride)-supported phosphonic acid resins

Wet diethyl phosphonate ester resin was placed in a Büchner funnel and aspirated for 5 min at 710 mm Hg. Approximately 40 g of the resin was placed in a 500 ml three-neck round bottom flask fitted with an overhead stirrer, condenser and a stopper. A volume of 200 ml of concentrated hydrochloric acid was added and the mixture refluxed for 17 h. The solution was siphoned off and the beads washed 3 times with water. The resin was then transferred to a fritted glass column and conditioned with 1 L elutions of water, 4 wt% NaOH, water, 4 wt% HCl and water (approximate flow rate of 1 L/h). The resin was then Soxlet extracted with water for 17 h and reconditioned.

Synthesis of polystyrene-supported phosphonic acid resins

Approximately 20 g of polystyrene beads were placed in a 300 ml three-neck round bottom flask fitted with an overhead stirrer, condenser and a stopper. A volume of 130 ml of PCl_3 was added and stirred. After 1 h of stirring, 29.92 g of $AlCl_3$ was added

and the solution refluxed for 4 h. The solution was siphoned off and the beads placed in a container of crushed ice. Water saturated with NaCl was added slowly with mixing until the hydrolysis was complete. The resin was washed 3 times with water and separated from any remaining ice. The resin was then transferred to a fritted glass column and conditioned with 1 L elutions of water, 4 wt% NaOH, water, 4 wt% HCl and water (approximate flow rate of 1 L/h). The resin was then placed in a 300 ml three-neck round bottom flask fitted with an overhead stirrer, condenser and a stopper. Approximately 300 ml of concentrated nitric acid was added and heated to 60°C for 4 h. The solution was siphoned off and the beads washed 3 times with water. The resin was then transferred to a fritted glass column and conditioned with 1 L elutions of water, 4 wt% NaOH, water, 4 wt% HCl and water (approximate flow rate of 1 L/h). The resin was then Soxlet extracted with water for 17 h and reconditioned.

Sulfonation of ion-exchange resins with chlorosulfonic acid

Wet resin was placed in a Büchner funnel and aspirated for 5 min at 710 mm Hg. Approximately 5 g of the resin was placed in a 500 ml three-neck round bottom flask fitted with an overhead stirrer, stopper, and a Dean Stark trap fitted with a condenser and drying tube. A volume of 100 ml of heptane was added and the mixture refluxed for 3 h. The solution was siphoned off, 200 ml of ethylene dichloride added and the solution stirred for 1 h. The Dean Stark trap was replaced with an addition funnel containing 66 ml ethylene dichloride and 16.5 ml of chlorosulfonic acid. The round bottom was placed in an ice bath and the addition funnel stopper opened to allow the solution to be added dropwise. After addition of the chlorosulfonic acid solution was complete, the ice bath

was removed and the reaction stirrer for 48 h. The solution was siphoned off and the beads washed with water:dioxane (1:9), water:dioxane (1:4), water:dioxane (1:1) and water (each solution stirred for 15 minutes). The resin was then transferred to a fritted glass column and conditioned with 1 L elutions of water, 4 wt% NaOH, water, 4 wt% HCl and water (approximate flow rate of 1 L/h). The resin was then Soxlet extracted with water for 17 h and reconditioned.

Sulfonation of ion-exchange resins with sulfuric acid

Wet resin was placed in a Büchner funnel and aspirated for 5 min at 710 mm Hg. Approximately 20 g of the resin was placed in a 500 ml three-neck round bottom flask fitted with an overhead stirrer, condenser and a stopper. A volume of 250 ml of concentrated sulfuric acid was added and the mixture heated to 110°C for 3 h. The solution was siphoned off and the beads washed 3 times with water. The resin was then transferred to a fritted glass column and conditioned with 1 L elutions of water, 4 wt% NaOH, water, 4 wt% HCl and water (approximate flow rate of 1 L/h). The resin was then Soxlet extracted with water for 17 h and reconditioned.

CHARACTERIZATION

Nitrogen capacity

Approximately 0.2 grams of dry resin, 0.25 g of $CuSO_4$, 10.0 g of K_2SO_4, 25 ml of concentrated H_2SO_4, and a few boiling chips were placed in a 500 ml 3-neck round bottom flask. The flask was fitted with a three foot condenser, two glass stoppers, and heated for 9 hours. The condenser was washed with 100 ml of distilled water, and

replaced with a distillation condenser fitted with a funnel piece. One stopper was removed, a magnetic stir bar and 250 ml addition funnel with pressure equalization arm were added. A 600 ml beaker containing 50.0 ml of standardized 0.1 N HCl was placed so that the funnel from the distillation was submerged in the solution. Approximately 150 ml of 6 N NaOH was added to the addition funnel and allowed to drip into the solution over a period of 5 minutes while stirring. After the NaOH was completely added, the flask was heated to reflux for approximately 45 minutes. When the solution distilling into the beaker tested neutral with pH paper, the HCl solution was quantitatively transfer to a 250 ml volumetric flask. Two 50.0 ml aliquots of the solution were titrated with standardized 0.1 N NaOH and bromocresol green indicator. The nitrogen capacity (in units of mmol / g) of the resin was then calculated using the equation:

$$\text{N capacity} = \frac{[(\text{N acid})(50.00\ \text{ml})] - [(5)(\text{N base})(\text{vol base titrated})]}{\text{weight of dry resin}}$$

Chlorine capacity

Approximately 0.2 g of oven-dried resin and 0.6 g mineral oil were placed in a Parr 1108 oxygen combustion bomb containing 5.0 ml of 5% sodium carbonate. The bomb was purged twice and then charged with 30 atm of oxygen. The bomb was moved to a water bath and ignited. Three minutes after ignition, the bomb was removed from the water bath, the pressure inside the bomb released, and the combustion solution quantitatively transferred to a 250 ml volumetric flask using nano-pure water. Approximately 3 ml of 2 N HNO_3 and exactly 5.0 ml of 0.50 N $AgNO_3$ was added to a 25 ml aliquot of the chlorine sample. The sample was boiled for two minutes, allowed to

cool, and the precipitate filtered. $FeNH_4(SO_4)_2$ indicator in 2 N HNO_3 was added to the filtered solution, and the excess $AgNO_3$ titrated for with a 0.0500 N NH_4SCN standard. The chlorine capacity (in units of mmol / g) was calculated using the following equation:

$$\text{Cl Cap.} = \frac{\{[(\text{N of } AgNO_3)(\text{vol. of } AgNO_3)] - [(\text{N of } NH_4SCN)(\text{vol. of } NH_4SCN)]\} \times 10}{\text{weight of dry resin}}$$

Nitrophenoxide capacity

Approximately 0.2 grams of oven dried resin was placed in a fritted glass column, and eluted with 0.9 liters of 1 N HCl over a period of 2.5 to 3 hours. The solution was collected in a 1 L volumetric flask, and a 25 ml aliquot diluted to 100 ml with 1 N HCl. The unknown solution and calibration standards were analyzed with a Hewlett-Packard 8452A diode array spectrophotometer. The absorbance of p-nitrophenol solutions was measured at 318 nm, and 330 nm for the m-nitrophenol solutions. All calibration curves employed solutions of 0, $2e^{-6}$, $1e^{-5}$, $2e^{-5}$, $1e^{-4}$, or $2.5e^{-4}$ M nitrophenol in 1 N HCl, and generated a regression greater than 0.999. The nitrophenoxide loading (in units of mmol / g) was calculated using the equation:

$$\text{capacity} = \frac{(\text{diluted solution's conc.})(\text{dilution factor of 4})(1\text{ L volume})(1000\text{ mmol/mol})}{\text{grams of dry resin}}$$

Phosphorus capacity

Approximately 20 mg of oven dried resin, 5 ml concentrated nitric acid and 10 ml concentrated perchloric acid was added to a clean 125 ml Erlenmeyer flask. The mixture was heated on a hot plate for 3 h to digest the resin. The solution was cooled and transferred to a 100 ml volumetric flask. A 5 ml aliquot of the solution was mixed with 3.5 ml perchloric acid, 4.5 ml amidol solution, 3.5 ml molybdate solution and diluted to

50 ml. (Amidol solution contained: 1 g recrystallized 2,4-diaminophenol dihydrochloride, 10 g Na_2SO_3, 2.7g concentrated H_2SO_4, and 90 g H_2O. Molybdate solution contained: 4.4 g in 50 ml H_2O.) The absorbance of the solution was measured to 700 nm on a Bausch and Lomb Spectronic 21, and the concentration determined from Beer's Law using a series of K_2HPO_4 standards. The phosphorus capacity (in units of mmol / g) was then calculated from the equation:

$$\text{P capacity} = \frac{(\text{Absorbance})(1000\ \text{ml})}{(\text{weight of dry resin})(\text{calibration slope ml/mg})(30.974\ \text{mg/mmol})}$$

Swelling ratios

Approximately 1.5 ml of oven dried resin is packed into a 10 ml graduated cylinder and then filled with solvent. After the resin has stopped swelling, the volume of the swollen resin is recorded and the swelling ratio calculated using the equation:

swelling ratio = (volume of swollen resin) / (volume of dry resin)

Percent solids

All ion-exchange resins used in the selective complexation of Eu(III) were stored under water. Wet resin was placed in a Büchner funnel and aspirated for 5 min at 710 mm Hg. A weighed sample of the resin (approximately 1-1.5 g) was then placed in a 20 ml scintillation vial and dried at 110°C for 16 h. The vial was then cooled in a desiccator and weighed. The percent solids was calculated using the equation:

% solids = (wt. of Büchner dried resin)/(wt. of oven dried resin)

Acid capacity

All ion-exchange resins used in the selective complexation of Eu(III) were stored

under water. Wet resin was placed in a Büchner funnel and aspirated for 5 min at 710 mm Hg. A weighed sample of the resin (approximately 1-1.5 g) was then placed in a 250 ml Erlenmeyer flask. The resin was gently stirred with 200 ml standardized 0.10 N NaOH containing 5 wt% NaCl for 17 h. Approximately 120 ml of the solution was removed and two 50 ml aliquots were titrated with 0.1 N HCl using a phenolpthalein indicator. The acid capacity (in units of mmol/g) was then calculated by the equation:

$$\text{acid capacity} = \frac{[\,(\text{ml NaOH})(\text{N NaOH})\,] - [\,4(\text{ml HCl})(\text{N HCl})]}{(\text{wt. of Büchner dried resin})(\%\ \text{solids})}$$

KINETIC STUDIES

Gas chromatographic analysis of the organic reactions

Changes in the reactant and product concentrations of an organic reaction were determined by gas chromatography (GC). The Hewlett-Packard 5890 GC was equipped with a split injection liner, dimethylpolysiloxane capillary column (15 m x 0.53 mm x 1.5 μm), flame ionization detector, and a Hewlett-Packard 3396 series 3 recording integrator. Typical GC settings included: a 300°C injection port temperature, 300°C detector port temperature, 70 kpascal head pressure, initial temperature of 35°C, and a heating ramp of 15°C per minute. Reaction samples were taken with a Hamilton 7000 series 1 μL positive displacement syringe.

Reagent concentrations were determined by the use of an internal standard. A calibration curve was constructed by plotting the peak area ratio of the reagent and internal standard against the mass ratio. Using a calibration curve with a regression

greater than 0.998, the mass of the reagent present at the time of the sampling was calculated by the equation:

$$W_n = \alpha (A_n / A_s) W_s$$

(W_n is the weight of the reagent, α is a constant obtained from the slope of the calibration curve, A_n is the reagent peak area, A_s is the internal standard peak area, and W_s is the weight of the internal standard.) The concentration of the reagent was then determined by converting the mass into moles and dividing by the known solution volume.

The Williamson ether synthesis

Small scale reactions were used to determine the suitable reaction conditions for the kinetic study. Alkyl halide was weighed into a 4 ml vial and diluted to 2 ml with toluene. The immobilized phenoxide resin was then added to the vial, a timer started, and the vial placed onto a wrist action shaker. A 1 μL sample of the mixture was analyzed at timed intervals by GC.

Large scale reactions were used to accurately measure the initial reaction rate. The phenoxide resin (7.19 mmol) was weighed into a 100 ml 3-neck round bottom flask. A stir shaft, thermometer, septum, and 79.20 ml of toluene or ethanol were added to the flask. The solution was stirred at 150 rpm overnight to ensure swelling of the beads. The stir rate was increased to 353 rpm and the system heated to 75^{0}C using a water bath. Benzyl chloride (7.093 mmol, 0.80 ml) was then pipetted into the reaction, and a timer started. A 1 μL sample of the mixture was taken every 30 minutes for the first 5.5 h and the concentration of benzyl chloride determined by GC analysis.

A plot of benzyl chloride concentration (M) vs. time (seconds) was constructed

for each reaction performed. The resulting curve was fit by a double or triple exponential decay equation with a regression greater than 0.99. The initial rate of the reaction was determined by calculating the derivative of the line equation at time zero.

The Mitsunobu etherification and esterification

Into a 100 ml three-neck roundbottom flask, 11.25 mmol m-cresol, 7.5 mmol phosphine reagent, 75 ml anhydrous tetrahydrofuran (THF), and 7.5 mmol dry benzyl alcohol were added. Under an argon atmosphere, the flask was placed in a water bath held at 25°C, and the mixture stirred at 252 rpm to prevent mass transfer effects. The etherification reaction was started by the addition of 12.7 mmol of diethyl azodicarboxylate (DEAD). The reaction rate was monitored by microliter samples analyzed by gas chromatography (GC). Reactant and product concentrations were determined from the integrated data using THF as an internal standard. To perform the esterification reaction, the same procedure was followed except for the amount of two reagents: 7.5 mmol benzoic acid and 15 mmol phosphine reagent.

Metal ion studies

All ion-exchange resins used in the selective complexation of Eu(III) were stored under water. Wet resin was placed in a Büchner funnel and aspirated for 5 min at 710 mm Hg. Contact studies were performed by weighing one milliequivalent of phosphorus ligands into a 20 ml scintillation vial. The resin was preequilibrated with 10 ml of the appropriate nitric acid solution and shaken for 15 minutes with a Burrell wrist-action shaker. The acid solution was then removed with a Pasteur pipet, and the process repeated three more times. The resin was then contacted with 10 ml of the appropriate

metal ion solution and shaken for 24 hours. The metal ion solution was removed with a Pasteur pipet and transferred to a second scintillation vial. The concentration of Eu(III) remaining in the solution was determined by atomic emission.

Atomic absorption/emission spectroscopy

Europium metal ion solutions were analyzed with a Perkin-Elmer 3100 atomic absorption/emission spectrometer. Europium emission was detected at 459.4 nm using a nitrous oxide/acetylene flame. Solutions were spiked with 4000 ppm KCl to prevent ionization. All calibration curves used standard solution containing 0, $1e^{-5}$, $2e^{-5}$, $5e^{-5}$ and$1e^{-4}$ N $Eu(NO_3)_3$ in either 0.01, 0.10, 0.50 or 1.00 N HNO_3, and generated a regression greater than 0.999.

REFERENCES

1. Synthesis and Separations Using Functional Polymers; Hodge, P., Sherrington, D.C.; Wiley: Chichester, 1988, Chapters 3-5.

2. Synthesis and Separations Using Functional Polymers; Hodge, P., Sherrington, D.C.; Wiley: Chichester, 1988, Chapters 1-2.

3. Synthesis and Separations Using Functional Polymers; Hodge, P., Sherrington, D.C.; Wiley: Chichester, 1988, Chapter 8.

4. Polymer-Supported Reactions in Organic Synthesis; Hodge, P., Sherrington, D.C.; Wiley: Chichester, 1980, Chapters 1-2.

5. Hallensleben, M.L. *Angew. Mokromol. Chem.* **1974**, *96*, 6469.

6. Merrifield, R.B. *J. Am. Chem. Soc.* **1963**, *85*, 2149.

7. Thompson, L.A.; Ellman, J.A. *Chem. Rev.*, **1996**, *96*, 555.

8. Fruchtel, J.S.; Jung, G. *Angew. Chem. Int. Ed. Engl.*, **1996**, *35*, 17.

9. Argonaut Technologies, 887 Industrial Road, Suite G, San Carlos CA 94070

10. Challa, G. *J. Mol. Catal.* **1983**, *21*, 1.

11. Capillon, J.; Richard, A.; Audebert, R.; Quivoron, C. *Polym. Bull.* **1985**, *13*, 185.

12. Guyot, A.; Bartholin, M. *Progr. Polym. Sci.* **1982**, *8*, 277.

13. Baker, G.L.; Fritschel, S.J.; Stille, J.K. *Am. Chem. Soc. Org. Coat. Appl. Polym. Sci. Proc.*, **1982**, *46*, 687.

14. Dumont, W.; Poulin, J.C.; Dang, T.P.; Kagan, H.B. *J. Am. Chem. Soc.* **1973**, *95*, 8295.

15. Harrison, C.R.; Hodge, P. *J. Chem. Soc. Perkin Trans. I*, **1982**, 509.

16. Emerson, D.W.; Emerson, R.R.; Joshi, S.C.; Sorensen, E.M.; Turek, J.E. *J. Org. Chem.*, **1979**, *44*, 4634.

17. Grubbs, R.H.; Gibbons, G.; Kroll, L.C; Bonds, W.D.; Brubaker, C.H. *J. Am. Chem. Soc.* **1973**, *95*, 2373.

18. Grubbs, R.H.; Gibbons, G.; Kroll, L.C; Bonds, W.D.; Brubaker, C.H.; Chandrasekaran E.S. *J. Am. Chem. Soc.* **1975**, *97*, 2128.

19. Hodge, P.; Khoshdel, E. *React. Polym.*, **1985**, *3*, 143.

20. Morawetz, H. *J. Macromol. Sci-Chem.* **1979**, *13*, 311.

21. Harrison, C.R.; Hodge, P.; Hunt, B.J.; Khoshdel, E.; Richardson, G. *J. Org. Chem.*, **1983**, *48*, 3721.

22. Deratani, A.; Darling, G.D.; Horak, D.; Frechet, J.M. *Macromolecules*, **1987**, *20*, 767.

23. Deratani, A.; Darling, G.D.; Frechet, J.M. *Polymer*, **1987**, *28*, 825.

24. Macroscale and Microscale Organic Experiments; Williamson, K.L.; D.C. Heath: Toronto, 1994.

25. Beauvais, R.; Alexandratos, S.D.; *Reactive & Functional Polymers*, **1998**, *36*, 113.

26. Capillon, J.; Richard, A.; Audebert, R.; Quivoron, C. *Polym. Bull.* **1985**, *13*, 185.

27. Challa, G. *J. Mol. Catal.* **1983**, *21*, 1.

28. Guyot, A.; Bartholin, M. *Progr. Polym. Sci.* **1982**, *8*, 277.

29. The Chemistry of the Ether Linkage; Patai, S.; Wiley: New York, 1967.

30. Barco, A.; Benetti, S.; De Risi, C.; Marchetti, P.; Pollini, G.; Zanirato, W. *Tetrahedron: Asymmetry* **1998**, *9*(16), 2857.

31. Yamazaki, O.; Togo, H.; Nogami, G.; Yokoyama, M. *Bull. Chem. Soc. Jpn.* **1997**, *70*(10), 2519.

32. Rozhanskii, I. L.; Tomita, I.; Endo, T. *Polymer* **1998**, *40*(6), 1581.

33. Chemical Kinetics The Study of Reaction Rates in Solution; Connors, K.A.; VCH: New York, 1990, Chapter 7.

34. Gelbard, G.; Colonna, S. *Synthesis* **1977**, *9*, 113.

35. Hudson, R.F.; Loveday, G. *J. Am. Chem. Soc.* **1962**, *84*, 1068.

36. Nassar, A.; Kharaba, M.A.; Youssef. A. *Revue Roumaine de Chimie* **1988**, *33*(5), 525.

37. Hudson, R.F.; Klopman, G.. *J. Am. Chem. Soc.* **1964**, *86*, 5.

38. Okamoto, K.; Kushiro, H.; Nitta, I.; Shingu, H. *Bull. Chem. Soc. Jpn.* **1967**, *40*, 1900.

39. Panigrahi, G.P.; Sinha, T.K. *Indian J. Chem.*. **1984**, *23B*, 57.

40. Schreck, J.O. *J. Chem.Ed.* **1971**, *48*(2), 103.

41. Leisten, J.; *J. Chem. Soc.* **1959**, 765.

42. Bunnett, J.; Zahler, R. *Chem. Revs.*, **1951**, *49*, 294.

43. Willi, A.; Robertson, R. *Can. J. Chem.* **1953**, *31*, 361.

44. Anderson, B.M.; Jencks, W.P. *J. Amer. Chem. Soc.*, **1964**, *86*, 837.

45. Hupe, D.J.; Jencks, W.P. *J. Am. Chem. Soc.* **1977**, *99*, 451.

46. Hupe, D.J.; Wu, D. *J. Am. Chem. Soc.* **1977**, *99*, 7653.

47. Jencks, W.P.; Brant, S.R.; Gandler, J.R.; Fendrich, G.; Nakamura, C.; *J. Am. Chem. Soc.* **1980**, *104*, 7045.

48. Stefanidis, D.; Cho S.; Dhe-Paganon, S.; Jencks, W.P. *J. Am. Chem. Soc.* **1993**, *115*, 1650.

49. Um, I.; Kim, G.; Kwon, D. *Bull. Korean Chem. Soc.* **1994**, *15*(7), 585.

50. Terrier, F.; Moutiers, G.; Xiao, L.; Guevel, E.L.; Guir, F. *J. Org. Chem.*, **1995**, *60*, 1748.

51. Um, I.; Chung, E.; Kwon, D. *Tetrahedron Lett.* **1997**, *38*(27), 4787.

52. Jencks, W.P.; Gilchrist, M. *J. Am. Chem. Soc.* **1962**, *84*, 2910.

53. Scott, J; McIver, R.; Bartmess, J. *J. Am. Chem. Soc.* **1979**, *101*, 6056.

54. Ruasse, M.; Moro, G.; Galland, B.; Bianchini, R.; Chiappe, C; Bellucci, G. *J. Am. Chem. Soc.* **1997**, *119*, 12492.

55. McDowell, M.J.; Draus, C.A. *J. Am. Chem. Soc.* **1951**, *73*, 3293.

56. CRC Handbook of Chemistry and Physics; CRC Press, Boca Raton, Florida, 1996.

57. Szczecinski, P. *Rocz. Chem.* **1977**, *51*(10), 2029.

58. Phase Transfer Catalysis; Dehmlow, E.V.; Dehmlow, S.S.; Verlag Chemie, Deerfield, Florida, 1980, Chapter 1.

59. Bordwell, F. *Acc. Chem. Res.* **1988**, *21*, 456.

60. Newton, T.; Arcand, G. *J. Am. Chem. Soc.*, **1953**, *75*, 2449.

61. Bauman, W.C. *J. Am. Chem. Soc.* **1947**, *69*, 2830.

62. Hassanein, M.; Ford, W.T. *J. Org. Chem.* **1989**, *54*, 3106.

63. Bauman, W.C. *J. Am. Chem. Soc.* **1960**, *82*, 1068.

64. Ancillotti, F.; Mauri, M.M.; Pescarollo, E. *J. Catal.* **1977**, *46*, 49.

65. Hodge, P.; *Chem. Soc. Rev.*, **1997**, *26*, 417.

66. Hughes, E.D.; Ingold, C.K. *J. Chem. Soc.* **1935**, 244.

67. Mitsunobu, O.; Yanagida, N. *Bull. Chem. Soc. Jpn.* **1967**, *40*, 2380.

68. Mitsunobu, O.; Kimura, J.; Iiizumi, K.; Yanagida, N. *Bull. Chem. Soc. Jpn.* **1976**, *49*, 510.

69. Bittner, S.; Assaf, Y. *Chem. Ind. (London)* **1975**, 281.

70. Manhas, M.S.; Hoffman, W.H.; Lal, B.; Bose, A.K. *J. Chem. Soc. Perkin Trans. 1* **1975**, 461.

71. Mitsunobu, O.; Eguchi, M. *Bull. Chem. Soc. Jpn.* **1971**, *44*, 3427.

72. Mitsunobu, O.; Wada, M.; Sano, T. *J. Am. Chem. Soc.* **1972**, *94*, 679.

73. Loibner, H.; Zbiral, E. *Helv. Chim. Acta* **1976**, *59*, 2100.

74. Wada, M.; Mitsunobu, O. *Tetrahedron Lett.* **1972**, 1279.

75. Hughes, D.L. *Org. Prep. Proced. Int.* **1996**, *28*(2), 127.

76. Richter, L.S.; Gadek, T.R. *Tetrahedron Lett.* **1994**, *35*(27), 4705.

77. Rano, T.A.; Chapman, K.T. *Tetrahedron Lett.* **1995**, *36*(22), 3789.

78. Krchnak, V.; Flegelova, Z; Weichsel, A.S.; Lebl, M. *Tetrahedron Lett.* **1995**, *36*(35), 6193.

79. Tsunoda, T.; Yamamiya, Y.; Ito, S. *Tetrahedron Lett.* **1993**, *34*(10), 1639.

80. Tsunoda, T.; Ozaki, F.; Ito, S. *Tetrahedron Lett.* **1994**, *35*(28), 5081.

81. Alexandratos, S.D.; Miller, D.H.J. *Macromolecules* **1996**, *29*, 8025.

82. Hughes, D.L.; Reamer, R.A.; Bergan, J.J.; Grabowski, E.J.J. *J. Am. Chem. Soc.* **1988**, *110*, 6487.

83. Hansch, C.; Leo, A.; Taft, R.W. *Chem. Rev.* **1991**, *91*, 165.

84. Hughes, E.D.; Ingold, C.K. *J. Chem. Soc.* **1935**, 244.

85. DeBruyn, C.; Steger, A. *Rec. Trav. Chim.* **1899**, *18*(41), 311.

86. LeRoux L.; Sugden S. *J. Chem. Soc.* **1939**, 1279.

87. Grubbs, R.; Kroll, L. *J. Am. Chem. Soc.* **1971**, *93*, 3062.

88. LaGrega, M. D.; Buckingham, P. L.; Evans, J.C. *Hazardous waste management*; McGraw-Hill, Inc.: New York, 1994.

89. Hirai, H.; Toshima, N. *Tailored Metal Catalysts*; Iwasawa, Y., Ed.; Reidel: Dordrecht, 1986; Fritz, J. S.; Gjerde, D.T.; Pohlandt, C. *Ion Chromatography*; Huthig: Heidelberg, 1982; Marhol, M. *Ion Exchangers in Analytical Chemistry*; Svehla, G., Ed.; Elsevier: Amsterdam, 1982; Comprehensive Analytical Chemistry, Vol. 14

90. Boyd, G. E.; Vaslow, F.; Lindenbaum, S. *J. Phys. Chem.* **1967**, *71*, 2214.

91. Shah, R.; Devi, S. *React. Funct. Polym.* **1996**, *31*, 1.

92. VanBerkel, P.M.; Driessen, W.L.; Reedijk, J.; Sherrington, D.C.; Zitsmanis, A. *React. Funct. Polym.* **1995**, *27*, 15.

93. Yi-Yong, C.; Xing-Zhong, Y. *React. Polym.* **1994**, *23*, 165.

94. Letho, J.; Vaaramaa, K.; Leinoen, H. *React. Funct. Polym.* **1997**, *33*, 13.

95. Yatsimirskii, K.B.; Zicmanis, A.; Strizhak, P.E.; Pavlishchuk, V.V. *Dokl Akad Nauk SSR.* **1989**, *307*, 888.

96. Gauthier, M.; Frank, P.C. *React. Funct. Polym.* **1996**, *31*, 67.

97. Alexandratos, S.D.; Wilson, D.L. *Macromolecules*, **1986**, *19*, 280.

98. Alexandratos, S.D.; Trochimczuk, A.W.; Crick, D.W., Horwitz, E.P.; Gatrone, R.C.; Chiarizia, R. *Macromolecules*, **1996**, *29*, 1021.

99. Horwitz, E.P.; Chiarizia, R.; Diamond, H.; Gatrone, R.C.; Alexandratos, S.D.; Trochimczuk, A.W.; Crick, D.W., *Solv. Extr. Ion Exch.* **1993**, *11*, 943.

100. Alexandratos, S.D.; Quillen, D.R. *React. Polym.* **1990**, *13*, 255.

101. Alexandratos, S.D.; Quillen, D.R. *Solv. Extr. Ion Exch.* **1989**, *7*, 511.

102. Alexandratos, S.D.; Trochimczuk, A.W. *J. App. Poly. Sci.*, **1994**, *52*, 1273.

103. Alexandratos, S.D.; Hussain, L.A. *Ind. Eng. Chem. Res.* **1995**, *34*, 251.

104. Solvent Extraction Chemistry, Sekine, T.; Hasegawa, Y., Marcel Dekker: New York, 1977.

105. Alexandratos, S.D.; Crick, D.W.; Quillen, D.R. *Ind. Eng. Chem. Res.* **1991**, *30*, 772.

106. Alexandratos, S.D.; Beauvais, R.; Duke, J.R.; Jorgensen, B.S. *J. App. Poly. Sci.*, **1998**, *68*, 1911.

107. Alexandratos, S.D.; Crick, D.W.; Quillen, D.R. *Ind. Eng. Chem. Res.* **1991**, *30*, 772.

108. Vedejs, E.; Diver, S.T. *J. Am. Chem. Soc.* **1993**, *115*, 3358.

109. Buckler, S.A. *J. Am. Chem. Soc.* **1962**, 3393.

APPENDIX

APPENDIX

POLYMER-SUPPORTED ACYLATION CATALYST

Nucleophiles such as amines and phosphines have been used to catalyze the acylation of alcohols by anhydrides.[108] In the present research, a series of nucleophiles were evaluated as potential polymer-supported catalyst to study the influence of the microenvironmental effect.

EXPERIMENTAL

Synthesis of poly(vinylbenzyldimethylamine)

In an 800 ml beaker, 500 ml of 40 wt% dimethylamine and 1 g of NaOH was mixed until homogenous. The mixture was then added to 500 mL 3 neck round-bottom flask containing 14 g of poly(vinylbenzyl chloride) gel beads. The round-bottom was fitted with a condenser, overhead stirrer, and stopper with Teflon tape in the ground glass joints. After the reaction had refluxed for 9 h and cooled to room temperature, the resin was then washed with water twice for 15 min. The resin was then moved to a column and conditioned with 1 L H_2O, 1N NaOH, H_2O, 1 N HCl, and H_2O with a 1 h elution time for each liter. The characterization of resin CS2-118, synthesized using this procedure, determined a nitrogen capacity of 1.88 mmol / g.

Acylation reaction conditions

Benzoic anhydride (0.08 mol) and benzyl alcohol (0.04) were weighed in a

graduated cylinder. The mixture was dilute to 80 ml with either acetonitrile (CH_3CN) or tetrahydrofuran (THF), and the mass of solvent determined. The mixture was transferred to a 3-neck 100 ml round-bottom flask fitted with a thermometer, overhead stirrer, and rubber septum. The round-bottom was placed in a water bath at room temperature and sweep with nitrogen for one minute. The reaction was started with the addition of the catalyst (0.008 mol) and the progress of the reaction monitored by GC analysis of samples. Reactant and product concentrations were determined from the integrated data using the solvent as an internal standard.

RESULTS AND DISCUSSION

Acylation reactions with tributylphosphine and diethylphenylphosphine were complete within 0.1 h and 0.5 h respectfully. Although the reactivity of these phosphines was ideal for a study of the microenvironmental effect on a polymer-supported catalyst, these phosphines are also highly susceptible to oxidation in air[109] which would complicate the synthesis and characterization of the polymer analog. Triphenylphosphine, which is not readily oxidized, showed no catalytic activity in the first 24 h. The results of the acylation reaction catalyzed with poly(vinylbenzyldiphenylphosphine) [supplied by Dr. Dorothy Miller, resin DM-03-115] were identical to the triphenylphosphine reaction. The poor reactivity of the triphenylphosphine and DM-03-115 was attributed to the reduced electron density at the phosphorus by the electron-withdrawing aromatics rings.

Although trialkylphosphines have been reported to be highly reactive in the catalysis of acylation reactions[108], their uncontrollable oxidation in air complicated the

study of a polymer-supported phosphine. The catalytic activity of several amines were then evaluated as a potential polymer-supported catalyst. Acylation reactions with triethylamine and benzyldimethylamine were complete within 2 h and 24 h respectfully. Unlike the small molecule reaction, the acylation with poly(vinylbenzyldimethylamine) [resin CS2-118] and poly(vinylbenzyldipropylamine) [supplied by Dr. Donna Quillen, resin DQ-04-218B] were incomplete within 24 h. A comparison of pyridine and poly(vinylpyridine) [supplied by Dr. Latiff Hussain, resin LH-02-218] determined both catalysts to have poor activity within the first 24 h.

VITA

Christopher Shelley was born in Freeport, Texas on July 10, 1971. He graduated from Eastern High School located in Louisville, Kentucky in 1989. In May of 1993, Christopher earned his Bachelor of science degree in Chemistry from the University of Kentucky. In August 1993 he accepted a teaching and research assistantship from the University of Tennessee Chemistry Department. The degree was awarded in May 2000. In June 1999 Christopher accepted a position as an Assistant Professor of Chemistry at Tennessee Wesleyan College located in Athens, Tennessee.